

Cluster Heads Selection and Cooperative Nodes Selection for Cluster-based Internet of Things Networks

by

Liumeng Song

A thesis submitted to the University of London for the degree of
Doctor of Philosophy

School of Electronic Engineering and Computer Science
Queen Mary University of London
United Kingdom

2016

Abstract

Clustering and cooperative transmission are the key enablers in power-constrained Internet of Things (IoT) networks. The challenges for power-constrained devices in IoT networks are to reduce the energy consumption and to guarantee the Quality of Service (QoS) provision. In this thesis, optimal node selection algorithms based on clustering and cooperative communication are proposed for different network scenarios, in particular:

- The QoS-aware energy efficient cluster heads (CHs) selection algorithm in one-hop capillary networks. This algorithm selects the optimum set of CHs and construct clusters accordingly based on the location and residual energy of devices.
- Cooperative nodes selection algorithms for cluster-based capillary networks. By utilising the spacial diversity of cooperative communication, these algorithms select the optimum set of cooperative nodes to assist the CHs for the long-haul transmission. In addition, with the regard of evenly energy distribution in one-hop cluster-based capillary networks, the CH selection is taken into consideration when developing cooperative devices selection algorithms.

The performance of proposed selection algorithms are evaluated via comprehensive simulations. Simulation results show that the proposed algorithms can achieve up to 20% network lifetime longevity and up to 50% overall packet error rate (PER) decrement. Furthermore, the simulation results also prove that the optimal tradeoff between energy efficiency and QoS provision can be achieved in one-hop and multi-hop cluster-based scenarios.

TO MY FAMILY

Declaration

I, Liumeng Song, confirm that the work presented in this thesis is my own work and it is original, except where due reference has been mentioned.

I attest that I have exercised reasonable care to ensure that the work is original, and does not to the best of my knowledge break any UK law, infringe any third party's copyright or other Intellectual Property Right, or contain any confidential material.

I accept that the College has the right to use plagiarism detection software to check the electronic version of the thesis. I confirm that this thesis has not been previously submitted for the award of a degree by this or any other university.

The copyright of this thesis rests with the author and no quotation from it or information derived from it may be published without the prior written consent of the author.

Signature _____

Date _____

Acknowledgments

First of all, I would like to express my sincere gratitude to my supervisor, Dr. Michael Chai, who has given me all the support, priceless guidance and encouragement throughout my Ph.D. study. Michael supported me not only by providing continuous guidance but also helping me go through all difficulties I encountered in my research work and thesis writing.

I would also like to express my profound gratitude to Prof. Yue Chen, for her helpful suggestions and discussions, and for being so dedicated to her role as my independent assessor. I would also like to thank Dr. Jonathan Loo and Dr. John Schormans, for their valuable suggestions and comments on my research.

Moreover, my gratitude to the colleagues and friends at Queen Mary, who made my time in London more enjoyable and memorable.

I would also like to thank the Chinese Scholarship Council (CSC), for the financial support in the past four years.

Finally, I would like to take this opportunity to express my gratitude to my parents and boyfriend, who gave me enormous support and courage during my Ph.D. stage.

Table of Contents

Abstract	i
Declaration	iii
Acknowledgments	iv
Table of Contents	v
List of Figures	ix
List of Tables	xii
List of Abbreviations	xiv
1 Introduction	1
1.1 Research Motivation	1
1.2 Research Scope	2
1.3 Contributions	3
1.4 Researcher Publication List	4
1.5 Thesis Outline	5
2 Background	6
2.1 Overview of Capillary Networks	6
2.1.1 Network Architecture	7
2.1.2 Clustering Protocol in Capillary networks	8

2.1.3	Cooperative Communication in Cluster-based Capillary Networks .	9
2.2	State-of-the-Art	12
2.2.1	Clustering Protocols in Capillary Networks	13
2.2.2	CMISO Systems in Cluster-based Networks	15
2.2.3	CMIMO Systems in Cluster-based Networks	17
2.3	Methodology	20
2.3.1	Node Selection Algorithms	20
2.3.2	Quantum Particle Swarm Optimisation	21
2.3.3	Multi-objective Optimisation	34
2.4	Summary	39
3	CHs Selection for the Capillary Networks	40
3.1	System Model	40
3.2	Energy Consumption Model	43
3.3	Energy Efficiency Problem Formulation	45
3.3.1	Energy Consumption in Intra-cluster Communication	46
3.3.2	Energy Consumption of Data Aggregation	46
3.3.3	Energy Consumption in Inter-cluster Communication	47
3.3.4	Network Lifetime Formulation	48
3.4	QPSO-based CHs Selection Algorithm	49
3.5	Simulation and Conclusions	53
3.5.1	Scenario Design and System Parameters	53
3.5.2	Simulation Platform	55
3.5.3	Simulation Results	58
3.5.4	Conclusions	63
3.6	Summary	64
4	CH and Cooperative Devices Selection for Single-Hop Networks	65
4.1	System Model	65
4.2	Energy Consumption Model	67

4.3	Energy Efficient CH and and Cooperative Devices Selection	68
4.3.1	Energy Efficiency Problem Formulation	68
4.3.2	Energy Efficiency CH and and Cooperative Devices Selection Algo- rithm	73
4.3.3	Simulation and Conclusions	75
4.4	QoS-based CH and Cooperative Devices Selection	83
4.4.1	QoS-based Problem Formulation	84
4.4.2	QoS-based CH and Cooperative Devices Selection Algorithm . . .	88
4.4.3	Simulation and Conclusions	90
4.5	CH and Cooperative Devices Selection for Joint Optimisation	95
4.5.1	Joint Optimisation Problem Formulation	95
4.5.2	CH and Coops Selection Algorithm for Joint Optimisation	96
4.5.3	Simulation and Conclusions	98
4.6	Summary	104
5	Cooperative Coalitions Selection for Multi-hop Networks	106
5.1	System Model	106
5.2	Energy Consumption Model	110
5.3	Energy Efficient Cooperative Coalitions Selection	110
5.3.1	Energy Efficient Problem Formulation	111
5.3.2	Energy Efficiency Cooperative Coalitions Selection Algorithm . . .	118
5.3.3	Simulation and Conclusions	119
5.4	QoS-based Cooperative Coalitions Selection	128
5.4.1	QoS-based Problem Formulation	128
5.4.2	QoS-based Cooperative Coalitions Selection Algorithm	134
5.4.3	Simulation and Conclusions	135
5.5	Cooperative Coalitions Selection for Joint Optimisation	139
5.5.1	Joint Optimisation Problem Formulation	139
5.5.2	Cooperative Coalitions Selection Algorithm for Joint Optimisation	140

5.5.3	Simulation and Conclusions	142
5.6	Summary	147
6	Conclusions and future work	149
6.1	Conclusions	149
6.2	Future work	150
6.2.1	Cooperative Coalitions Selection in Energy Harvesting Networks .	150
6.2.2	Cooperative Coalitions Selection in Heterogeneous Wireless Net- works	151
Appendix A	Simulation Validation	153
References		155

List of Figures

2.1	Network Architecture	7
2.2	Clusters in capillary networks	8
2.3	CMISO Systems in cluster-based capillary networks	10
2.4	CMIMO systems in cluster-based capillary networks	12
2.5	Population representation in evolutionary algorithms	21
2.6	Flowchart of general evolutionary algorithm	22
2.7	Qubit-based QPSO updating process	24
2.8	Single-point crossover to get local attractor	28
2.9	Number of generations versus fitness value of Rastrigin function	32
2.10	Number of generations versus fitness value of Griewank function	33
3.1	System model for clustering in capillary networks	41
3.2	Transmission structure in cluster-based capillary networks	42
3.3	Particle position representation for CH candidates	51
3.4	Scenario diagram for cluster-based capillary networks	53
3.5	Flowchart of the proposed clustering algorithm	56
3.6	Flowchart of scenario initialisation in cluster-based capillary networks	57
3.7	Flowchart of algorithm initialisation in Algorithm 4	57
3.8	Particle number and generation number selection	60
3.9	Convergence of QPSO	60
3.10	Number of hours versus overall residual battery capacity	61

3.11	Number of hours versus number of alive nodes	62
3.12	Number of hours versus number of CHs	63
4.1	System model for CMISO system in cluster-based capillary networks	66
4.2	Time slots of TDMA scheduling using CMISO systems	67
4.3	Particle position representation for cooperative devices candidates	74
4.4	Scenario diagram for capillary networks using the CMISO system	75
4.5	Flowchart of the proposed CH and Coops selection algorithm	78
4.6	Particle number and generation number selection	80
4.7	Location of capillary gateway versus network lifetime	81
4.8	Location of capillary gateway versus number of Coops	82
4.9	BER threshold versus network lifetime	82
4.10	BER threshold versus number of Coops	83
4.11	Convergence of QPSO	91
4.12	Energy constraint E_t versus overall PER	92
4.13	Energy constraint E_t versus number of Coops	93
4.14	Location of capillary gateway versus overall PER	93
4.15	Location of capillary gateway versus number of Coops	94
4.16	Flowchart of the proposed CH and Coops selection algorithm	100
4.17	Flowchart of NSGA-II module	101
4.18	Pareto optimal solution of NSQPSO	102
4.19	\bar{E}_b/N_0 versus network lifetime	102
4.20	\bar{E}_b/N_0 versus number of Coops	103
4.21	\bar{E}_b/N_0 versus number of Coops	104
5.1	System model for CMIMO systems	107
5.2	Intra-cluster transmission for multi-hop cluster-based capillary networks .	109
5.3	Inter-cluster communication for multi-hop cluster-based capillary networks	109
5.4	Time slots of TDMA scheduling for a cluster using CMIMO systems . . .	110
5.5	Particle position representation for cooperative coalitions candidates . . .	119

5.6	Scenario design with three clusters	121
5.7	Simulation scenario for cluster-based capillary networks	121
5.8	Flowchart of the proposed cooperative coalitions selection algorithm . . .	122
5.9	Particle number and generation number selection	124
5.10	Convergence of QPSO algorithm	124
5.11	Network lifetime versus long-haul cluster distance	125
5.12	Network lifetime versus BER threshold	127
5.13	Energy constraint E_t versus overall PER	137
5.14	Long-haul distance versus overall PER	138
5.15	Flowchart of the proposed cooperative coalitions selection algorithm . . .	143
5.16	Pareto optimal solution of NSQPSO	144
5.17	\bar{E}_b/N_0 versus network lifetime	145
5.18	\bar{E}_b/N_0 versus overall PER	146

List of Tables

2-A	Optimum Number of Coops in Terms of Long-haul Distance	16
3-A	System Parameters for Cluster-based Capillary Networks	54
3-B	Particle Number and Generation Number Selection	58
4-A	System Parameters in Scenario Using CMISO system	77
4-B	Particle Number and Generation Number Selection	79
5-A	Particle Number and Generation Number Selection	123
5-B	Size of Cooperative Coalitions in terms of Long-haul Cluster Distance . .	126
5-C	Size of Cooperative Coalitions in terms of BER Threshold	127
5-D	Size of Cooperative Coalitions in terms of Energy Constraint E_t	137
5-E	Size of Cooperative Coalitions versus Long-haul Cluster Distance	138
5-F	Size of Cooperative Coalitions for Link 1 in terms of \bar{E}_b/N_0	146
5-G	Size of Cooperative Coalitions for Link 2 in terms of \bar{E}_b/N_0	147
5-H	Size of Cooperative Coalitions for Link 3 in terms of \bar{E}_b/N_0	147

List of Abbreviations

AWGN	Additive White Gaussian Noise
BER	Bit Error Rate
CH	Cluster Head
CM	Cluster Member
CMIMO	Cooperative Multiple-Input-Multiple-Output
CMISO	Cooperative Multiple-Input-Single-Output
Coops	Cooperative devices
ETE	End-to-End
IoT	Internet of Things
LEACH	Low Energy Adaptive Clustering Hierarchy
MIMO	Multiple-Input-Multiple-Output
MISO	Multiple-Input-Single-Output
NP-hard	Non-deterministic Polynomial-time hard
NSGA-II	Non-dominated Sorting Genetic Algorithm II
NSQPSO	Non-dominated Sorting Quantum-inspired Particle Swarm Optimisation
PAR	Peak-to-Average Ratio
PER	Packet Error Rate
PSO	Particle Swarm Optimisation
QAM	Quadrature Amplitude Modulation
QGA	Quantum Genetic Algorithm

QoS	Quality of Service
QPSO	Quantum-inspired Particle Swarm Optimisation
RCoops	Cooperative Receivers
SCoops	Cooperative Senders
SIMO	Single-Input-Multiple-Output
SNR	Signal-to-Noise Ratio
STBC	Space Time Block Coding
TDMA	Time Division Multiple Access

Chapter 1

Introduction

Internet of Things (IoT) was first proposed in 1999 when Auto-ID Center launched their initial vision of the Electronic Product Code network for automatically identifying and tracing the flow of goods in supply-chains. Nowadays, the IoT networks represent a new revolutionary era of computing technology which enables a wide variety of devices to interoperate through the existing Internet infrastructure. The IoT networks promote the virtual world of information technology to integrate seamlessly with the real world of things. The capillary networks were introduced in the IoT networks to support huge number of devices in the IoT networks via wireless technologies [CVAG12].

1.1 Research Motivation

Energy efficiency of the long-haul transmission is one of the main challenging issues considering the fact that most of the wireless devices involved in capillary connections are powered by batteries and have limited energy supply. The clustering protocol was then proposed as an energy efficient cross-layering technique to solve the aforementioned issue [LG97]. The clustering protocol employs cluster heads (CHs) which consequently transmit the aggregated data to the capillary gateway for the long-haul transmission.

There remains a problem that it is difficult to determine the number of CHs and the distribution of CHs to ensure the energy efficiency [GP10].

In addition, although the clustering protocol improves energy efficiency in capillary networks, the CHs consume a considerable energy compared to other devices, bringing the unequal energy depletion among the wireless devices [ZD07]. As a result, the energy of CHs are run out earlier as compared to other devices in the network, which may limit the network lifetime. Cooperative communication was introduced in cluster-based capillary networks to increase spatial diversity and distribute the energy consumption evenly in the network [Lan06]. It uses cooperative devices to assist CHs in long-haul transmission. However, cooperative devices may result in extra energy consumption and Quality of Service (QoS) requirement. There is no effective strategy to decide how many and which cooperative devices should participate in the long-haul transmission with different objectives, such as energy efficiency, QoS provision optimisation and the optimum tradeoff between energy efficiency and QoS provision optimisation.

1.2 Research Scope

This thesis focuses on the node selections algorithm for capillary networks. The following research objectives are achieved:

- a) energy efficiency maximisation,
- b) QoS provision improvement,
- c) the optimum tradeoff between energy efficiency and QoS provision.

The following novel node selection algorithms are proposed to achieve these objectives for different network scenarios:

- a) The CHs selection algorithm aims to prolong the network lifetime in single-hop capillary networks.

- b) The CH and cooperative devices selection algorithm in single-hop cluster-based capillary networks aims to maximise network lifetime, to minimise overall packet error rate (PER), and also to strike the optimum tradeoff between network lifetime and overall PER.
- c) The cooperative coalitions selection algorithm in multi-hop cluster-based capillary networks aims to maximise network lifetime, to minimise overall PER, and also to strike the optimum tradeoff between network lifetime and overall PER.

1.3 Contributions

The contributions of this thesis are list as follows:

- a) A QoS aware energy efficient CHs selection algorithm in one-hop capillary networks is proposed by using Quantum-inspired Particle Swarm Optimisation (QPSO) to maximise the network lifetime. The proposed algorithm is able to select the optimum set of CHs and construct clusters accordingly based on the location and residual energy of devices.
- b) The CH and cooperative devices selection algorithms for one-hop capillary networks based on cooperative multiple-input-single-output (CMISO) are proposed to maximise the network lifetime, minimise the overall PER, and also achieve the optimum tradeoff between network lifetime and overall PER. These algorithms apply exhaustive search to determine the optimum CH, utilise QPSO to select the optimum set of cooperative devices to assist CH for long-haul transmission, and also employs Non-dominated Sorting Genetic Algorithm-II (NSGA-II) for the Pareto solutions of the cooperative devices set to prolong network lifetime and decrease overall PER.
- c) Cooperative coalitions selection algorithms for multi-hop capillary networks based on multi-hop cooperative multiple-input-multiple-output (CMIMO) are proposed to maximise the network lifetime, minimise the overall PER, and also achieve the opti-

mum tradeoff between network lifetime and overall PER. The cooperative coalitions selection algorithms apply QPSO to select the optimum set of cooperative senders and cooperative receivers of each cluster in the routing path, and also employ NSGA-II for the Pareto solutions of cooperative coalitions to prolong network lifetime and decrease overall PER.

1.4 Researcher Publication List

1. **L. Song**, K. K. Chai, Y. Chen, J. Loo, and J. Schormans, "Cooperative Coalition Selection for Quality of Service Optimisation in Cluster-based Capillary Networks of the Internet of Things Systems", *IEEE Systems Journal*, 2016.
2. **L. Song**, K. K. Chai, Y. Chen and J. Schormans, "QoS-aware Energy Efficient Cooperative Scheme for Cluster-based IoT Systems", *IEEE Systems Journal*, 2015.
3. **L. Song**, K. K. Chai, Y. Chen and J. Schormans, "Energy efficient cooperative MISO scheme for cluster-based M2M capillary networks", *2016 IEEE 27th Annual IEEE International Symposium on Personal, Indoor and Mobile Radio Communications (PIMRC)*, Valencia, Spain, 2016.
4. **L. Song**, K. K. Chai, Y. Chen, J. Loo, S. Jimaa and J. Schormans, "QoS-aware Energy Efficient Cooperative Scheme for Cluster-based IoT Systems", *2016 IEEE Wireless Communications and Networking Conference (WCNC)*, Doha, Qatar, 2016.
5. **L. Song**, K. K. Chai, Y. Chen and J. Schormans, "Energy efficient cooperative MISO scheme for cluster-based M2M capillary networks", *2014 International Symposium on Wireless Personal Multimedia Communications (WPMC)*, Sydney, NSW, 2014.

1.5 Thesis Outline

Chapter 2 provides the architecture of capillary networks and background information of clustering and cooperative communication, summarises the state-of-the-art clustering protocols and cooperative communication, as well as presents relevant methodologies used in this thesis.

Chapter 3 presents an energy efficient CHs selection algorithm by using QPSO to maximise the network lifetime. The performance evaluation is carried out for the proposed CHs selection algorithm.

Chapter 4 addresses the CH and cooperative devices selection problem in CMISO enabled one-hop capillary networks, where the CH and cooperative devices selection algorithms are developed with the objective of energy efficiency, QoS provision optimisation and the optimum tradeoff between energy efficiency and QoS provision. The performance evaluation are conducted during the development of proposed algorithms.

Chapter 5 investigates the cooperative coalitions selection algorithms in CMIMO enabled multi-hop capillary networks. The proposed cooperative coalitions selection algorithm aims at energy efficiency, QoS provision and the optimum tradeoff between energy efficiency and QoS provision. The performance evaluations are conducted during the development of proposed algorithms.

Chapter 6 consists of conclusions and some thoughts for future work.

Chapter 2

Background

This chapter presents the introduction of capillary networks. Taking the network performance into consideration, special focuses are given to the clustering protocol and cooperative communications for capillary networks. Correspondingly, the current research efforts on clustering protocol and cooperative communication are provided. At the end of this chapter, the methodologies used in the following chapters are described.

2.1 Overview of Capillary Networks

The Internet of Things (IoT) represents a new revolutionary era of computing technology that enables a wide variety of devices to interoperate through the existing Internet infrastructure [NBO⁺15]. The potential of this era is boundless, bringing in new communication opportunities in which ubiquitous devices blend seamlessly with the environment and embrace every aspect of people's daily lives. Cellular communication technologies can play a crucial role in the development and expansion of IoT [SYY⁺13]. Cellular networks can leverage their ubiquity, network management and advanced backhaul connectivity capabilities into IoT networks. In this regard, capillary networks aim to provide the capabilities of cellular networks to constrained networks while enabling connectivity

between wireless devices and cellular networks [SBE⁺14]. Hence, a capillary network provides local connectivity to devices using short-range radio access technologies while it connects to the backhaul cellular network.

2.1.1 Network Architecture

An end-to-end architecture from the capillary networks to the IoT platform through the mobile networks is given in Figure 2.1.

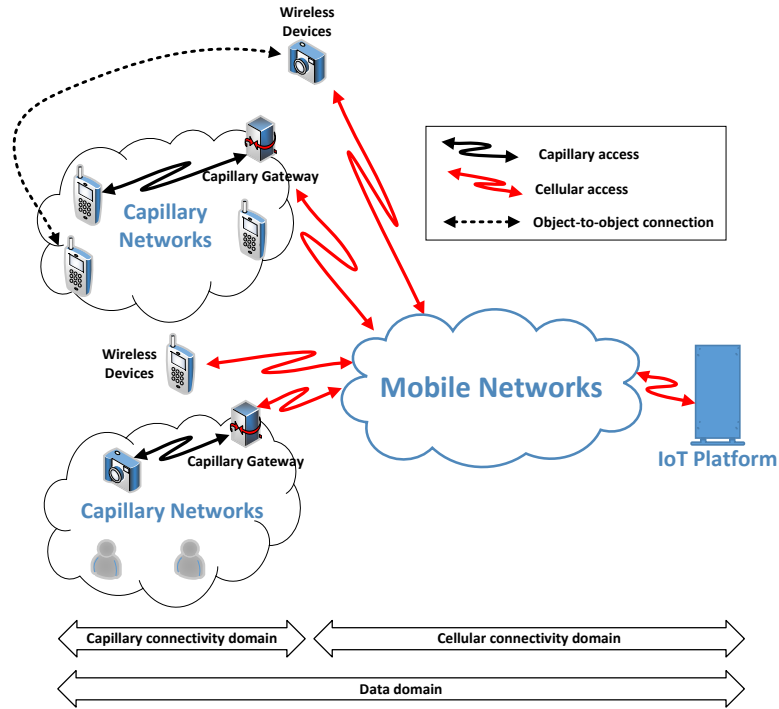


Figure 2.1: Network Architecture

This architecture consists of three domains: the capillary connectivity domain, the cellular connectivity domain, and the data domain. In capillary connectivity domain, some wireless devices communicate with the mobile networks through a capillary gateway while some communicate to the mobile networks via cellular connectivity directly. The cellular connectivity domain provides connectivity in the mobile networks and IoT platform. The data domain includes all devices and infrastructure that provide data pro-

cessing functionality for a desired service from the devices to the IoT platform [SBE⁺14].

2.1.2 Clustering Protocol in Capillary networks

Although capillary networks can provide reliable connectivity to devices within a specific local area, energy efficiency is a challenging issue [ABBR⁺12]. Additionally, if every device in capillary network communicates with the capillary gateway independently and directly, it stands a good chance that a huge number of packet collisions occur at the capillary gateway due to lots of simultaneous access requests. Moreover, a great amount of signalling overhead is another significant issue if direct connection between every device and the sink is allowed.

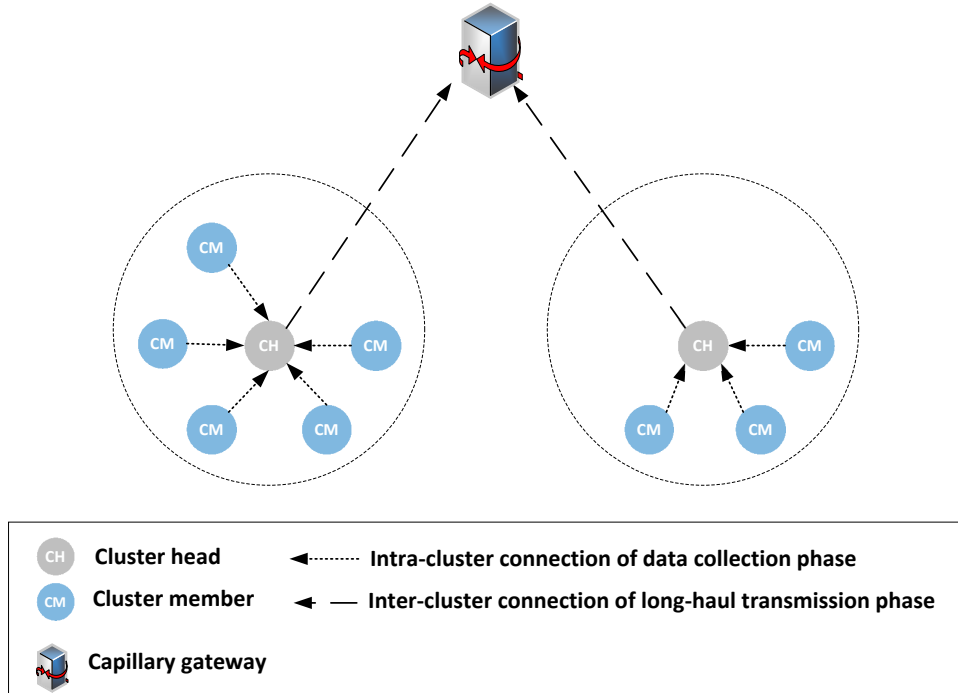


Figure 2.2: Clusters in capillary networks

The clustering protocol was proposed as an energy efficient cross-layering technique to solve the aforementioned issues [HCB00]. The clustering protocol organizes all devices in the network into several groups, as shown in Figure 2.2. A cluster consists of two kinds of devices: one CH and several cluster members (CMs). In particular, the CH is responsible

for collecting data packets from its CMs, aggregating the collected data based on some computations (e.g. average, standard deviation or gradient data aggregation algorithms), and preparing a single aggregated packet that is sent to the capillary gateway in the long-haul transmission. Therefore, there are two phases in the cluster-based transmission protocol:

- Data collection phase. Every CM transmits a data packet to its CH through the intra-cluster connection.
- Long-haul transmission phase. Every CH transmits an aggregated data packet to the capillary gateway through the inter-cluster connection.

The advantage of clustering lies on the reduction of transmission distance in both intra-cluster and inter-cluster communication, because the intra-cluster distances between the CMs and the CH are normally shorter than the long-haul distance between the CM and the capillary gateway. Besides, the number of CHs is less than the number of CMs in the network, therefore, clustering technique also decreases the signalling overhead and releases traffic congestion at the capillary gateway.

2.1.3 Cooperative Communication in Cluster-based Capillary Networks

In cluster-based capillary networks, the CHs consume a considerable energy in the long-haul transmission compared to the CMs within the same cluster. The unequal energy depletion among the devices in the capillary networks may cause CHs to run out of battery power earlier than CMs, which severely limits the network lifetime [KCY⁺08]. In this case, multi-antenna systems have been introduced in cluster-based capillary networks to increase channel capacity and reduce transmission energy consumption in fading channels [CSSI06]. Due to the limited physical size of a wireless device which can typically support one single antenna, cooperative communication systems allow single-antenna devices to reap some of the benefits of multi-antenna systems.

To form such a cooperative communication system, devices must first exchange the data packet that is utilized to decide the long-haul data. Then, the source device and cooperative devices jointly transmit the long-haul data to the destination. And the destination side can have one or more devices to receive the long-haul data.

2.1.3.1 Cooperative Multiple-Input-Single-Output Systems

In small-scale cluster-based capillary networks where clusters are located relatively close to the capillary gateway, CMISO systems are employed in the long-haul transmission between clusters and capillary gateway. In particular, the CH and cooperative devices (Coops) within the same cluster form the cooperative multiple-input antennas to transmit the long-haul data to the capillary gateway which is equipped with one antenna to receive data [FGZW10], as shown in Figure 2.3.

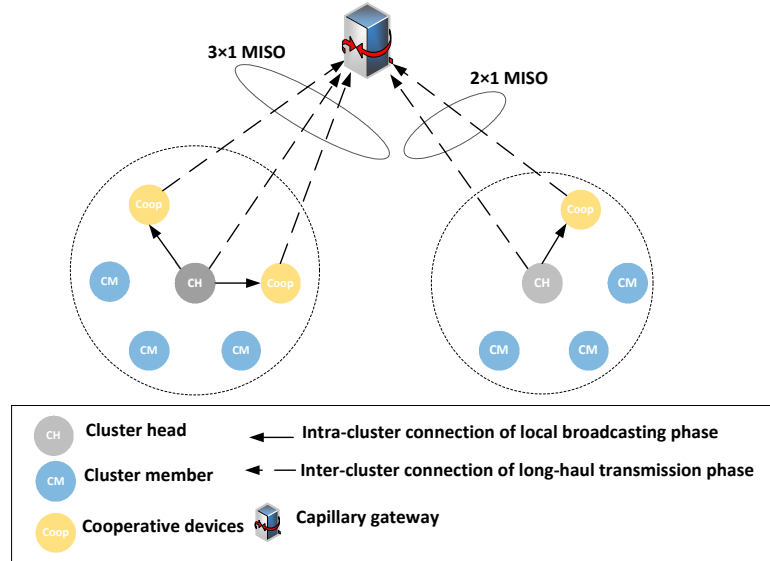


Figure 2.3: Cooperative Multiple-Input-Single-Output systems in cluster-based capillary networks

The CMISO transmission consists of two phases:

- Local broadcasting phase. The CH shares the aggregated data with its Coops by broadcasting it within the cluster.

- Long-haul transmission phase. The CH and its Coops modulate the local broadcasting data to be the long-haul data based on diversity modulation techniques, such as space-time block coding (STBC). Then the CH and Coops jointly transmit the MISO-modulated long-haul data to the capillary gateway.

2.1.3.2 Cooperative Multiple-Input-Multiple-Output Systems

In large-scale cluster-based capillary networks where several clusters are located far away from the capillary gateway, cooperative Multiple-Input-Multiple-Output (CMIMO) systems are employed in the multi-hop long-haul transmission [MR13]. In CMIMO systems, the source CH with its cooperative senders (SCoops) at the transmission side form the cooperative multi-antennas system to send the long-haul data to the destination CH and its cooperative receivers (RCoops) at the reception side.

The CMIMO transmission consists of three phases:

- Local broadcasting phase. At the transmission side, the source CH shares the aggregated data with its SCoops by broadcasting it within the cluster.
- Long-haul transmission. At the transmission side, the source CH and its SCoops modulate the local broadcasting data to be the long-haul data based on diversity modulation techniques, and then transmit the MIMO-modulated data to the reception side. At the reception side, the destination CH together with its RCoops receive the MIMO-modulated data from all the source CH and SCoops.
- Local forwarding phase. At the reception side, all RCoops transmit the received MIMO-modulated data to the destination CH.

An example of multi-hop CMIMO systems in cluster-based capillary network is shown in Figure 2.4. For instance, Cluster 1 in the Routing path 1 have data to transmit to the capillary gateway through Cluster 2. In the long-haul transmission between Cluster 1 and Cluster 2, a 3×2 MIMO system is employed with one CH and two SCoops at the

transmission side as well as one CH and one RCoop at the reception side. And in the long-haul transmission between Cluster 2 and the capillary gateway, a 3×1 MISO system is employed, including one CH and two SCoops at the transmission side. Similarly, in Routing path 2, the Cluster 3 send data to the capillary gateway through Cluster 4 and Cluster 5 by 2×2 MIMO, 2×3 MIMO and 2×1 MISO systems, respectively.

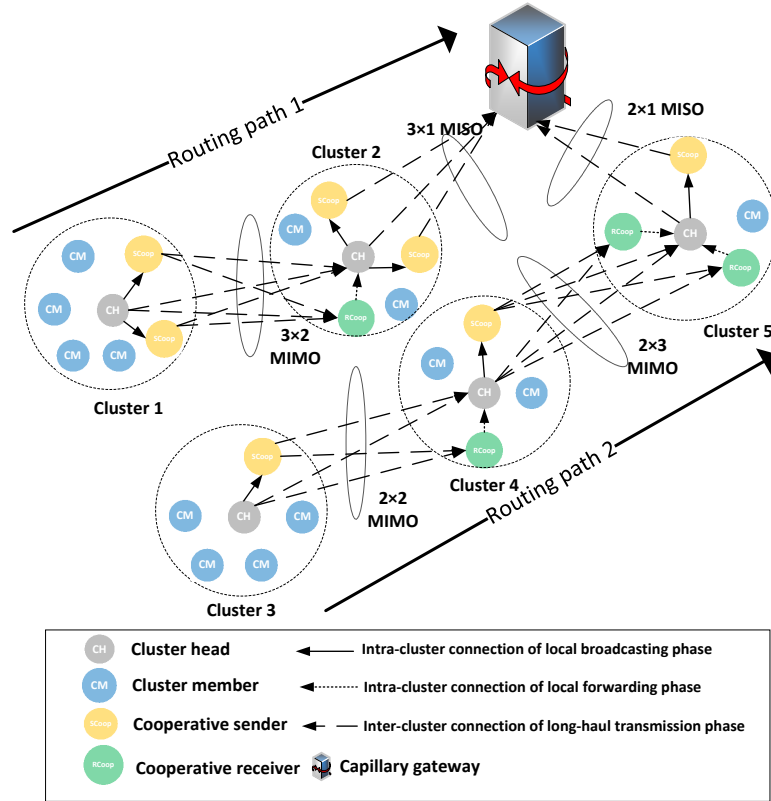


Figure 2.4: Cooperative Multiple-Input-Multiple-Output systems in cluster-based capillary networks

2.2 State-of-the-Art

In this section, several recent research work on clustering protocols and cooperative communication are reviewed.

2.2.1 Clustering Protocols in Capillary Networks

Clustering protocols are able to achieve energy efficiency in a scalable and effective manner by organizing wireless devices into small groups. The clustering protocols can be classified into distributed, centralised and hybrid ones [AY07].

In distributed clustering protocols, devices are usually not aware of their network position, and all the clustering and routing decisions have to be made based on devices' internal information and information exchange with their neighbours. Some well-known distributed clustering protocols include low energy adaptive clustering hierarchy (LEACH) Protocol [HCB00], energy efficient hierarchical clustering (EEHC) [BC03], and scalable energy efficient clustering hierarchy (SEECH) [TKS14], with the objectives of overall energy consumption minimisation.

In centralised clustering protocols, the network consists of a number of location-aware wireless devices. That is, all devices report their individual information to a centre sink, e.g. the capillary gateway, and all the clustering and routing decisions are made in the centre sink. Some well-known centralised clustering protocols include centralised LEACH (LEACH-C) [HCB02], base-station controlled dynamic clustering protocol (BCDCP) [MMBF05], and cluster head election mechanism using Fuzzy logic (CHEF) [KPHC08], with the objectives of overall energy consumption minimisation.

Hybrid clustering protocols are composed of both centralised and distributed approaches. In hybrid clustering protocols, distributed approaches are usually used for coordination between CHs, and centralised manners are performed for CHs to build individual clusters. Typical hybrid clustering strategies include hybrid energy-efficient distributed (HEED) clustering algorithm [YF04] and non-probabilistic approach and fuzzy logic based on HEED algorithm (HEED-NPF) [TNKY10], with the objectives of overall energy consumption minimisation or even energy distribution.

The capillary gateway is assumed to be capable of processing complicated algorithms

and supplying unlimited energy [SH11], because the centre sink, e.g. capillary gateway, is usually connected to the power grid and has high data processing capability. Therefore, the capillary gateway is able to execute the centralised clustering algorithms. From an optimisation perspective, clustering is a kind of non-deterministic polynomial-time hard (NP-hard) grouping problem [Fal98]. A problem is in NP if there exists a non-deterministic polynomial-time solution [LKH93]. If a problem is NP-hard, it indicates that any problem in NP can be reduced to that problem [Woe03]. Particularly, centralised clustering protocols involving evolutionary algorithms are widely believed to be effective on NP-hard problems. And evolutionary algorithms are able to provide near-optimal solutions to such problems in a reasonable time [LKH93]. Evolutionary algorithms in [LTS07] [LTSL08] [GSDL14] have been applied in centralised clustering protocols recently.

In [LTS07], the authors proposed a centralised energy-aware clustering protocol using Particle Swarm Optimisation (PSO) algorithm, with the objective of simultaneously minimising the intra-cluster distance and optimising the energy consumption of the network. The base station runs the proposed PSO-based algorithm to select a pre-determined number of CHs that can minimise the cost function, as defined by,

$$\begin{aligned}
 cost &= \omega_{weight} \times f_1 + (1 - \omega_{weight}) \times f_2 \\
 f_1 &= \max_{k=1,2,\dots,K} \left\{ \sum_{\forall n \in C_{p,k}} \frac{d(n_i, CH_{p,k})}{|C_{p,k}|} \right\} \\
 f_2 &= \sum_{i=1}^N E(n_i) / \sum_{k=1}^K E(CH_{p,k})
 \end{aligned} \tag{2.1}$$

where K is the pre-determined number of CHs, f_1 is the maximum average Euclidean distance of devices to their associated CHs, $|C_{p,k}|$ is the number of devices belong to cluster C_k of particle p , f_2 is the ratio of total initial energy of all devices n_i , $i = 1, 2, \dots, N$ in the network with the total energy of the CH candidates in the current round. The constant ω_{weight} is a user-defined constant used to weigh the contribution of each of the sub-objectives. The simulation results suggest that the performance of

proposed PSO-based algorithm outperforms LEACH and LEACH-C.

In [GSDL14], the authors proposed a quantum genetic algorithm (QGA) based clustering protocol to determine the CHs selection, aiming at the energy consumption balance between CMs and CHs. Particularly, the proposed QGA algorithm deals with cluster formation based on different events, CH selection and aggregation of the sensed data within a cluster, and also the long-haul aggregated data transmission to the base station in an energy efficient way. The simulation result illustrates that the performance of the proposed algorithm is better than other distributed clustering algorithms. By applying the proposed algorithm, average residual energy of the network is not going down very quickly, and thus increasing network lifetime.

2.2.2 CMISO Systems in Cluster-based Networks

Single-hop CMISO communication between the cluster and the sink or the relay cluster is preferred, when all clusters are located close to the capillary gateway. And the capillary gateway uses one single antenna to receive the MISO-modulated data from CHs and Coops. Recent literature focused on the protocol design involving CMISO systems to optimise energy efficiency or QoS provision [AK10] [YHC06].

2.2.2.1 Energy Efficiency in Cluster-based CMISO Systems

Some studies about CMISO aiming at energy efficiency have been conducted. In [AK10], the authors proposed a cooperative LEACH protocol by introducing a cross layer approach to obtain higher order diversity without sacrificing any spectral efficiency. In [HOKK12], the authors investigated different data aggregation schemes in wireless networks with CMISO communication.

In [BZL08], the authors proposed a cluster formation scheme based on LEACH using CMISO system. The proposed scheme takes residual energy and the long-haul distance

into consideration aiming at overall energy consumption minimisation as well as the energy balance among the whole network. In particular, the optimum number of Coops is determined by the distance between CH and the base station, as illustrated in Table 2-A. Moreover, Coops are selected from the CMs with highest energy level within the cluster. The energy balance is improved by varying cluster size based on the long-haul distance and the preferred number of Coops. Simulation results have shown that the energy imbalance problem can be greatly improved by varying the cluster size.

Table 2-A: Optimum Number of Coops in Terms of Long-haul Distance

Distance between CH and BS (m)	Optimal number of Coops
0-60	1
60-80	2
80-140	3
140-200	4

In [LLW⁺13], the authors conducted a systematic analysis on the energy consumption of CMISO communication in a randomly distributed scenario. Based on the performance analysis, a closed form expression of overall PER is obtained and an optimisation problem is formulated to minimise the overall energy consumption subject to the device active rate. Meanwhile, the authors also considered the effect of the various system constraints on the optimisation. Devices which can correctly decode the local-broadcasting packet are selected as Coops. Besides, a node sleep strategy is proposed to achieve the tradeoff between the overall energy consumption and the number of active devices. The simulation results have shown that the total energy consumption can be optimised by adjusting intra-cluster broadcasting energy consumption under different overall PER requirements. Besides, it is proved that the proposed protocol has significant energy savings compared to non-cooperative long-haul transmissions.

2.2.2.2 QoS Optimisation in Cluster-based CMISO Systems

In [YHC06], authors proposed a cross-layer design to jointly improve the energy efficiency, reliability, and end-to-end (ETE) QoS provision in cluster-based wireless networks. In the

proposed protocol, the original LEACH protocol is extended by incorporating the CMISO communication. The ETE latency and throughput of the protocol is modelled in terms of the bit error rate (BER) performance in the long-haul transmission. Besides, a non-linear constrained optimisation model is developed to seek the optimum BER performance for each link to meet the QoS requirements with a minimum energy consumption. The PSO algorithm is employed to solve the programming problem. Simulation results have shown the effectiveness of the proposed protocol to achieve the goals of minimizing energy consumption and ETE QoS provisioning.

In [WCZW12], authors used a cooperative communication scheme to achieve the optimal solution of a random tradeoff between the outage performance and the network lifetime in a cluster-based wireless networks. The outage performance is evaluated as the QoS provision by a system design parameter and the outage probability threshold. Particularly, the research problem is formulated as a multi-variable optimisation problem, and is transformed into the concatenation of two sub-problems:

- a) Long-haul transmit power per device, which is solved by using convex optimisation theory combined with the Lambert W function.
- b) Set of Coops, which is solved by using a coalition formation game framework in the context of the results in the former sub-problem.

Extensive simulation results have shown that the proposed algorithm can achieve the tradeoff between outage performance and network lifetime by choosing the appropriate value of the system parameter.

2.2.3 CMIMO Systems in Cluster-based Networks

In large-scale capillary networks, the source CH and its SCoops at the transmission side send the MIMO-modulated data to the capillary gateway or the relay cluster. And there are usually more than one receiver antennas at the reception side. Recent literature

focus on the protocol design involving CMIMO systems to optimise energy efficiency or QoS provision.

2.2.3.1 Energy Efficiency in Cluster-based CMIMO Systems

In [PLC12], the authors proposed a novel fair cooperative communication scheme which encourages devices to participate in cooperative communication by giving the extra reward. First, the source header node finds its potential source member nodes by broadcasting the cluster-formation message. After the potential source member nodes receive message from source header node, SCoops are selected from the source member nodes within the same cluster if two conditions are satisfied:

- a) The signal-to-noise ratio (SNR) of the received signal is larger than a predefined SNR threshold level which is a minimum required level to decode the local-broadcasting message.
- b) Potential RCoops at the reception side must be within the transmission range of SCoops at the transmission side.

Then the proposed scheme finds the optimum radii of transmission and reception cluster to minimise the energy consumption under the given outage requirement. It has been shown that the proposed scheme consumes much less energy than unfair cooperative scheme and non-cooperative scheme.

In [APW08], the authors proposed a solution for non-uniform energy consumption in the cluster-based multi-hop wireless networks through adaptive selection of CMIMO schemes. The objective function is as follows,

$$\frac{1}{N_{total}} \times E_{bt} \approx C \quad (2.2)$$

where N_{total} is the number of clusters in the network, E_{bt} is the energy consumption per bit and C is a constant used to maintain the non-uniform energy consumption. The

number of SCoops and RCoops are determined by the given cooperative transmission energy per bit. The authors also showed that CMIMO system is able to reduce the energy consumption per bit by increasing the number of SCoops and RCoops for a given BER performance. It is proved that the multi-hop CMIMO system in relay clusters can reduce energy consumption as compared to the non-cooperative system, and the adaptive selection of cooperative transmission provides uniform energy consumption in all the clusters.

2.2.3.2 QoS Optimisation in Cluster-based CMIMO Systems

In [DCSI07], authors proposed a cluster-based wireless network using CMIMO systems which is optimally designed for minimum ETE outage probability by giving a per link energy constraint. The authors assumed that the energy consumption in the cluster-to-cluster hop is limited to E_t , and the research problem is expressed as

$$E_t = \vartheta p_1 + (1 - \vartheta)p_2 \quad (2.3)$$

where p_1 is the power consumption in the local broadcasting phase, p_2 is the power consumption in the long-haul transmission phase, ϑ is the optimum fraction of time dedicated to the local broadcast channel and to the long-haul transmission channel. The transmission performance is further optimised from a judicious choice of p_1 , p_2 and ϑ . Meanwhile, the authors proposed a simplified sub-optimum time allocation with a negligible performance loss to obtain closed form expressions. Moreover, the per-hop minimum outage probability is obtained by searching for the optimum number of SCoops and RCoops. In the proposed CMIMO scheme, the spatial diversity converges to the product of the total number of antennas available for cooperation at both transmission and reception clusters. Simulation results have shown that the proposed scheme achieves spatial diversity equal to the equivalent MIMO system and significantly reduces energy consumption with respect to the non-cooperative system.

2.3 Methodology

This section introduces the node selection algorithms, and the relevant methodologies used to solve the node selection algorithms in this thesis.

2.3.1 Node Selection Algorithms

Node selection problem in wireless networks has been widely studied in many research areas including base station selection for mobile nodes [SB12], relays selection in routing protocols [AY05], camera sensors selection for target localization [LZM10], CHs selection in wireless sensor networks [TT10], cooperative devices selection in CMIMO system [HOKK12] and so on.

Evolutionary algorithms have been applied in node selection problems to meet certain requirement [DDCM02]. Due to its broad applicability, evolutionary algorithms have natural advantages in solving the node selection problems [Fog97]. Generally, evolutionary algorithms require a data structure to represent solutions, a performance index to evaluate solutions, and variation operators to generate new solutions from old solutions [LES08]. The search space of possible solutions can be disjoint and can encompass infeasible regions, and the performance index can be time varying [Lee05]. The human designer can choose a representation that follows their intuition. In this sense, the procedure is representation independent, in contrast with other numerical techniques which might be applicable for only continuous values or other constrained sets. Representation should allow for variation operators that maintain a behavioural link between parent and offspring. Small changes in the structure of a parent should lead to small changes in the resulting offspring, and likewise large changes should engender gross alterations.

Figure 2.5 shows an example of data structure to represent solutions. In this example, the binary string is used to represent one population, and each binary bit represents an individual of the potential candidate. In Figure 2.5, the first individual represents Node

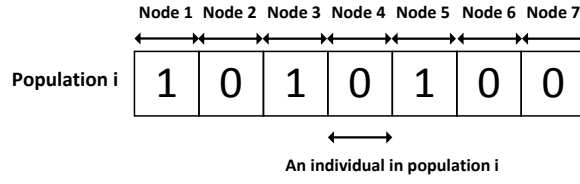


Figure 2.5: Population representation in evolutionary algorithms

1, and so on. Moreover, the value of the first individual that equals to 1 indicates Node 1 is selected, and the value of the second individual that equals to 0 indicates Node 2 is not selected. In this way, the optimum set of nodes can be selected by updating the value of individual in the following procedure [Bác96]:

- a) Generate the initial population of individuals randomly (first generation).
- b) Evaluate the fitness of each individual in that population.
- c) Repeat on this generation until termination (time limit, sufficient fitness achieved, etc.):
 - i. Select the best-fit individuals for reproduction (parents).
 - ii. Breed new individuals through crossover and mutation operations to give birth to offspring.
 - iii. Evaluate the individual fitness of new individuals.
 - iv. Replace least-fit population with new individuals.

A general flowchart of evolutionary algorithms is summarised in Figure 2.6 .

2.3.2 Quantum Particle Swarm Optimisation

QPSO is one of the evolutionary algorithms which introduces quantum coding mechanism into PSO [GCD11]. PSO models after the social behaviour of a flock of birds, which was proposed by Kennedy and Eberhart in 1995 [KE95]. It searches for the optima by

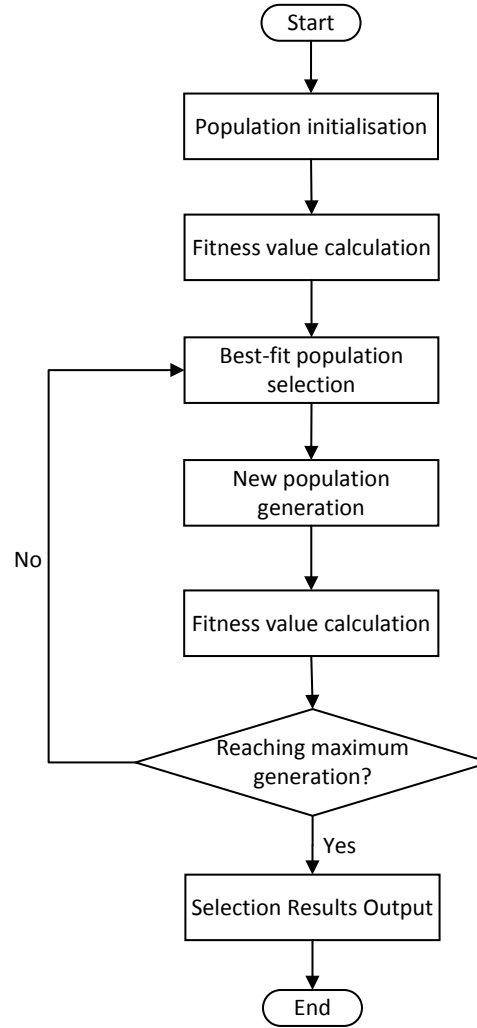


Figure 2.6: Flowchart of general evolutionary algorithm

updating generations. Besides, PSO and QPSO introduced the term “particle”, and each particle represents a solution to find the best particle with respect to a given fitness function.

Two QPSO algorithms have been proposed recently: qubit-based QPSO by [GCD11] and Ψ -based QPSO [SFX04]. Although both QPSO algorithms apply quantum coding mechanism, the procedures to encode and update the particles are different. Particularly, Ψ -based QPSO uses quantum delta potential well model to encode particles, while qubit-based QPSO uses quantum theory to encode each particle by quantum bit (qubit). Besides, Ψ -based QPSO adopts mean optimum position and local attractor to update

particles, while qubit-based QPSO adopts local optimum position and global optimum position to update particles. In this subsection, the qubit-based QPSO is described in detail and the performance of both QPSO algorithms are compared by benchmark functions.

2.3.2.1 Qubit-based Quantum Particle Swarm Optimization

There are three main parameters to update the particles in qubit-based QPSO, including quantum velocity, position and rotation angle. Quantum velocity indicates the moving speed of a particle in the search space and is represented by a string of qubits. Quantum position represents the location of the particle in the search space. Quantum rotation angle indicates the direction of a particle's movement. In addition, individual optimum and global optimum are another two parameters affecting the moving direction of particles. Individual optimum is a particle's individual best known position and fitness value in the search space, and the global optimum is the entire swarm's best known position and fitness value.

The updating process of quantum rotation angle, velocity, position, individual optimum and global optimum are shown in Figure 2.7.

A. Quantum Velocity

Qubit-based QPSO encodes each particle by a qubit for probabilistic representation [GCD11]. A qubit has a state, either '0' or '1', and is defined as a pair of composite numbers (α, β) , where $|\alpha|^2 + |\beta|^2 = 1$ and $\alpha > 0, \beta > 0$. $|\alpha|^2$ gives the probability that the quantum bit is found in '0' state and $|\beta|^2$ gives the probability that the quantum bit is found in '1' state. The quantum velocity of particle m at generation t is defined as

$$\mathbf{v}_m^t = \begin{bmatrix} \alpha_{m1}^t & \alpha_{m2}^t & \cdots & \alpha_{m\mathcal{R}}^t \\ \beta_{m1}^t & \beta_{m2}^t & \cdots & \beta_{m\mathcal{R}}^t \end{bmatrix} \quad (2.4)$$

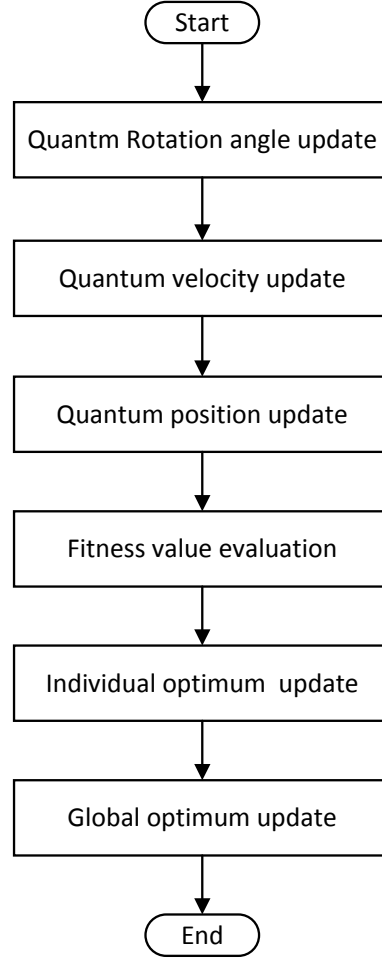


Figure 2.7: Qubit-based QPSO updating process

where $m \in [1, 2, \dots, \mathcal{N}_{particle}]$, $\mathcal{N}_{particle}$ is the number of particles and \mathcal{R} is the dimension of the research problem, i.e. the number of candidates to be selected. Since $\beta_{mn} = \sqrt{1 - \alpha_{mn}^2}$, (2.4) can be simplified as

$$\mathbf{v}_m^t = [\alpha_{m1}^t \quad \alpha_{m2}^t \quad \dots \quad \alpha_{m\mathcal{R}}^t] \quad (2.5)$$

The updated velocity of the quantum particle m at $t + 1$ generation is

$$v_{mn}^{t+1} = \begin{cases} \sqrt{1 - (v_{mn}^t)^2}, & \text{if } \theta_{mn}^{t+1} = 0 \text{ and } \delta < c_1 \\ \left| v_{mn}^t \cos \theta_{mn}^{t+1} - \sqrt{1 - (v_{mn}^t)^2} \sin \theta_{mn}^{t+1} \right|, & \text{otherwise} \end{cases} \quad (2.6)$$

where θ_{mn}^{t+1} is the rotation angle in generation $t + 1$ and can be obtained by (2.12), δ is a uniform random number between 0 and 1, and c_1 is a constant which refers to the mutation probability, $c_1 \in [0, 1/\mathcal{R}]$.

B. Quantum Position

The quantum particle position can be expressed as,

$$x_{mn}^t = \begin{cases} 1 & \text{if } \delta_{mn} > (v_{mn}^t)^2 \\ 0 & \text{if } \delta_{mn} \leq (v_{mn}^t)^2 \end{cases} \quad (2.7)$$

where $\delta_{mn} \in [0, 1]$ is a uniform random number between 0 and 1. The position of a particle represents a possible solution to a specific research problem, as indicated in Figure 2.5.

C. Individual Optimum and Global Optimum

In a single objective optimisation problem, the research objective can be either minimisation or maximisation.

In a minimisation problem, denote the fitness value of particle m at generation t to be f_m^t , the local individual optimum fitness value $f_m^{pbest_{min}}$ is defined as the minimum fitness value of particle m from the first generation to the current generation t , and the corresponding local individual optimum position $\mathbf{x}_m^{pbest_{min}}$ is defined as follows

$$\begin{aligned} f_m^{pbest_{min}} &= \min\{f_m^1, f_m^2, \dots, f_m^t\} \\ t_{min} &= \arg \min\{f_m^1, f_m^2, \dots, f_m^t\} \\ \mathbf{x}_m^{pbest_{min}} &= \mathbf{x}_m^{t_{min}} \end{aligned} \quad (2.8)$$

where t_{min} is the generation number for which attains the minimum fitness value.

The global optimum fitness value, denoted by $f^{gbest_{min}}$, is defined as the minimum local individual optimum fitness value of all particles, and the corresponding global

optimum position $\mathbf{x}^{gbest_{min}}$ is defined as below

$$\begin{aligned} f^{gbest_{min}} &= \min\{f_1^{pbest_{min}}, \dots, f_m^{pbest_{min}}, \dots, f_{N_{particle}}^{pbest_{min}}\} \\ m_{min} &= \arg \min\{f_1^{pbest_{min}}, \dots, f_m^{pbest_{min}}, \dots, f_{N_{particle}}^{pbest_{min}}\} \\ \mathbf{x}^{gbest_{min}} &= \mathbf{x}_{m_{min}}^{pbest_{min}} \end{aligned} \quad (2.9)$$

where m_{min} is the particle index for which attains the minimum fitness value of local individuals.

In a maximisation problem, the local individual optimum fitness value $f_m^{pbest_{max}}$ is defined as the maximum fitness value of particle m from the first generation to the current generation t , and the corresponding local individual optimum position $\mathbf{x}_m^{pbest_{max}}$ is defined as follows

$$\begin{aligned} f_m^{pbest_{max}} &= \max\{f_m^1, f_m^2, \dots, f_m^t\} \\ t_{max} &= \arg \max\{f_m^1, f_m^2, \dots, f_m^t\} \\ \mathbf{x}_m^{pbest_{max}} &= \mathbf{x}_m^{t_{max}} \end{aligned} \quad (2.10)$$

where t_{max} is the generation number for which attains the maximum fitness value.

The global optimum fitness value, denoted by $f^{gbest_{max}}$, is defined as the maximum local individual optimum fitness value of all particles, and the corresponding global optimum position $\mathbf{x}^{gbest_{max}}$ is defined as below

$$\begin{aligned} f^{gbest_{max}} &= \max\{f_1^{pbest}, \dots, f_m^{pbest}, \dots, f_{N_{particle}}^{pbest}\} \\ m_{max} &= \arg \max\{f_1^{pbest_{max}}, \dots, f_m^{pbest_{max}}, \dots, f_{N_{particle}}^{pbest_{max}}\} \\ \mathbf{x}^{gbest_{max}} &= \mathbf{x}_{m_{max}}^{pbest_{max}} \end{aligned} \quad (2.11)$$

where m_{max} is the particle index for which attains the maximum fitness value of local individuals.

D. Quantum Rotation Angle

At generation $t + 1$, the quantum rotation angle θ_{mn}^{t+1} is updated by

$$\theta_{mn}^{t+1} = k_1(x_{mn}^{pbest} - x_{mn}^t) + k_2(x_{mn}^{gbest} - x_{mn}^t) \quad (2.12)$$

where k_1 and k_2 are two positive learning factors of cognitive and social acceleration, respectively. The cognitive acceleration factor k_1 represents the attraction that a particle has toward its individual success and the social acceleration factor k_2 represents the attraction that a particle has toward the success of its neighbours.

2.3.2.2 Ψ -based Quantum Particle Swarm Optimization

According to [SFX04], wave function ($\Psi(\cdot)$) based QPSO is comprised of three parts: mean optimum position at generation t (\mathbf{mp}^t), local attractor at generation t (\mathbf{l}_m^t) and evolutionary equation at generation $t + 1$ (\mathbf{x}_m^{t+1}). Denote the local individual optimum position to be \mathbf{p}_m^t and the global optimum position to be \mathbf{p}_g^t at generation t . Assume the number of particles is $\mathcal{N}_{particle}$, mp_n^t is determined by the states of the p_{mn}^t where $m \in [1, 2, \dots, \mathcal{N}_{particle}]$, $n \in [1, 2, \dots, \mathcal{R}]$ where \mathcal{R} is the dimension of research problem,

$$mp_n^t = \begin{cases} 1, & \text{if } \sum_{m=1}^{\mathcal{R}} p_{mn}^t > \frac{\mathcal{R}}{2} \quad \text{or} \quad \left(\sum_{m=1}^{\mathcal{R}} p_{mn}^t = \frac{\mathcal{R}}{2} \quad \text{and} \quad \delta < 0.5 \right) \\ 0, & \text{if } \sum_{m=1}^{\mathcal{R}} p_{mn}^t < \frac{\mathcal{R}}{2} \quad \text{or} \quad \left(\sum_{m=1}^{\mathcal{R}} p_{mn}^t = \frac{\mathcal{R}}{2} \quad \text{and} \quad \delta \geq 0.5 \right) \end{cases} \quad (2.13)$$

where δ is a uniform random number in the range 0 and 1.

The local attractor \mathbf{l}_m^t is generated from \mathbf{p}_m^t and \mathbf{p}_g^t by single-point crossover or multipoint crossover technique. Figure 2.8 shows an example of single-point crossover process. The process is as follows:

- a) Randomly selected the crossover point in the range of 1 and R .
- b) Generate two offspring $\mathbf{l}_m^t(1)$ and $\mathbf{l}_m^t(2)$ from \mathbf{p}_m^t and \mathbf{p}_g^t at the selected crossover

point.

- c) Randomly select one offspring from $\mathbf{I}_m^t(1)$ and $\mathbf{I}_m^t(2)$ as \mathbf{I}_m^t .

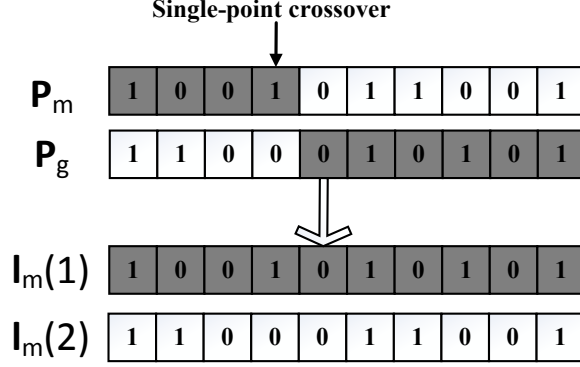


Figure 2.8: Single-point crossover to get local attractor

The evolutionary equation is given by

$$d_H [x_{mn}^{t+1}, l_{mn}^t] = \varpi d_H [x_{mn}^t, mp^t] \ln \frac{1}{\delta} \quad (2.14)$$

where $d_H [y_1, y_2]$ is the hamming distance between two binary string y_1 and y_2 , ϖ is contraction expansion coefficient, and δ is a random variable between 0 and 1. (2.14) can be regarded as the procedure of inverting the value of every bit in l_m^t with an inverse probability \mathcal{P}_{inv} , where

$$\mathcal{P}_{inv}^{t+1} = \begin{cases} \varpi d_H [x_{mn}^t, mp^t] \ln \frac{1}{\delta}, & \text{if } \varpi d_H [x_{mn}^t, mp^t] \ln \frac{1}{\delta} < 1 \\ 1, & \text{otherwise} \end{cases} \quad (2.15)$$

Assume all bits in the same decision variable have the same inverse probability, then the position of m -th particle at generation $t + 1$ can be obtained according to (2.14),

$$x_{mn}^{t+1} = \begin{cases} l_{mn}^t, & \text{if } \delta > \mathcal{P}_{inv}^{t+1} \\ Rev^{-1}(l_{mn}^t), & \text{if } \delta \leq \mathcal{P}_{inv}^{t+1} \end{cases} \quad (2.16)$$

where δ is a random number between 0 and 1 and $Rev^{-1}(\cdot)$ is the inverse equation of

binary string.

2.3.2.3 Other Reference Evolutionary Algorithms

PSO [LTS07] and QGA [GSDL14] are selected as the reference algorithms in this thesis. In particular, PSO is selected as a reference algorithm to verify that quantum coding is a better way to encode particles compared with the axis coding of PSO, because QPSO introduces quantum coding into PSO. QGA applies quantum coding and quantum rotation gate to update the population. QGA is adopted as a reference algorithm to demonstrate that the particle updating process of QPSO is more effective.

A. Particle swarm optimisation

Similar to qubit-based QPSO, the particle velocity and position are two main parameters in PSO. The updated velocity of particle m at the $t + 1$ generation is,

$$v_m^{t+1} = \omega \times v_m^t + c_1 \delta_1 \times (x_{mn}^{pbest} - x_{mn}^t) + c_2 \delta_2 \times (x^{gbest} - x_{mn}^t) \quad (2.17)$$

where ω is the inertia weight, c_1 and c_2 are two learning factors, δ_1 and δ_2 are random numbers between 0 and 1, x_{mn}^{pbest} is the local individual optimum of particle m , x^{gbest} is the global optimum of all particles, and x_{mn}^t is the particle position for particle m at generation t . The local individual optimum x_{mn}^{pbest} and the global optimum x^{gbest} are defined as the same as qubit-based QPSO.

The updated position of particle m at generation $t + 1$ is,

$$x_{mn}^{t+1} = x_{mn}^t + v_{mn}^{t+1} \quad (2.18)$$

After updating the particles, the position of particles are mapped with the closet (x, y) coordinate in a specific research problem [SBY⁺12].

B. Quantum genetic algorithm

The quantum genetic algorithm applies quantum gates to update the position of particles. The quantum rotation gate \mathbb{G}_{mn}^t of particle m at generation t is chosen as quantum logic gate and is expressed as

$$\mathbb{G}_{mn}^t = \begin{bmatrix} \cos\theta_{mn}^t & -\sin\theta_{mn}^t \\ \sin\theta_{mn}^t & \cos\theta_{mn}^t \end{bmatrix} \quad (2.19)$$

where θ_{mn}^t is a pre-determined parameter which represents the rotation angle of the quantum rotation gate for particle m at generation t .

The updated position of chromosome m at generation $t + 1$ is,

$$x_{mn}^{t+1} = \mathbb{G}_{mn}^t \times x_{mn}^t \quad (2.20)$$

The position of a chromosome represents a possible solution to a specific research problem, as indicated in Figure 2.5.

2.3.2.4 Performance Evaluation of Evolutionary Algorithms

The performance of qubit-based QPSO algorithm is evaluated by the Rastrigin function and the Griewank function, which have been employed as benchmark functions for global optimisation algorithms. In this subsection, the Rastrigin function is employed to evaluate the convergence rate, while the Griewank function is used to measure the convergence value.

The Rastrigin function [Dic06] is defined as follows

$$F_1(\mathbf{x}) = \sum_{i=1}^n (x_i^2 - 10 \cos(2\pi x_i) + 10) \quad (2.21)$$

where $\mathbf{x} = \{x_1, \dots, x_i, \dots, x_n\}$ and $-5.12 \leq x_i \leq 5.12$. According to [GGP⁺15], the Rastrigin function is a typical example of non-linear multi-modal function, and its minimum value is 0 and all the local minima are regularly distributed.

The Griewank function [Dic06] is defined as follows

$$F_2(\mathbf{x}) = \frac{1}{4000} \left(\sum_{i=1}^n (x_i - 100)^2 \right) - \left(\prod_{i=1}^n \cos \left(\frac{x_i - 100}{\sqrt{i}} \right) \right) + 1 \quad (2.22)$$

where $\mathbf{x} = \{x_1, \dots, x_i, \dots, x_n\}$ and $-600 \leq x_i \leq 600$. The global minimum value of Griewank function is 0 and the global minimum is located in the origin. The Griewank function also has a huge number of local minima with regular distribution, which indicates that an optimisation algorithm can easily be trapped in a local optimum on its way toward the global optimum. The Griewank function is similar to the Rastrigin function, but the number of local optimum of Griewank function is larger.

Matlab is used as the simulation tool. The simulation process is comprised of 50 simulation iterations for both proposed and references algorithms. In the following simulation, binary strings are used to encode the input \mathbf{x} of the benchmark functions. For simplification, set the size of \mathbf{x} to be 2. Denote the two input variables to be x_1 and x_2 with the length of 15 bits each. Following steps are executed through Matlab (2.21) and (2.22) through the two 15-bit binary numbers:

- a) Convert the 15 bits binary numbers to decimal numbers according to the number base conversion method [CADM91]. Denote the converted decimal number to be χ_i , where $i = 1, 2$.
- b) Convert the decimal number into the pre-defined range, i.e. $[-5.12, 5.12]$ for (2.21) and $[-600, 600]$ for (2.22). Denote the pre-defined range to be $[R_{min}, R_{max}]$, the decimal number in the pre-defined range can be obtained by $x_i = R_{min} + \frac{R_{max} - R_{min}}{2^{15} - 1} \cdot \chi_i$, where $i = 1, 2$.
- c) Obtain the Rastrigin function value and Griewank function value by substituting the set of input variables \mathbf{x} into (2.21) and (2.22), respectively, where $\mathbf{x} = \{x_1, x_2\}$.

In addition, the qubit-based QPSO is compared with another three evolutionary algorithms: Ψ -based QPSO [SFX04], PSO [LTS07] and QGA [GSDL14]. For qubit-

based QPSO, Ψ -based QPSO, PSO and QGA algorithms, the population size $\mathcal{N}_{particle}$ is set to be 20, the dimension of particle \mathcal{R} is set to be 30 for two 15 bits input variables. In terms of PSO, the two acceleration coefficients are 2 and velocity limitation is 4. As for QGA, the rotation angle of quantum gates decreases linearly from 0.1π at the first generation to 0.005π at the last generation.

Figure 2.9 evaluates the convergence rate of the four evolutionary algorithms. It can be seen that both qubit-based QPSO and Ψ -based QPSO can achieve the same convergence value after 400 generations, while PSO and QGA both get trapped in one of the local optima, due to their less effective generation updating process.

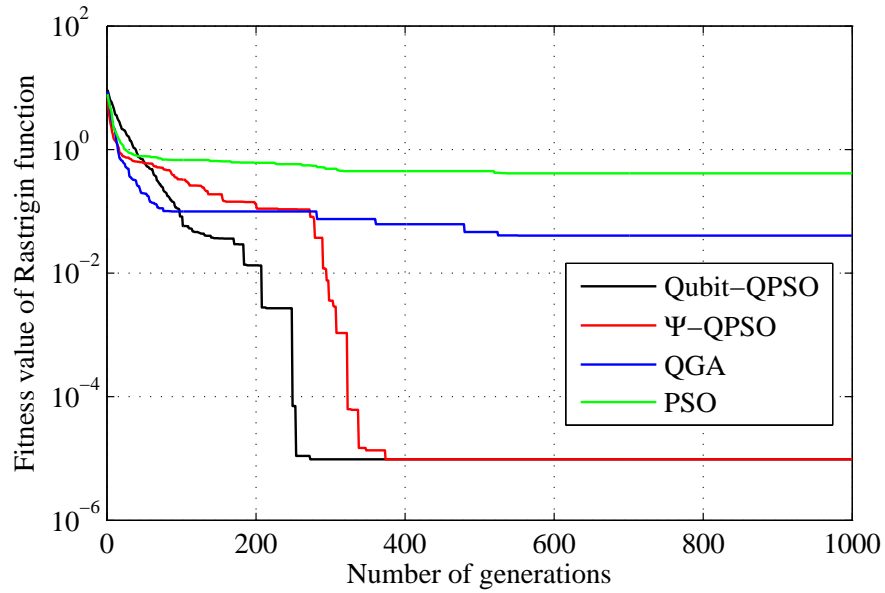


Figure 2.9: Number of generations versus fitness value of Rastrigin function

Figure 2.10 shows the convergence value of the four evolutionary algorithms. The qubit-based QPSO outperforms other algorithms by fast convergence rate and more accurate convergence value. Considering the fact that the Griewank function has more number of local optima compared with the Rastrigin function, the result suggests that the qubit-based QPSO has better capacity in getting out of local optimum.

The computational complexity of evolutionary algorithms depends on the size of pop-

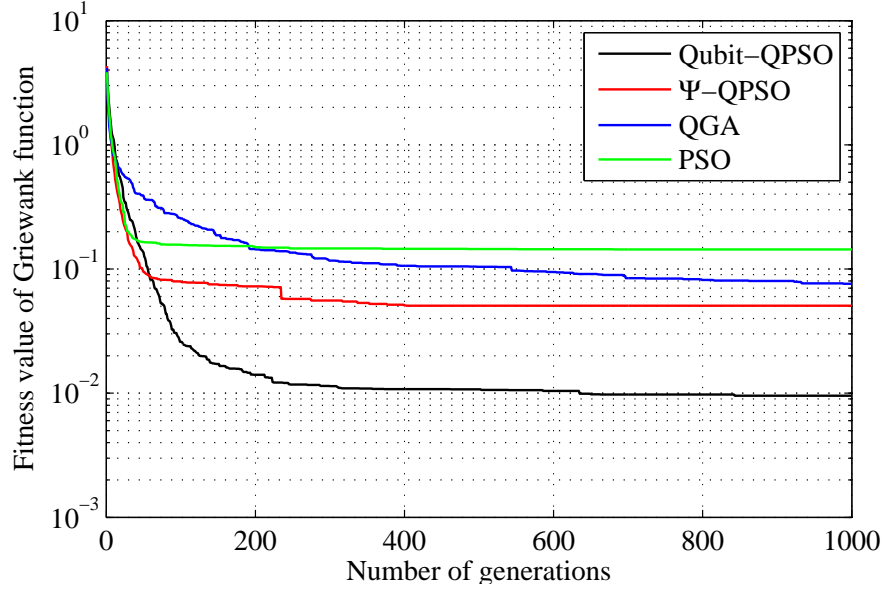


Figure 2.10: Number of generations versus fitness value of Griewank function

ulation $\mathcal{N}_{particle}$ and the dimension of research problem (\mathcal{R}) [Sud08], that is, $O(\mathcal{R}\mathcal{N}_{particle})$ for PSO, QGA, qubit-based QPSO and Ψ -based QPSO.

Although PSO, QGA, qubit-based QPSO and Ψ -based QPSO are of the same computational complexity, the qubit-based QPSO is proved to be more competitive with other three algorithms by employing better evolutionary equations and simpler updating equations. It can be seen from Figure 2.9 that qubit-based QPSO outperforms PSO, QGA and Ψ -based QPSO in terms of convergence rate. Furthermore, although Ψ -based QPSO and qubit-based QPSO both applies quantum computing and swarm intelligence, Figure 2.10 proved that qubit-based QPSO outperforms PSO, QGA and Ψ -based QPSO in terms of more accurate convergence value. Therefore, the qubit-based QPSO is adopted as the algorithm to solve the CHs and cooperative nodes selection algorithms in the following chapters. Also, the term “QPSO” is used to represent “qubit-based QPSO” for simplification in the following chapters.

2.3.3 Multi-objective Optimisation

2.3.3.1 Definition of Multi-objective Optimisation

A general multi-objective optimisation problem consists of a number of objectives and is associated with a number of inequality and equality constraints [DK01]. Mathematically, the problem can be written as follows

$$\begin{aligned}
 & \text{Minimise/Maximise} \quad f_i(\mathbf{x}) \quad i = 1, 2, \dots, N \\
 & \text{Subject to} \quad g_j(\mathbf{x}) \leq 0 \quad j = 1, 2, \dots, \mathcal{J} \\
 & \quad \quad \quad h_k(\mathbf{x}) = 0 \quad k = 1, 2, \dots, \mathcal{K}
 \end{aligned} \tag{2.23}$$

The parameter \mathbf{x} uses a p dimensional vector having p design or decision variables. Solutions to a multi-objective optimisation problem are mathematically expressed in terms of non-dominated or superior points, known as Pareto-optimal solutions.

As referred to [CEC05], a vector $\mathbf{x} = [x_1, x_2, \dots, x_p]^T$ is said to dominate $\mathbf{y} = [y_1, y_2, \dots, y_p]^T$ in a maximisation problem, denoted by $\mathbf{x} \succ \mathbf{y}$, if $\forall i \in \{1, 2, \dots, p\} : x_i \geq y_i$ and $\exists i \in \{1, 2, \dots, p\} : x_i > y_i$. That is, no value in \mathbf{y} is more than \mathbf{x} and at least one value of \mathbf{x} is strictly greater than \mathbf{y} .

Similarly, a solution \mathbf{x}^* is said to dominate \mathbf{x} in a multi-objective maximisation problem, if $\forall i \in \{1, 2, \dots, M\} : f_i(\mathbf{x}^*) \geq f_i(\mathbf{x})$ and $\exists i \in \{1, 2, \dots, M\} : f_i(\mathbf{x}^*) > f_i(\mathbf{x})$. That is, a solution \mathbf{x}^* is Pareto optimal if there exists no feasible solution \mathbf{x} which would increase some criteria without causing a simultaneous decrease in at least other criterion. It also applies for the multi-objective minimisation research problem.

Classical optimisation methods suggest converting the multi-objective optimisation problem to a single-objective optimisation problem by emphasizing one particular Pareto-optimal solution at a time [BS13]. However, one Pareto-optimal solution cannot be said to be better than the other. This demands a user to find as many Pareto-optimal solutions as possible. The non-dominated sorting Genetic algorithm-II (NSGA-II) [DPAM02]

is proposed to be an effective algorithm to find these Pareto optimal solutions.

2.3.3.2 Non-dominated Sorting Genetic Algorithm II

NSGA-II applies a fast non-dominated sorting procedure to sort a population into different non-domination levels, a fast crowded distance estimation procedure to get an estimate of the density of solutions surrounding a particular solution in the population, and a crowded-comparison operator to guide the selection process toward a uniformly spread-out Pareto-optimal front.

A. Fast Non-dominated Sorting

In NSGA-II, each solution has two entities:

- n_p , the domination count which is defined as the number of solutions which dominate individual p .
- S_p , which is the set containing all the individuals that are being dominated by p .

In fast non-dominated sorting, all solutions in the first non-dominated front will have their domination count as zero. For each solution p with $n_p = 0$, visit each member (q) of its set S_p and reduce its domination count by one. In doing so, if for any member q the domination count becomes zero, put it in a separate list \mathcal{Q} . These members belong to the second non-dominated front. Now, the above procedure is continued with each member of \mathcal{Q} and the third front is identified. This process continues until all fronts are identified. The execution process of fast non-dominated sorting is summarised in Algorithm 1.

B. Fast Crowded Distance Estimation

Crowded distance is proposed to maintain the diversity among population members.

Algorithm 1: non-dominated sorting

Input: A set of solutions \mathbb{P}

```

1 for each  $p \in \mathbb{P}$  do
2    $\mathcal{S}_p = \emptyset$ 
3    $n_p = 0$ 
4   for each  $q \in \mathbb{P}$  do
5     if  $p \prec q$  then
6       /* if  $p$  dominates  $q$  */
7        $\mathcal{S}_p = \mathcal{S}_p \cup \{q\}$ 
8       else if  $q \prec p$  then
9          $n_p = n_p + 1$ 
10      end
11    end
12  if  $n_p = 0$  then
13    /*  $p$  belongs to the first front  $\mathcal{F}_1$  */
14     $p_{rank} = 1$ 
15     $\mathcal{F}_1 = \mathcal{F}_1 \cup \{p\}$ 
16  end
17 end
18 /* Initialise the front counter */
19  $i = 1$ 
20 while  $\mathcal{F}_i \neq \emptyset$  do
21   /*  $\mathcal{Q}$  is used to store members of the next front */
22    $\mathcal{Q} = \emptyset$ 
23   for each  $p \in \mathcal{F}_i$  do
24     for each  $q \in \mathcal{S}_p$  do
25        $n_q = n_q - 1$ 
26       /*  $q$  belongs to the next front */
27       if  $n_q = 0$  then
28          $q_{rank} = i + 1$ 
29          $\mathcal{Q} = \mathcal{Q} \cup \{q\}$ 
30       end
31     end
32   end
33    $i = i + 1$ 
34    $\mathcal{F}_i = \mathcal{Q}$ 
35 end
36 return the set of all fronts  $\mathcal{F}$ 

```

The crowded distance is the average distance of two points along each of the objectives. The crowded distance computation requires sorting the population according to each objective value in ascending order of magnitude for every front. Therefore, for

each objective function, the boundary solutions, i.e. solutions with smallest and largest function values, are assigned an infinite distance value. All other intermediate solutions are assigned a distance value equal to the absolute normalized difference in the function values of two adjacent solutions. The calculation is continued with other objective functions. The overall crowded distance value is calculated as the sum of individual distance values corresponding to each objective. The process of fast crowded distance estimation is summarised in Algorithm 2.

Algorithm 2: Crowded distance assignment

```

Input: Front  $\mathcal{L}$ 
/* Set  $l$  to be the number of solutions in front  $\mathcal{L}$  */
1 for  $i \in \{1, 2, \dots, l\}$  do
2   |  $\mathcal{L}_{distance}(i) = 0$ 
3 end
/* Set  $N_{obj}$  to be the number of objectives */
4 for  $m \in \{1, 2, \dots, N_{obj}\}$  do
5   | /* Sort  $\mathcal{L}$  in descending order */
6   |  $\mathcal{L}_{sort} = \text{sort}(\mathcal{L}, m)$ 
7   | /* Set the distance of boundary points to be infinity so that
8   |   they are always selected */
9   |  $\mathcal{L}_{sort}^{distance}(1) = \mathcal{L}_{sort}^{distance}(l) = \infty$ 
10  | for  $i \in \{2, \dots, l-1\}$  do
11  |   |  $\mathcal{L}_{sort}^{distance}(i) = \mathcal{L}_{sort}^{distance}(i) + \frac{\mathcal{L}_{sort}^{distance}(i+1).m - \mathcal{L}_{sort}^{distance}(i-1).m}{f_m^{max} - f_m^{min}}$ 
12  |   end
13 end
14 return the crowded distance  $\mathcal{L}_{sort}^{distance}$  of all solutions in front  $\mathcal{L}$ 

```

C. Crowded-comparison Operator

The crowded-comparison operator, denoted by \prec_n , guides the selection process at the various stages of the algorithm toward a uniformly spread-out Pareto-optimal front. Assume that every individual i in the population has two attributes:

- Non-domination rank, denoted by i_{rank} .
- Crowded distance, denoted by $i_{distance}$.

The crowded-comparison operator is defined as below

$$i \prec_n j, \quad \text{if } (i_{rank} < j_{rank}) \text{ or } [(i_{rank} = j_{rank}) \text{ and } (i_{distance} > j_{distance})] \quad (2.24)$$

That is, between two solutions with differing non-domination ranks, the solution with the lower (better) rank is preferred. Otherwise, if both solutions belong to the same front, then the solution that is located in a less crowded region is preferred.

D. Main Loop of NSGA-II

In NSGA-II algorithm, first, a combined population $\mathcal{Z}_t = \mathcal{P}_t \cup \mathcal{Q}_t$ is formed, where \mathcal{P}_t is the parent population and \mathcal{Q}_t is the offspring population. Assume the population size of \mathcal{P}_t is \mathcal{N}_{pop} , then combined population \mathcal{Z}_t is of size $2\mathcal{N}_{pop}$. Then, the population \mathcal{Z}_t is sorted according to non-domination. Since all parent and offspring population members are included in \mathcal{Z}_t , elitism is ensured. Solutions belonging to the best non-dominated set \mathcal{F}_1 are of best solutions in the combined population and must be emphasized more than any other solution in the combined population. If the size of \mathcal{F}_1 is smaller than \mathcal{N}_{pop} , all members of the set \mathcal{F}_1 are selected for the new population \mathcal{P}_{t+1} . The remaining members of the population \mathcal{P}_{t+1} are chosen from subsequent non-dominated fronts in the order of their ranking. Thus, solutions from the set \mathcal{F}_2 are chosen next, followed by solutions from the set \mathcal{F}_3 , and so on. This procedure is continued until no more sets can be accommodated. Say that the set \mathcal{F}_l is the last non-dominated set beyond which no other set can be accommodated. In general, the count of solutions in all sets from \mathcal{F}_1 to \mathcal{F}_l would be larger than the population size. To choose exactly \mathcal{N}_{pop} population members, solutions of the last front \mathcal{F}_l is sorted using the crowded-comparison operator \prec_n in descending order and choose the best solutions needed to fill all population slots. The main loop of NSGA-II is summarised in Algorithm 3.

Algorithm 3: Main Loop of NSGA-II

Input: Patent population \mathcal{P}_t and offspring population \mathcal{Q}_t

```

1  $\mathcal{Z}_t = \mathcal{P}_t \cup \mathcal{Q}_t$ 
2 Get the non-dominated fronts  $\mathcal{F}$  by executing Algorithm 1 and taking  $\mathcal{Z}_t$  as input
3 Set  $\mathcal{P}_{t+1} = \emptyset$  and  $i = 1$ 
  /* Loop ends when the parent population is filled */
4 while  $|\mathcal{P}_{t+1}| + |\mathcal{F}_i| \leq \mathcal{N}_{pop}$  do
5   Get  $\mathcal{F}_i^{distance}$  by executing Algorithm 2 and taking  $\mathcal{F}_i^{distance}$  as input
6    $\mathcal{P}_{t+1} = \mathcal{P}_{t+1} \cup \mathcal{F}_i^{distance}$ 
7    $i = i + 1$ 
8 end
  /* Sort in descending order using  $\prec_n$  */
9 Sort( $\mathcal{F}_i, \prec_n$ )
  /* Choose the first  $(\mathcal{N}_{pop} - |\mathcal{P}_{t+1}|)$  elements of  $\mathcal{F}_i^{distance}$  */
10  $\mathcal{P}_{t+1} = \mathcal{P}_{t+1} \cup \mathcal{F}_i^{distance} [1 : (\mathcal{N}_{pop} - |\mathcal{P}_{t+1}|)]$ 
11 Get  $\mathcal{Q}_{t+1}$  by executing evolutionary algorithms, e.g. genetic algorithm and taking
     $\mathcal{P}_{t+1}$  as input
12 return Offspring population  $\mathcal{Q}_{t+1}$ 

```

2.4 Summary

In this chapter, Section 2.1 provided an overview of the architecture of capillary networks in IoT networks. Clustering protocol and cooperative communications were also introduced to improve the network performance of capillary networks in this section. Also, the existing research outcomes on clustering and cooperative communications were surveyed and categorised according to different performance metrics in Section 2.2. In clustering and cooperative communications, how to select the CHs and cooperative coalitions in the long-haul transmission are important node selection problems. Thereby, an overview of node selection algorithms was given special attention in Section 2.3. To solve the node selection problem, QPSO algorithm was adopted as the methodology and was described in detail. Moreover, Section 2.3 also presented NSGA-II as the tool to address the multi-objective optimisation problem in this thesis.

Chapter 3

CHs Selection for the Capillary Networks

This chapter focuses on the CHs selection in cluster-based capillary networks. The system model for cluster-based capillary networks is presented, followed by the energy consumption model. The cluster-based energy efficiency problem is formulated into the CHs selection aiming at network lifetime maximisation. Following this, the clustering scheme and proposed CHs selection algorithm using QPSO algorithm are presented. The simulation platform, numerical simulation results and conclusions are given at last.

3.1 System Model

In this chapter, the system model considers the capillary networks for IoT platform with \mathcal{N}_{total} power-constrained wireless devices. All wireless devices are classified into CHs and non-CH devices (i.e. CMs in this chapter), as shown in Figure 3.1. Denote the number of CHs in the network to be \mathcal{N}_{CH} and the number of CMs belongs to CH i to be n_i , thus $\mathcal{N}_{total} = \mathcal{N}_{CH} + \sum_{i=1}^{\mathcal{N}_{CH}} n_i$.

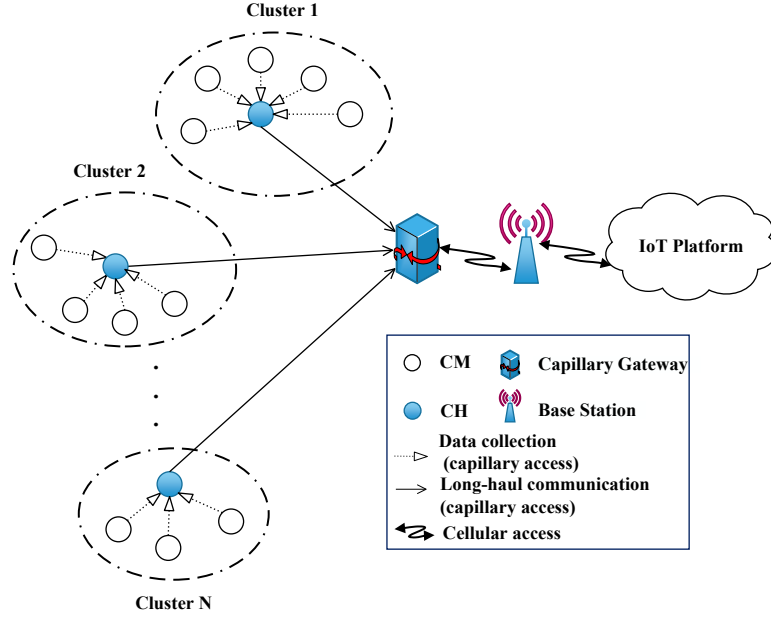


Figure 3.1: System model for clustering in capillary networks

All devices are randomly distributed over the capillary networks with following assumptions:

- \mathcal{N}_{total} wireless devices perform data collection task periodically and always have data to send to the capillary gateway. The data collected by every device is of the same size that is denoted by L_{data} and the data type is delay-insensitive.
- \mathcal{N}_{total} wireless devices are homogeneous and energy constrained.
- \mathcal{N}_{total} wireless devices are capable of adjusting their transmit powers dynamically to reach the intended recipients with the minimum required energy consumption.
- \mathcal{N}_{total} wireless devices are aware of their geographical locations and residual energies.
- \mathcal{N}_{total} wireless devices are equipped with short-range local area wireless radio, e.g. IEEE 802.15.4.
- \mathcal{N}_{total} wireless devices are capable to perform as either CH or CM.

- \mathcal{N}_{total} devices are capable of operating in data collection and aggregation mode.
- Uniform data aggregation is adopted as the aggregation scheme, where the amount of data after aggregation in every cluster is fixed as a constant [HOKK12].
- M -ary Quadrature Amplitude Modulation ($MQAM$) is adopted as the modulation scheme. $MQAM$ is a modulation scheme where data bits select one of M combinations of amplitude and phase shifts that are applied to the carrier wave [Das10].
- The intra-cluster communications within the cluster is modelled by the Additive White Gaussian Noise (AWGN) channel with squared power path loss.
- The long-haul transmission between CHs and the capillary gateway is modelled by the frequency-nonselective and slow Rayleigh fading.
- The energy consumption of signalling communications are omitted, compared to the energy consumption on large amount of data packets.
- A static capillary gateway is equipped with two radio interfaces: the local area capillary radio to communicate with the capillary networks and the cellular radio to communicate with the IoT platform through the base station. The energy consumption on capillary gateway is omitted.

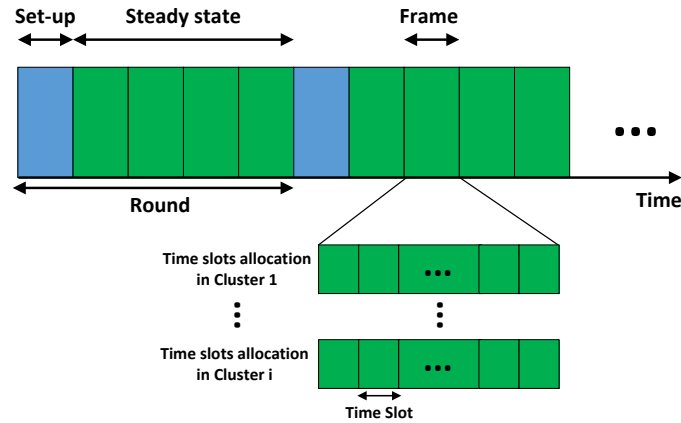


Figure 3.2: Transmission structure in cluster-based capillary networks

Similar to the communication protocol in LEACH [HCB00], the operation is broken

up into rounds. As shown in Figure 3.2, the transmission is operated in two phases of one round:

- Set-up phase. During the set-up phase, the gateway executes the clustering algorithm and informs every device with its role.
- Steady state phase. The steady state phase consists of several time frames. Each time frame operates the time division multiple access (TDMA) scheduling. In one time frame, every CM is allocated with a time slot to collect and transmit data to its CH. Also, every CH is allocated with a time slot to aggregate all data from its CMs and transmit the aggregated data to the capillary gateway. During one frame, every cluster performs intra-cluster data transmission simultaneously based on its own TDMA scheduling.

Denote the duration of one time frame to be t_Δ and the time frame number of the steady state phase in one round to be \mathcal{N}_{frame} . In general, compared with the duration of the steady state phase, the duration of set-up phase is much shorter, which can be omitted, therefore the time duration of one round is $T_{round} = t_\Delta \times \mathcal{N}_{frame}$.

3.2 Energy Consumption Model

In this thesis, the power consumption model is as specified in [CGB04]. The total power consumption along the single path can be divided into two main components: power consumption of power amplifiers P_{PA} and power consumption of all other circuit blocks P_c .

The power consumption of power amplifiers is linearly dependant on the transmit power P_t . Then the power consumption per link is expressed as

$$P = P_{PA} + P_c = (1 + \varphi_{amp})P_t + P_c \quad (3.1)$$

where $\varphi_{amp} = \xi/\eta - 1$ with η being the drain efficiency of the radio frequency power amplifier, and ξ being the peak-to-average ratio (PAR), which is dependent on the modulation scheme and the associated constellation size. In MQAM coded communication, $\xi = 3(M - 2\sqrt{M} + 1)/(M - 1)$.

Denote the number of transmitters and receivers to be \mathcal{N}_t and \mathcal{N}_r respectively, the circuit power consumption P_c is given by

$$P_c \approx \mathcal{N}_t(P_{DAC} + P_{mix} + P_{filt}) + 2P_{syn} + \mathcal{N}_r(P_{LNA} + P_{mix} + P_{IFA} + P_{filr} + P_{ADC}) \quad (3.2)$$

where P_{DAC} , P_{mix} , P_{filt} , P_{syn} , P_{LNA} , P_{IFA} , P_{filr} and P_{ADC} are the power consumption values of the D/A converter, the mixer, the active filters at the transmitter side, the frequency synthesizer, the low noise amplifier, the intermediate frequency amplifier, the active filters at the receiver side and the A/D converter at the receiver side, respectively. P_c is composed of the transmitter circuit blocks power consumption, denoted by P_{ct} , and the receiver circuit blocks power consumption, denoted by P_{cr} .

In the MQAM coded connection, the transmit power P_t in (3.1) is expressed according to the link budget relationship as follows

$$P_t = \frac{(4\pi)^2 M_l N_r}{G_t G_r \lambda^2} \cdot R_b \cdot \frac{\bar{E}_b}{N_0} \cdot d^\kappa \quad (3.3)$$

where d is the distance between the transmitter and the receiver, κ is the channel path loss exponent, G_t and G_r are the transmitter and receiver antenna gains, respectively, M_l is the link margin which indicates the difference between the receiver sensitivity and the actual received power, N_r is the single-sided power spectral density of the receiver noise, λ is the carrier wavelength, \bar{E}_b/N_0 is the normalized average energy per bit required for a given BER specification to the noise spectral density (also known as SNR per bit), R_b is the bit rate for MQAM and $R_b = B_{band} \cdot \log_2 M$ with B_{band} to be the modulation bandwidth.

The average \bar{E}_b/N_0 of the intra-cluster communication with a square constellation MQAM in AWGN channel [DZ04] is given by

$$\left. \frac{\bar{E}_b}{N_0} \right|_{intra} \doteq \frac{M-1}{3 \log_2 M} \cdot \left[Q^{-1} \left(\frac{\bar{P}_{BER}^{intra} \log_2 M}{4(1-1/\sqrt{M})} \right) \right]^2 \quad (3.4)$$

where $Q(x) = \int_x^\infty \frac{1}{\sqrt{2\pi}} e^{-\frac{u^2}{2}} du$ and \bar{P}_{BER}^{intra} is the average BER of intra-cluster communication.

The average \bar{E}_b/N_0 of the inter-cluster communication with a square constellation MQAM in Rayleigh fading channel [ZD07] is given by

$$\left. \frac{\bar{E}_b}{N_0} \right|_{inter} \doteq \frac{2(M-1)}{3 \log_2 M} \cdot \left[\left(\frac{(1-1/\sqrt{M})}{\bar{P}_{BER}^{inter} \log_2 M} \right) - 1 \right] \quad (3.5)$$

where \bar{P}_{BER}^{inter} is the average BER of inter-cluster communication.

The energy consumption per bit of the source device consists of the energy consumption on power amplifier block and the transmitter circuit block, which is expressed as follows

$$E_{bt} = (1 + \varphi_{amp}) \frac{P_t}{R_b} + \frac{P_{ct}}{R_b} \quad (3.6)$$

On the other hand, when a destination device receives data from a source device, the receiver circuit block dissipates energy. Therefore, the energy consumption per bit of the destination device is

$$E_{br} = \frac{P_{cr}}{R_b} \quad (3.7)$$

3.3 Energy Efficiency Problem Formulation

In this section, the energy consumption of the intra-cluster communication, data aggregation and inter-cluster communication in one round are formulated. Following this, the individual device lifetime and network lifetime are derived. The research problem of

network lifetime maximisation in this chapter is given at last.

3.3.1 Energy Consumption in Intra-cluster Communication

Intra-cluster communication operates in data collection phase within the clusters. In every time frame, each CM transmits data to its CH in its allocated time slots. Denote the current round to be r . In cluster i , the overall energy consumption includes the transmission energy consumption of n_i^r CMs to send the collected data to CH i and the overall reception energy consumption of CH i to receive data from n_i^r CMs. Thus the overall intra-cluster energy consumption for the i -th cluster in round r , denoted by $E_{intra}^r(i)$, is expressed as

$$\begin{aligned} E_{intra}^r(i) &= L_{data} \left(\sum_{j=1}^{n_i^r} E_{bt}^r(j) + n_i^r E_{br}^r(i) \right) \\ &= L_{data} \left(\sum_{j=1}^{n_i^r} \left[(1 + \varphi_{amp}) \cdot \frac{(4\pi)^2 M_l N_r}{G_t G_r \lambda^2} \cdot d_{j,i}^2 \cdot \frac{\bar{E}_b}{N_0} \Big|_{intra} + \frac{P_{ct}}{R_b} \right] + \frac{n_i^r P_{cr}}{R_b} \right) \end{aligned} \quad (3.8)$$

where $d_{j,i}$ is the distance between CM j and CH i and n_i^r is the number of CMs in the i -th cluster during round r .

3.3.2 Energy Consumption of Data Aggregation

After receiving all data packets from its CMs, CH i performs data aggregation to process its own data and CMs' data into a single packet. Denote the aggregation factor to be γ_{agg} . Then the packet size after data aggregation of CH i in round r is as follows

$$L_{agg}^r(i) = \frac{n_i^r + 1}{(n_i^r + 1)\gamma_{agg} - \gamma_{agg} + 1} L_{data} \quad (3.9)$$

The energy dissipation of data aggregation depends on the complexity of data aggre-

gation algorithm which is denoted by $O(n)$. In uniform data aggregation, the energy dissipation is formulated as

$$E_{da} = C_0 + C_1 l \quad (3.10)$$

where C_0 and C_1 are coefficients depending on the software and CPU parameters, and l is the number of bits required to be aggregated. Then the energy consumption per bit for data aggregation is given by

$$E_{bf} = \frac{C_0 + C_1 l}{l} = \frac{C_0}{l} + C_1 \quad (3.11)$$

Note that C_0/l can be omitted with a large l . Hence, the energy consumption per bit of algorithm complexity with $O(n)$ is approximately constant. In terms of the experiment results described in [WHC99], E_{bf} is set to be 5 nJ/bit/signal for simulation experiments.

In this chapter, the data aggregation energy consumption of CH i in round r is

$$E_{agg}^r(i) = L_{agg}^r(i) E_{bf} \quad (3.12)$$

3.3.3 Energy Consumption in Inter-cluster Communication

Inter-cluster communication operates in the long-haul transmission between the CHs and the capillary gateway. After data collection and aggregation, CHs transmit the aggregated data to the capillary gateway. Therefore, the inter-cluster energy consumption of CH i in round r is the transmission energy consumption to send the aggregated data with size $L_{agg}^r(i)$ to the capillary gateway, which is expressed as

$$\begin{aligned} E_{inter}^r(i) &= L_{agg}^r(i) E_{bt}^r(i) \\ &= L_{agg}^r(i) \left[(1 + \varphi_{amp}) \cdot \frac{(4\pi)^2 M_l N_r}{G_t G_r \lambda^2} \cdot d_{i,g}^{\kappa_{i,g}} \cdot \frac{\bar{E}_b}{N_0} \right]_{inter} + \frac{P_{ct}}{R_b} \end{aligned} \quad (3.13)$$

where $d_{i,g}$ is the distance between CH i and the capillary gateway, and $\kappa_{i,g}$ is the path loss exponent of the long-haul transmission and is in the range between 2 and 3.

3.3.4 Network Lifetime Formulation

The overall network energy consumption in round r includes the intra-cluster energy consumption, data aggregation energy consumption and inter-cluster energy consumption in \mathcal{N}_{CH} clusters, and can be derived from (3.8) to (3.13) as follows

$$E_{net}^r = \sum_{i=1}^{\mathcal{N}_{CH}} (E_{intra}^r(i) + E_{agg}^r(i) + E_{inter}^r(i)) \quad (3.14)$$

In terms of individual energy consumption, CM j transmits data to its CH i , dissipating the transmission energy consumption. Therefore, the energy consumption of CM j in round r denoted by $E_{CM}^r(j)$ is expressed as

$$E_{CM}^r(j) = (1 + \varphi_{amp}) \cdot \frac{(4\pi)^2 M_l N_r}{G_t G_r \lambda^2} \cdot d_{j,i}^2 \cdot \frac{\bar{E}_b}{N_0} \Big|_{intra} + \frac{P_{ct}}{R_b} \quad (3.15)$$

Furthermore, CH i receives data from its CMs dissipating the reception energy consumption, aggregates all data within cluster i dissipating the data aggregation energy consumption, and transmits the aggregated data to the capillary gateway dissipating the transmission energy consumption. Therefore, the energy consumption of CH i in round r , denoted by $E_{CH}^r(i)$, is given by

$$E_{CH}^r(i) = \frac{P_{cr}}{R_b} + L_{agg}^r \bar{E}_{agg} + \left[(1 + \varphi_{amp}) \cdot \frac{(4\pi)^2 M_l N_r}{G_t G_r \lambda^2} \cdot d_{i,g}^2 \cdot \frac{\bar{E}_b}{N_0} \Big|_{inter} + \frac{P_{ct}}{R_b} \right] \quad (3.16)$$

The lifetime of a device is derived by taking the residual energy devices into consideration. Denote the residual energy of device n to be $E_{re}^r(n)$. Then the lifetime of CM j in round r , denoted by $T_{CM}^r(j)$, is given by

$$T_{CM}^r(j) = \frac{E_{re}^r(j)}{E_{CM}^r(j)} \quad (3.17)$$

Similarly, the lifetime of CH i in round r , denoted by $T_{CH}^r(i)$, is given by

$$T_{CH}^r(i) = \frac{E_{re}^r(i)}{E_{CH}^r(i)} \quad (3.18)$$

In this chapter, the network lifetime is defined as the average lifetime of devices in the capillary network. Denote the network lifetime in round r to be T_{net}^r . The network lifetime is expressed as

$$T_{net}^r = \frac{\sum_{i=1}^{\mathcal{N}_{CH}} T_{CH}^r(i) + \sum_{i=1}^{\mathcal{N}_{CH}} \sum_{j=1}^{n_i} T_{CM}^r(j)}{\mathcal{N}_{total}} \quad (3.19)$$

The research problem in this chapter is to find the optimum set of CHs at round r with the objective to maximise T_{net}^r . Denote the optimum set of CHs to be $\mathcal{CH} = \{CH_1^r, \dots, CH_{\mathcal{N}_{CH}}^r\}$. The research problem is expressed as

$$\underset{\mathcal{CH}}{\text{maximise}} T_{net}^r \quad (3.20)$$

3.4 QPSO-based CHs Selection Algorithm

The clustering protocol is described in Algorithm 4. The whole transmission consists of lots of rounds, and each round consists of one set-up phase and one steady-state phase, as shown in Figure 3.2.

Particularly, the set-up phase is comprised of initialisation, CHs selection and cluster formation and the steady-state phase is comprised of several time frames for data transmission.

Firstly, every device reports its individual information (i.e. location and residual energy) to the capillary gateway at the beginning of the set-up phase. Secondly, capillary gateway selects the CH candidates beforehand to ensure the selected CHs are of sufficient

Algorithm 4: Clustering scheme in capillary networks for IoT platform

Input: $r = 0$

- 1 **while** $\exists n. E_{re}^r(n) > 0$ **do**
- 2 Set-up phase initialisation. Every device reports its location and residual energy to the gateway.
- 3 CHs selection. The capillary gateway selects \mathcal{N}_{cand} CH candidates, executes Algorithm 5 to select CHs, and also assign every non-CH device to its closest CH.
- 4 Cluster formation. The gateway broadcasts a message to notify each device about its role.
- 5 **for each** $i \in [1, 2, \dots, \mathcal{N}_{frame}]$ **do**
- 6 Steady-state phase data transmission. The network performs intra-cluster and inter-cluster data transmission in frame i .
- 7 **end**
- 8 $r \leftarrow r + 1$
- 9 **end**
- 10 **return** set r as the final number of rounds when all devices run out of energy.

energy. Denote the percentage of CH candidates to be \mathbb{P}_{cand} , then the number of CH candidates is $\mathcal{N}_{cand} = \mathbb{P}_{cand} \times \mathcal{N}_{total}$. Only first \mathcal{N}_{cand} devices with the highest residual energy level in the scenario are eligible to be CHs for this round. If different devices are of the same energy level, the long-haul distance is taken as another criteria to select the CH candidates, i.e. devices close to the gateway is more likely to be selected as CH candidates. The optimum set of CHs is selected from the CH candidates. Then the capillary gateway executes Algorithm 5 to select the optimum set of CHs by QPSO algorithm. In order to form clusters, the capillary gateway assigns every non-CH device to its closest CH. Thirdly, in order to notify each device about its role, the gateway broadcasts a message which contains all CHs' ID for every device: if the CH's ID of the device matches with its own ID, the device is a CH; otherwise, the device is a CM and it determines its time slot in TDMA scheduling for data transmission. Finally, the network performs cluster-based data transmission process in the steady-state phase. The whole communication terminates when all devices run out of energy.

In this chapter, the quantum position of a particle is composed of CH candidates, as shown in Figure 3.3. Therefore, the dimension of particles is the number of CH

candidates \mathcal{N}_{cand} . The value of quantum position indicates whether the device n in particle m is a CH in generation t : $x_{mn}^t = 1$ represents that the candidate n in particle m is a CH at generation t ; otherwise, the candidate n in particle m is a CM at generation t . Every particle in this chapter represents a possible set of CHs.

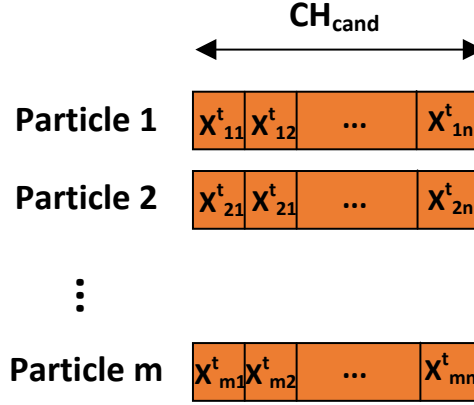


Figure 3.3: Particle position representation for CH candidates

The QPSO-based CHs selection algorithm aiming at maximising the network lifetime is described in Algorithm 5. Denote the maximum generation to be T_{max} . In this chapter, the dimension of particles is the size of CH candidates. The input of this algorithm is the set of CH candidates. Firstly, the position, velocity, local optimum and global optimum of all particles are initialised, as described from line 1 to line 10. Secondly, the swarm updating process is performed from line 11 to line 29. In particular, line 13 to line 17 describes the updating process of particle m , including the regeneration of rotation angle by (2.12), velocity by (2.6) and position by (2.7). Then the fitness value (i.e. network lifetime) of particle m is updated by mapping the particle position at the current generation to the selected CHs from the CH candidates in line 18. Furthermore, line 19 to line 22 updates the individual optimum fitness values and position at the current generation by comparing the updated fitness value with the previous individual optimum fitness value. Then the temporary global optimum at current generation is updated by (2.11) in line 24, which is further compared with global optimum fitness value at previous generation. From line 25 to line 27, the final global optimum at the current generation is updated. Finally, the optimum set of CHs is returned as the output

in line 30.

Algorithm 5: QPSO-based CHs selection scheme

Input: Set of CH candidates

```

1 for each  $m \in [1, 2, \dots, \mathcal{N}_{particle}]$  do
2   for each  $n \in [1, 2, \dots, \mathcal{N}_{cand}]$  do
3     Set the quantum position  $x_{mn}^1$  by 0 or 1 randomly
4     Set the quantum velocity  $v_{mn}^1$  to be  $1/\sqrt{2}$ 
5   end
6   Update the network lifetime  $f_m^1$  by (3.19)
   /* The local optimum is the initialised particles at the first
   generation */
7   Set the local optimum fitness value  $f_m^{pbest_{max}}$  to be  $f_m^1$ 
8   Set the local optimum position  $\mathbf{x}_m^{pbest_{max}}$  to be  $\mathbf{x}_m^1$ 
9 end
   /* Update the global optimum */
10 Update  $f^{gbest_{max}}$  and  $\mathbf{x}^{gbest_{max}}$  by (2.11)
11 for each  $t \in [1, 2, \dots, T_{max}]$  do
12   for each  $m \in [1, 2, \dots, \mathcal{N}_{particle}]$  do
13     for each  $n \in [1, 2, \dots, \mathcal{N}_{cand}]$  do
14       Update the quantum rotation angle  $\theta_{mn}^{t+1}$  by (2.12)
15       Update the quantum velocity  $v_{mn}^{t+1}$  by (2.6)
16       Update the quantum position  $x_{mn}^{t+1}$  by (2.7)
17     end
18     Update the network lifetime  $f_m^{t+1}$  by (3.19)
     /* Find the updated local optimum */
19     if  $f_m^{t+1} > f_m^{pbest_{max}}$  then
20       Set  $f_m^{pbest_{max}} = f_m^{t+1}$ 
21       Set  $\mathbf{x}_m^{pbest_{max}} = \mathbf{x}_m^{t+1}$ 
22     end
23   end
24   Update the temporary global optimum fitness value  $g^{gbest_{max}}$  by (2.11)
   /* Update the final global optimum at generation  $t+1$  */
25   if  $g^{gbest_{max}} > f^{gbest_{max}}$  then
26     Set  $f^{gbest_{max}} = g^{gbest_{max}}$ 
27     Update  $\mathbf{x}^{gbest_{max}}$  according to  $g^{gbest_{max}}$ 
28   end
29 end
30 return  $\mathbf{x}^{gbest_{max}}$  as the optimum set of CHs

```

3.5 Simulation and Conclusions

This section presents the simulation scenario, system parameters setting, simulation platform design and the simulation results. PSO [LTS07] and QGA [GSDL14] are simulated as the references in this chapter.

3.5.1 Scenario Design and System Parameters

Assume 200 devices powered by AAA Carbon-zinc battery ($1.1V$, $320mAh$) [Bat11] are randomly distributed within a square with 500m side length. The gateway is located at position $(250m, 750m)$ in the scenario. The position of all devices and the capillary gateway is shown in Figure 3.4.

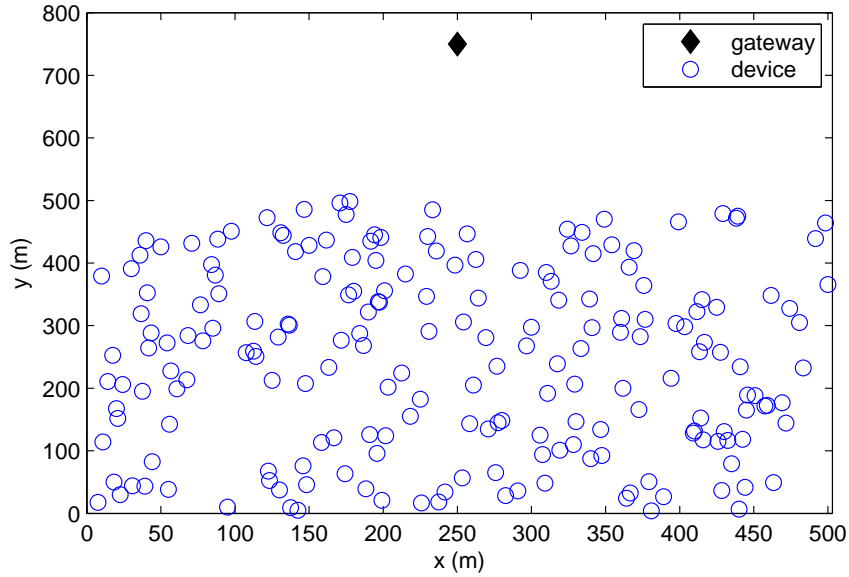


Figure 3.4: Scenario diagram for cluster-based capillary networks

In terms of battery energy conversion, the following battery capacity model in [Rap14] is used to convert the energy consumption in Joule $E(J)$ to the energy consumption in

Watt-hours $E(Wh)$,

$$E(J) = Q(mAh) \times V(v) \times 3600$$

$$E(Wh) = Q(mAh) \times V(v) \quad (3.21)$$

$$E(Wh) = \frac{E(J)}{3600}$$

where $Q(mAh)$ is the electric charge in milliamp-hours and voltage $V(v)$ in volts. By (3.21), the initial battery capacity of all devices is $1268J$ in energy and $0.35Wh$ in Watt-hours in the scenario.

Table 3-A: System Parameters for Cluster-based Capillary Networks

Parameter	Value	Meaning
k_1	0.06 [CZZL13]	learning factors of cognitive acceleration in QPSO
k_2	0.03 [CZZL13]	learning factors of social acceleration in QPSO
M_l	40dB [CGB04]	link margin
N_f	10dB [CGB04]	receiver noise figure
N_r	-161dBm/Hz [CGB04]	single-sided spectral density of the receiver noise
$G_T G_R$	5dBi [CGB04]	transmitter and receiver antenna gain
λ	0.12m [CGB04]	carrier wavelength
B_{band}	10kHz [CGB04]	channel bandwidth
P_{BER}^{intra}	10^{-5} [LLW ⁺ 13]	intra-cluster BER requirement
P_{BER}^{inter}	10^{-5} [LLW ⁺ 13]	inter-cluster BER requirement
φ_{amp}	0.47 [CGB04]	a constant in power amplification
L_{data}	100bits [HOKK12]	individual packet size
M	16 [ZD07]	QAM constellation size
R_b	10kbps [CGB04]	transmission bit rate
P_{LNA}	20mW [CGB04]	power consumption of low noise amplifier
P_{DAC}	15.5mW [CGB04]	power consumption of D/A converter
P_{mix}	30.3mW [CGB04]	power consumption of the mixer
P_{filt}	2.5mW [CGB04]	power consumption of the active transmitter filters
P_{filr}	2.5mW [CGB04]	power consumption of the active receiver filters
P_{IFA}	3mW [CGB04]	power consumption of the frequency amplifier
P_{ADC}	9.8mW [CGB04]	power consumption of A/D converter
γ_{agg}	0.5 [HOKK12]	data aggregation factor
\mathcal{N}_{frame}	24 [MQ10]	number of time frames in one round
\mathbb{P}_{cand}	0.2 [HCB02]	the percentage of CH candidates in the scenario
t_{Δ}	30 min [MQ10]	duration of one time frame
E_{agg}	5nJ/bit [WHC99]	energy consumption per bit in data aggregation

The system parameters used in this chapter are given in Table 3-A.

3.5.2 Simulation Platform

Matlab is used as the simulation tool. The simulation process is comprised of 50 simulation iterations for both proposed and references algorithms. The simulation process of the proposed clustering algorithm in Section 3.4 consists of a number of logic blocks and simulation loops, as shown in Figure 3.5.

3.5.2.1 Scenario Initialisation Module

This module initialises the individual information of 200 devices and the capillary gateway. Particularly, the position of capillary gateway and all devices are initialised as shown in Figure 3.4. The battery capacity of every device is set to be $1268J$. This module also initialises the long-haul path loss between devices and the capillary gateway to be a random value between 2 and 3. The function flow of this module is shown in Figure 3.6.

3.5.2.2 CH Candidates Selection Module

This module selects the CH candidates according to the residual energy and long-haul distance. In specific, only first \mathcal{N}_{cand} devices with the highest residual energy level in the scenario are eligible to be CHs for this round. If different devices are of the same residual energy, the long-haul distance is considered as another criteria to select CH candidates, i.e. devices close to the gateway is more likely to be selected as CH candidates.

3.5.2.3 QPSO-based CHs Selection Process

This module performs QPSO algorithm to select the CHs from the set of CH candidates. It includes particle initialisation, particle updating, generation iteration process and the output of optimum CHs set after a predetermined maximum number of generations.

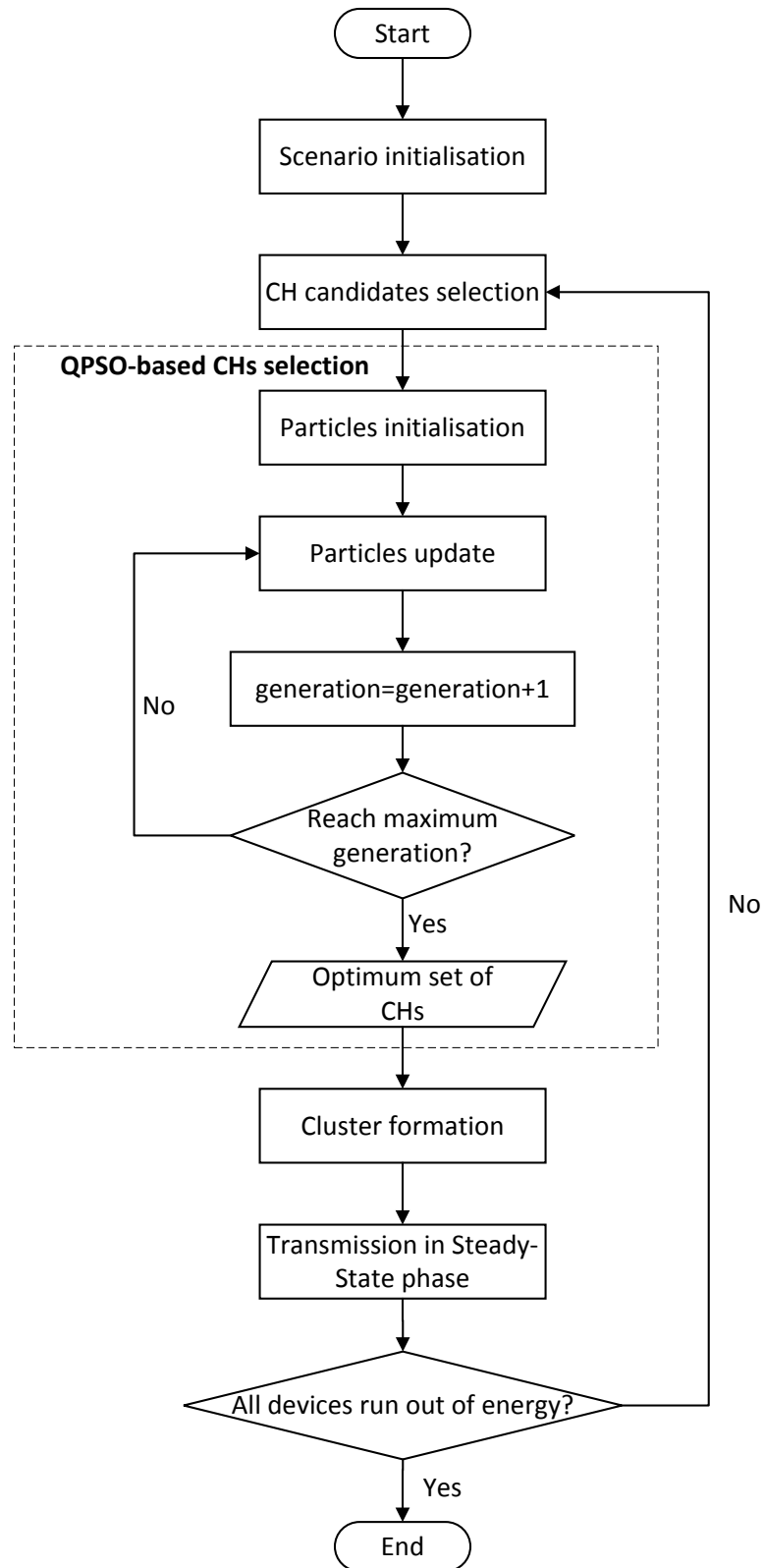


Figure 3.5: Flowchart of the proposed clustering algorithm (Algorithm 4)

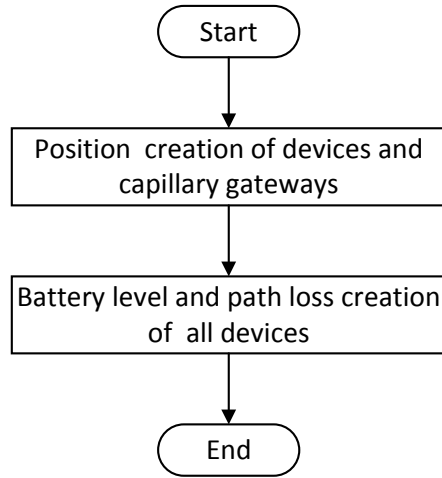


Figure 3.6: Flowchart of scenario initialisation in cluster-based capillary networks

A. Particle Initialisation Module

This sub-module initialises the position and velocity of all particles first. The position of all particles are mapped to a particular set of CHs, and the fitness values can be further obtained. In this chapter, the fitness value refers to the network lifetime in (3.19). Finally, the individual optimum and global optimum are updated.

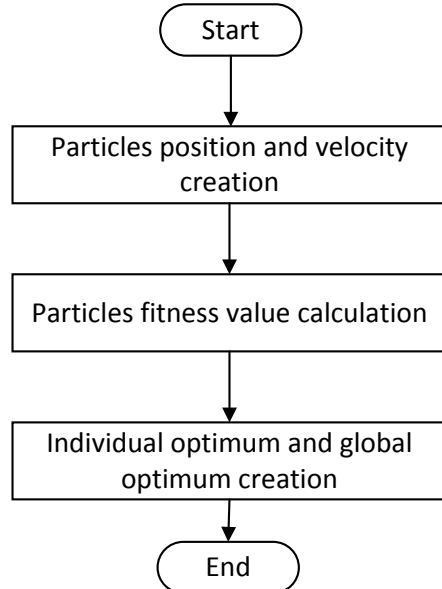


Figure 3.7: Flowchart of algorithm initialisation in Algorithm 4

B. Particle Updating Module

This sub-module generates a new swarm by updating the rotation angle, velocity and position of all particles, as shown in Figure 2.7.

3.5.2.4 Cluster Formation Module

This module produces the clusters in the capillary network based on the optimum set of CHs. The distance between a non-CH device and all selected CHs are calculated, and then it is assigned to its closest CH to form clusters. By this way, all non-CH devices join a particular CH to form clusters.

3.5.2.5 Steady-state Phase Module

This module calculates the energy consumption of every device in steady-state phase and also the residual energy of every device after the current round. If the residual energy of a device is 0, this device is regarded to run out of its energy and will be removed from the scenario.

3.5.3 Simulation Results

Table 3-B: Optimum generation number and function evaluation in terms of the particle number

Particle number $\mathcal{N}_{particle}$	Optimum generation number T_{opt}	Function evaluation FE
6	803	4818
8	601	4808
10	486	4860
12	391	4692
14	286	4004
16	253	4048
18	242	4356
20	225	4550
22	216	4752

First, one of the main difficulties of applying an evolutionary algorithm to a given

problem is to decide an appropriate set of parameter values, such as the particle number and generation number [LLM07]. Denote the optimum generation number to be T_{opt} , which shows the number of generations required to first produce the final optimum global fitness value. In addition, as referred to [CMBR14], the function evaluations denoted by \mathbb{FE} is defined as $\mathbb{FE} = T_{opt} \times \mathcal{N}_{particle}$, which indicates the algorithm complexity with respect to different number of particles. Table 3-B shows the optimum generation number and function evaluation for different number of particles to converge to the same final optimum global fitness value. The simulation iteration is set to be 50 times. Figure 3.8 shows the trend of optimum generation and function evaluation in Table 3-B. In Figure 3.8, the optimum generation number decreases dramatically with the increase of particle number from 6 to 14 particles. This is because more particles mean better opportunity to find the optimum fitness value within a limited generations. However, as the particle number increases from 14 to 22, the optimum generation number varies within a small range. Therefore, the performance of QPSO is not sensitive to the number of particles when there are more than 14 particles. Focusing on the function evaluations, it can be seen that the minimum \mathbb{FE} is achieved at the point where the particle number is 14 and the optimum generation number is 286. In this chapter, the particle number is set to be 14 and the generation number is set to be 300 to decrease the algorithm complexity as well as ensure the performance of QPSO.

Next, Figure 3.9 illustrates the convergence of QPSO. The overall residual energy increases with the number of generations, because the objective of this chapter is to find the maximum network lifetime. It can be seen that the final overall residual energy can be achieved after a certain number of generations for different number of particles, which indicates the convergence of QPSO algorithm.

Figure 3.10 shows the overall residual battery capacity of all devices with respect to the number of hours. The overall residual battery capacity of all algorithms decrease significantly after 2000 hours. This can be explained by the fact that the number of disabled devices increases after 2000 hours. Nevertheless, the advantage of QPSO emerges after

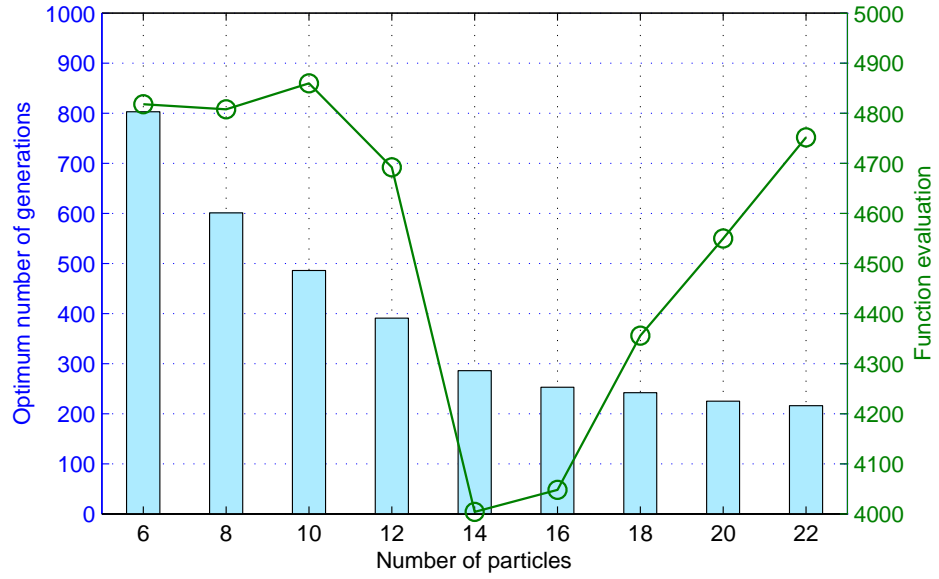


Figure 3.8: Optimum generation number and function evaluation in terms of the particle number

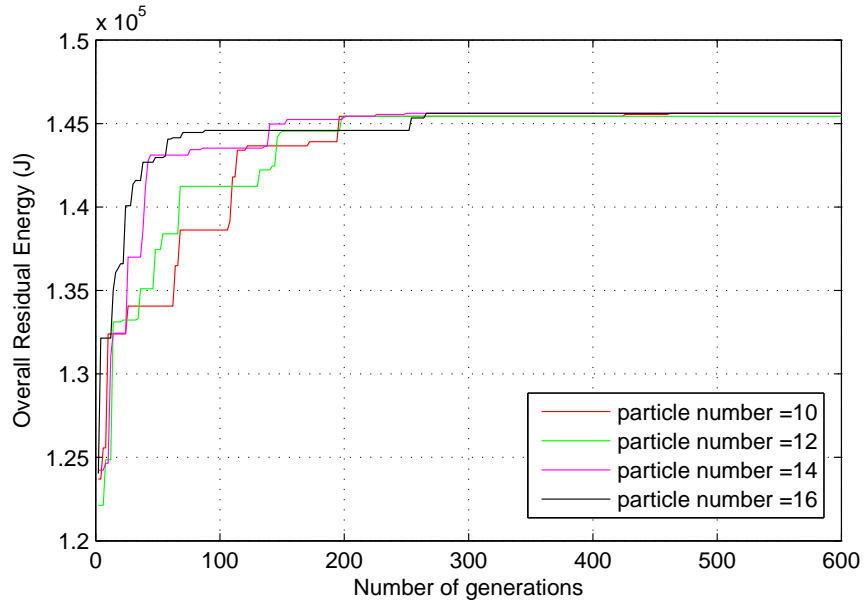


Figure 3.9: Convergence of QPSO

about 4000 hours when more and more devices run out of their energy. It is observed that all devices dissipate their total battery capacity after about 5400 hours using the PSO-based and QGA-based CH selection, but QPSO is able to prolong network lifetime by about 10% compared with PSO and QGA, because the proposed QPSO algorithm can

select a better set of CHs that can help more evenly distribute the energy consumption among the capillary networks in each round. This figure also indicates that the residual battery capacity of devices at last round are not enough to support the long-haul transmission, which is the reason why the overall battery capacity is not 0 for all three algorithms at the last round.

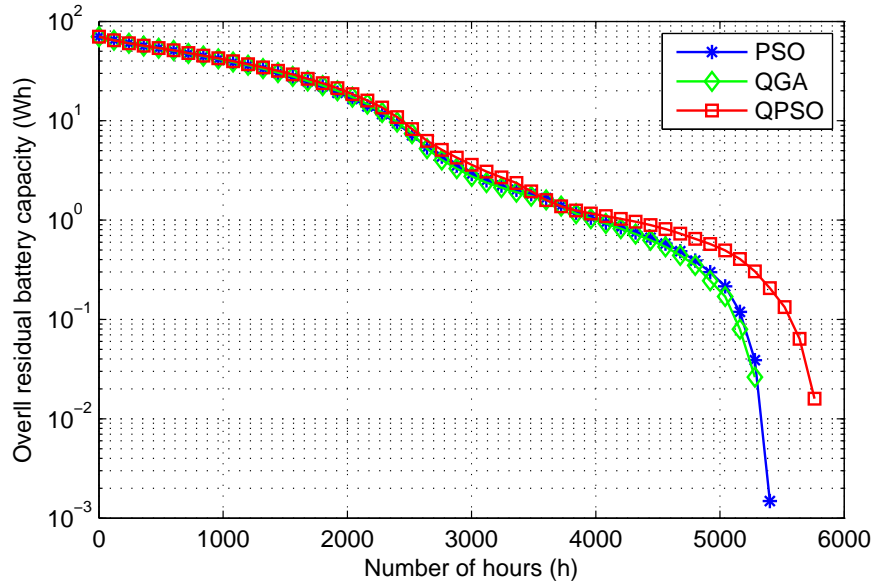


Figure 3.10: Overall residual battery capacity in terms of the number of hours for cluster-based capillary networks

Figure 3.11 shows the number of alive nodes with respect to the number of hours. It is shown that the first device runs out of energy after about 2000 hours for QPSO, PSO and QGA algorithms, followed by an increasing number of disabled devices from 2000 hours to 4000 hours. This is due to that fact that devices closer to the gateway is more likely to be selected as CHs, which results in these devices running out of energy quicker than other devices during the first 2000 hours, thereby more energy dissipation in the long-haul transmission after the unavailability of these devices after 2000 hours. In addition, as for PSO and QGA algorithms, all devices dissipate the battery capacity after about 5500 hours, however, the clustering scheme using the proposed QPSO-based CH selection can prolong the network lifetime by another 500 hours compared with PSO and QGA.

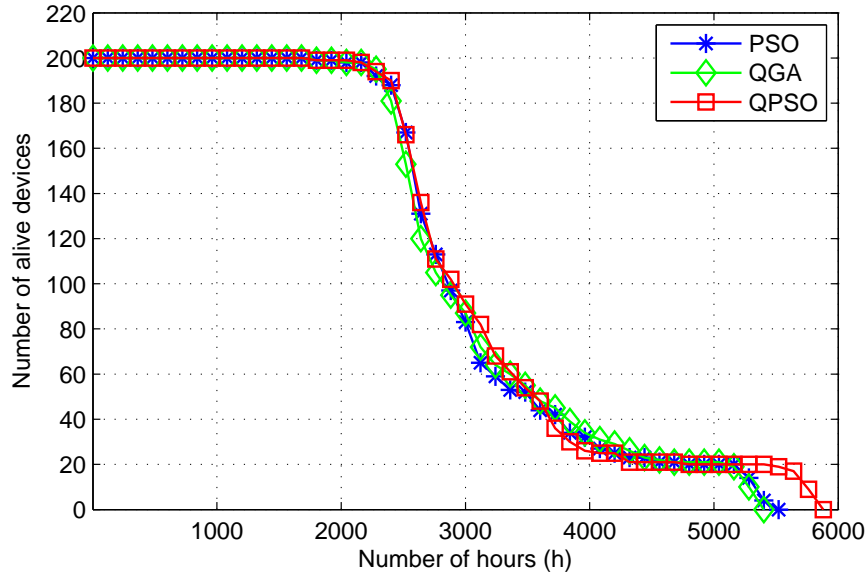


Figure 3.11: Number of alive nodes in terms of the Number of hours for cluster-based capillary networks

Finally, Figure 3.12 depicts the number of selected CHs by QPSO, PSO and QGA algorithms in terms of the number of hours. It is shown that the number of selected CH varies with the number of hours. For example, the number of selected CHs by QPSO, PSO and QGA algorithms at the beginning of the transmission are between 9 to 13, which is lower than the number of selected CHs between 17 to 28 at about 100 hours. This is explained by the proposed even energy distribution CHs selection strategy which takes the residual energy of devices into consideration. Specifically, all devices are of equal energy level at the beginning, devices closer to the capillary gateway are selected as CHs. However, after a few rounds, devices closer to the capillary gateway dissipate more energy than other devices, and thus devices that are relatively far away from the capillary gateway will be selected as CHs, thereby more CHs in this case are required to support farther long-haul distance. Additionally, due to the same reason that there are less alive devices after about 2000 hours in Figure 3.11, the number of CHs decreases dramatically from 2000 hours to 3000 hours. Furthermore, it can be seen that after 3000 hours, the number of selected CHs remains to be in the small range and is less than 5, since there is no enough CH candidates and less alive devices in the scenario. In addition,

although the QPSO outperforms other algorithms in Figure 3.10 and Figure 3.11, the number of CHs selected by the proposed QPSO algorithm is not the maximum at most time. It can be concluded that higher number of CHs is not necessary.

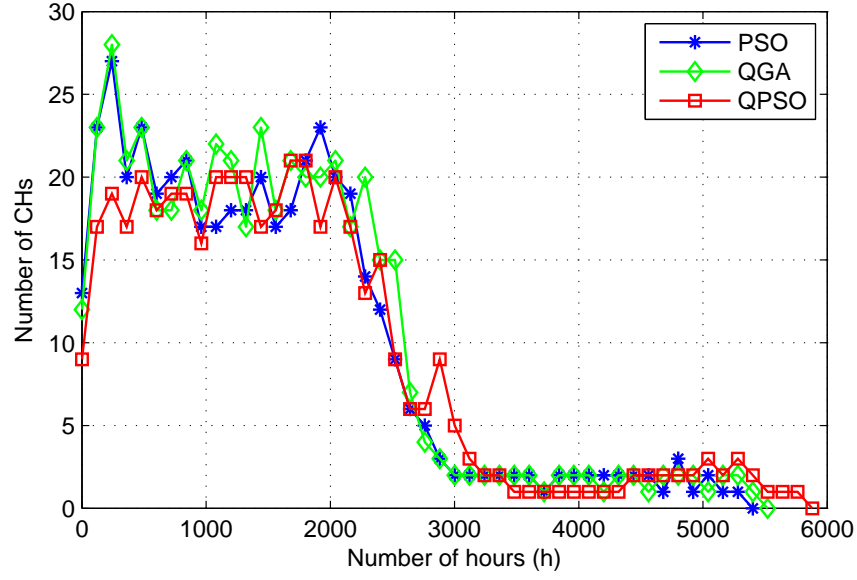


Figure 3.12: Number of selected CHs in terms of number of hours for cluster-based capillary networks

3.5.4 Conclusions

In this chapter, cluster structure design using QPSO is investigated with the aim of network lifetime longevity in cluster-based capillary networks. It is shown that the CHs selection plays an important role in data forwarding. The QPSO algorithm is proposed in order to select the optimum CHs coalition. Simulation results show that the proposed QPSO scheme outperforms PSO and QGA algorithms in terms of network lifetime by approximately 10%.

3.6 Summary

In this chapter, Section 3.1 specified the system model for cluster-based capillary networks and Section 3.2 provided the energy consumption model used in this thesis. The overall energy consumption in the network and individual energy consumption for every device were formulated to evaluate the network lifetime in Section 3.3. In order to maximise the network lifetime in every round, Section 3.4 developed an optimum CHs selection algorithm. The proposed algorithm employed QPSO to select the optimum set of CHs in the set-up phase of every round, thereby forming clusters to transmit data packet in steady-state phase. Section 3.5 presented the simulation platform design, simulation results and conclusions. The simulation results demonstrated that the proposed QPSO-based algorithm is able to choose the optimum set of CHs and can prolong network lifetime.

Chapter 4

CH and Cooperative Devices Selection for Single-Hop Networks

The CHs can be selected after the cluster formation phase in order to balance the energy consumption among the devices located at different areas in the networks [CL15] [RD16]. The cooperative communication can release the burden of CHs by employing cooperative devices in the long-haul transmission [AK10]. This chapter proposes a new CH and cooperative devices selection algorithm in post cluster formation phase for the single-hop cluster-based capillary networks. The proposed CH and cooperative devices selection algorithm chooses the optimum set of CH and cooperative devices with the objectives of energy efficiency, QoS provision, and the tradeoff between energy efficiency and QoS provision.

4.1 System Model

In this chapter, the system model considers a cluster in capillary networks for IoT platform with \mathcal{N}_{total} devices: one CH, \mathcal{N}_{CM} CMs and \mathcal{N}_{Coop} Coops, as shown in Figure 4.1, where $\mathcal{N}_{total} = 1 + \mathcal{N}_{CM} + \mathcal{N}_{Coop}$. The same assumptions in Section 3.1 are also made

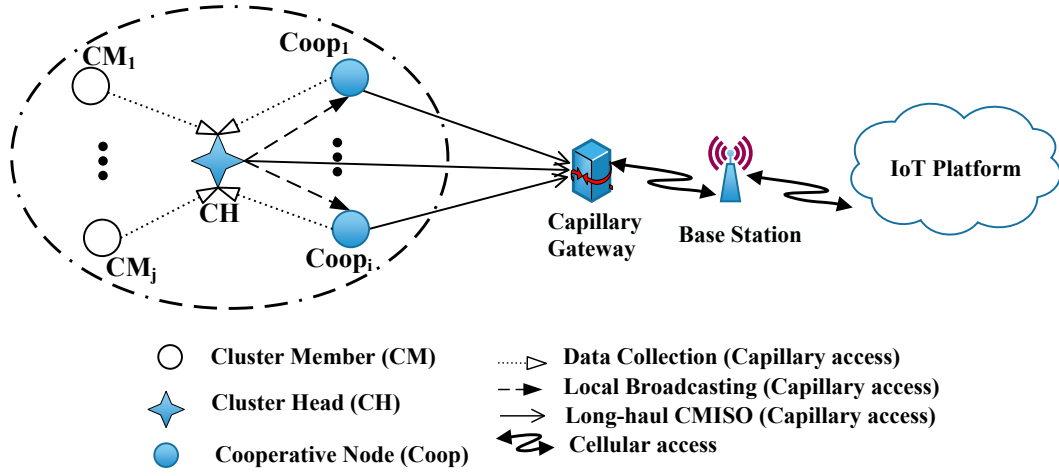


Figure 4.1: System model for CMISO system in cluster-based capillary networks

for this system model.

Furthermore, the communication in this chapter focuses on one time frame, which consists of the following three phases:

- Data collection (DC) phase: CH collects and aggregates data from all CMs and Coops.
- Local broadcasting (LB) phase: CH broadcasts the aggregated data to all Coops.
- Long-haul cooperative transmission (LH) phase: CH and Coops jointly encode and transmit the aggregated data to the capillary gateway based on orthogonal space-time block codes (STBC). STBC is a cooperative technique investigated in [LW03] such that the CH and cooperative devices share their antennas to create a virtual array through distributed transmission and signal processing. Then the data information is further forwarded to the IoT platform through the capillary gateway and the base station.

The transmission using CMISO systems consists of the local broadcasting phase and long-haul cooperative transmission phase. Furthermore, the communication in the data collection phase and the local broadcasting phase are performed within the cluster, i.e.

intra-cluster transmission, while the long-haul cooperative transmission phase performs inter-cluster communication.

Figure 4.2 illustrates the time slots of the above three phases in TDMA scheduling. Firstly, every non-CH device (i.e. CM or Coop) is allocated with a time slot to transmit the individual data to the CH in the data collection phase; secondly, CH uses one time slot to broadcast the aggregated data to all Coops in the local broadcasting phase; finally, CH together with all Coops are allocated with different time slots to transmit the STBC-coded data to the capillary gateway.

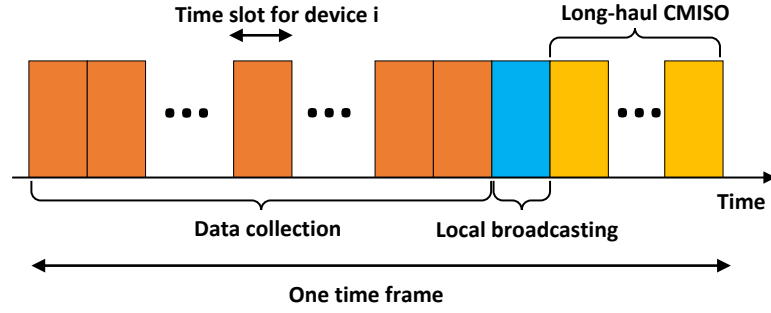


Figure 4.2: Time slots of TDMA scheduling using CMISO systems

4.2 Energy Consumption Model

This chapter uses the energy model of power consumption and intra-cluster communication in Section 3.2. For the inter-cluster communication of long-haul transmission phase, taking CMISO system into consideration, the average $\left. \frac{\bar{E}_b}{N_0} \right|_{inter}$ with a square constellation MQAM in Rayleigh fading channel [ZD07] is given by

$$\left. \frac{\bar{E}_b}{N_0} \right|_{inter} \doteq (N_{coop} + 1) \cdot \frac{2(M-1)}{3 \log_2 M} \cdot \left[\frac{1}{4} \left(\frac{4(1 - 1/\sqrt{M})^{(2(N_{coop}+1)-1)}}{\bar{P}_{BER}^{inter} \log_2 M} \right)^{\frac{1}{N_{coop}+1}} - 1 \right] \quad (4.1)$$

where \bar{P}_{BER}^{inter} is the average BER of inter-cluster communication.

4.3 Energy Efficient CH and Cooperative Devices Selection

This section investigates the cooperative devices selection using CMISO systems in one-hop cluster-based capillary networks with the objective of energy efficiency. The energy efficiency problem formulation is presented first, followed by the proposed CH and cooperative devices selection algorithm and simulation.

4.3.1 Energy Efficiency Problem Formulation

This subsection presents the battery model, the overall power consumption and active time of every device, as well as the network lifetime derivation.

4.3.1.1 Battery Model

The battery model in [ZCSA10] is used in this thesis to estimate the device lifetime. When a battery is discharge at current rate I_c in time period $[t_s, t_e]$, the available capacity $C_{avl}(I_c, T_{op}, t_s, t_e, \varrho^2)$ is as follows

$$C_{avl}(I_c, T_{op}, t_s, t_e, \varrho^2) = C_{init} - I_c F(T_{op}, t_s, t_e, \varrho^2) \quad (4.2)$$

$$F(T_{op}, t_s, t_e, \varrho^2) = (t_e - t_s) + 2 \sum_{k=1}^{\infty} \frac{e^{-\varrho^2 k^2 (T_{op} - t_e)} - e^{-\varrho^2 k^2 (T_{op} - t_s)}}{\varrho^2 k^2}$$

where C_{init} is the initial battery capacity, ϱ^2 is a constant related to the diffusion rate of the battery, which can be determined by data fitting [RV01], and T_{op} is the total operating time of battery.

4.3.1.2 Power Consumption and Active Time

In this thesis, the active time of a wireless device is defined as the cumulative operation time during the transmission. The part investigates the power consumption and active time of CH, Coop and CM for data collection phase, local broadcasting phase and the long-haul cooperative transmission phase.

A. Data collection phase

In the data collection phase, the CH acts as the receiver dissipating the reception power consumption while all CMs and Coops transmit data to the CH, dissipating the transmission power consumption. As the assumption of squared power path loss in intra-cluster communication, the power consumption per bit of CH, $Coop(i)$ where $i \in 1, \dots, \mathcal{N}_{Coop}$ and $CM(j)$ where $j \in 1, \dots, \mathcal{N}_{CM}$, are expressed as

$$\begin{aligned} P_{CH}^{DC} &= P_{cr} \\ P_{Coop}^{DC}(i) &= \frac{(4\pi)^2 M_l N_r}{G_t G_r \lambda^2} \cdot R_b d_{i,CH}^2 \cdot \frac{\bar{E}_b}{N_0} \Big|_{intra} + P_{ct} \\ P_{CM}^{DC}(j) &= \frac{(4\pi)^2 M_l N_r}{G_t G_r \lambda^2} \cdot R_b d_{j,CH}^2 \cdot \frac{\bar{E}_b}{N_0} \Big|_{intra} + P_{ct} \end{aligned} \quad (4.3)$$

where $d_{i,CH}$ is the distance between Coop i and CH, and $d_{j,CH}$ is the distance between CM j and CH. Correspondingly, the active time of devices in the data collection phase are given by

$$\begin{aligned} T_{CH}^{DC} &= (\mathcal{N}_{CM} + \mathcal{N}_{Coop}) \frac{L_{data}}{R_b} \\ T_{Coop}^{DC}(i) &= \frac{L_{data}}{R_b} \\ T_{CM}^{DC}(j) &= \frac{L_{data}}{R_b} \end{aligned} \quad (4.4)$$

After collecting data from all non-CH devices, the CH performs data aggregation technique. As for the CH, the time duration to aggregate the collected data is rather short compared to other transmission phases [SL13], and thus the active time and power con-

sumption for data aggregation is omitted in this section. The packet size after data aggregation in [YCK06] is as follows

$$L_{agg} = \frac{\mathcal{N}_{total}}{\mathcal{N}_{total}\gamma_{agg} - \gamma_{agg} + 1} L_{data} \quad (4.5)$$

where γ_{agg} is the aggregation factor.

B. Local broadcasting phase

In the local broadcasting phase, CH acts as transmitter to broadcast the STBC-coded data to Coops, dissipating the transmission power consumption, and all Coops receive data information from the CH, dissipating the reception power consumption. Due to the broadcast nature of the wireless channel, if the Coop with the maximum distance from CH, denoted by d_{max} , can receive the broadcast data, the other Coops can simultaneously receive these data. Then the power consumption per bit of CH, $Coop(i)$ where $i \in 1, \dots, \mathcal{N}_{Coop}$ and $CM(j)$ where $j \in 1, \dots, \mathcal{N}_{CM}$, are given by

$$\begin{aligned} P_{CH}^{LB} &= \frac{(4\pi)^2 M_t N_r}{G_t G_r \lambda^2} \cdot R_b d_{max}^2 \cdot \frac{\bar{E}_b}{N_0} \Big|_{intra} + P_{ct} \\ P_{Coop(i)}^{LB} &= P_{cr} \\ P_{CM(j)}^{LB} &= 0. \end{aligned} \quad (4.6)$$

Correspondingly, the active time of devices in the local broadcasting phase are as follows

$$\begin{aligned} T_{CH}^{LB} &= \frac{L_{agg}}{R_b} \\ T_{Coop(i)}^{LB} &= \frac{L_{agg}}{R_b} \\ T_{CM(j)}^{LB} &= 0 \end{aligned} \quad (4.7)$$

C. Long-haul cooperative transmission phase

In the long-haul transmission phase, CH and Coops jointly transmit the aggregated data to the capillary gateway, dissipating the transmission power consumption. Thus, the

power consumption per bit of CH , $Coop(i)$ where $i \in 1, \dots, \mathcal{N}_{Coop}$ and $CM(j)$ where $j \in 1, \dots, \mathcal{N}_{CM}$, are expressed as

$$\begin{aligned} P_{CH}^{LH} &= \frac{(4\pi)^2 M_l N_r}{G_t G_r \lambda^2} \cdot R_b d_{g,CH}^{\kappa_{g,CH}} \cdot \frac{\bar{E}_b}{N_0} \bigg|_{inter} + P_{ct} \\ P_{Coop}^{LH}(i) &= \frac{(4\pi)^2 M_l N_r}{G_t G_r \lambda^2} \cdot R_b d_{i,g}^{\kappa_{i,g}} \cdot \frac{\bar{E}_b}{N_0} \bigg|_{inter} + P_{ct} \\ P_{CM}^{LH}(j) &= 0 \end{aligned} \quad (4.8)$$

where $d_{g,CH}$ and $d_{i,g}$ are the distance between CH/Coops i and capillary gateway, $\kappa_{g,CH}$ and $\kappa_{i,g}$ are the path loss exponent between CH/Coops i and capillary gateway in the range between 2 and 3.

Furthermore, all Coops together with the CH encode the transmission sequence based on the aggregated data packet according to orthogonal STBC. Training symbols are prepended, appended and embedded in data packets for the purpose of channel estimation [Jay04]. Therefore, the packet size in the long-haul transmission is

$$L_c = \frac{F_{block}}{F_{block} - \rho_{train}(\mathcal{N}_{Coop} + 1)} L_{agg} \quad (4.9)$$

where F_{block} is the block size of STBC code and $\rho_{train}(\mathcal{N}_{Coop} + 1)$ is the number of training symbol. The effective system bit rate in the long-haul transmission [HH03] is given by

$$R_b^{eff} = \frac{F_{block} - \rho_{train}(\mathcal{N}_{Coop} + 1)}{F_{block}} R_b \quad (4.10)$$

Then the active time of devices in the long-haul transmission phase are expressed as follows

$$\begin{aligned} T_{CH}^{LH} &= \frac{L_c}{R_b^{eff}} \\ T_{Coop}^{LH}(i) &= \frac{L_c}{R_b^{eff}} \\ T_{CM}^{LH}(j) &= 0 \end{aligned} \quad (4.11)$$

4.3.1.3 Network Lifetime Formulation

Taking the battery model into consideration, the average current required to power a device during period $[t_s, t_e]$ is obtained by

$$\bar{I}_c = \frac{P_{total}}{\phi \mathbb{V}} \quad (4.12)$$

where P_{total} is the overall power consumption of the device during period $[t_s, t_e]$, ϕ and \mathbb{V} denote the DC-DC converter output efficiency and voltage, respectively [ZCSA09].

The battery operating time can then be expressed as

$$\begin{aligned} T_{op} &= \frac{C_{avl}(I_c, T_{op}, t_s, t_e, \varrho^2)}{\bar{I}_c} \\ &= \frac{C_{init}\phi\mathbb{V}}{P_{total}} - (t_e - t_s) - 2 \sum_{k=1}^{\infty} \frac{e^{-\varrho^2 k^2 (T_{op} - t_e)} - e^{-\varrho^2 k^2 (T_{op} - t_s)}}{\varrho^2 k^2} \end{aligned} \quad (4.13)$$

where P_{total} can be obtained from (4.3), (4.6) and (4.8); similarly, t_e can be obtained from (4.4), (4.7) and (4.11). Thus, denote the initialising time to be t_0 , the battery operating time of CH , $Coop(i)$ where $i \in 1, \dots, \mathcal{N}_{Coop}$ and $CM(j)$ where $j \in 1, \dots, \mathcal{N}_{CM}$, are expressed as

$$\begin{aligned} T_{CH}^{op} &= \frac{C_{init}(CH)\phi\mathbb{V}}{L_{data}P_{CH}^{DC} + L_{agg}P_{CH}^{LB} + L_cP_{CH}^{LH}} - (T_{CH}^{DC} + T_{CH}^{LB} + T_{CH}^{LH} - t_0) \\ &\quad - 2 \sum_{k=1}^{\infty} \frac{e^{-\varrho^2 k^2 (T_{CH}^{op} - (T_{CH}^{DC} + T_{CH}^{LB} + T_{CH}^{LH}))} - e^{-\varrho^2 k^2 (T_{CH}^{op} - t_0)}}{\varrho^2 k^2} \end{aligned} \quad (4.14)$$

$$\begin{aligned} T_{Coop}^{op}(i) &= \frac{C_{init}(i)\phi\mathbb{V}}{L_{data}P_{Coop}^{DC}(i) + L_{agg}P_{Coop}^{LB}(i) + L_cP_{Coop}^{LH}(i)} - (T_{Coop}^{DC}(i) + T_{Coop}^{LB}(i) + T_{Coop}^{LH}(i) - t_0) \\ &\quad - 2 \sum_{k=1}^{\infty} \frac{e^{-\varrho^2 k^2 (T_{Coop}^{op}(i) - (T_{Coop}^{DC}(i) + T_{Coop}^{LB}(i) + T_{Coop}^{LH}(i)))} - e^{-\varrho^2 k^2 (T_{Coop}^{op}(i) - t_0)}}{\varrho^2 k^2} \end{aligned} \quad (4.15)$$

$$\begin{aligned} T_{CM}^{op}(j) &= \frac{C_{init}(j)\phi\mathbb{V}}{L_{data}P_{CM}^{DC}(j)} - (T_{CM}^{DC}(j) - t_0) - 2 \sum_{k=1}^{\infty} \frac{e^{-\varrho^2 k^2 (T_{CM}^{op}(j) - T_{CM}^{DC}(j))} - e^{-\varrho^2 k^2 (T_{CM}^{op}(j) - t_0)}}{\varrho^2 k^2} \end{aligned} \quad (4.16)$$

In this thesis, the network lifetime is represented by the average battery operating

time of all devices within the cluster, which can be expressed as $\bar{T}_{avg}^{op} = \frac{\sum_{k=1}^{\mathcal{N}_{total}} T^{op}(k)}{\mathcal{N}_{total}}$. The research problem is to find the optimum set of cooperative devices $\mathcal{C} = \{CH, Coop_1, \dots, Coop_{\mathcal{N}_{Coop}}\}$, with the objective to maximise the average battery operating time \bar{T}_{avg}^{op} under given BER threshold \bar{P}_{BER}^{THR} . Therefore, the research problem in this section is expressed as

$$\begin{aligned} & \underset{\mathcal{C}}{\text{maximise}} \bar{T}_{avg}^{op} = \frac{\sum_{k=1}^{\mathcal{N}_{total}} T^{op}(k)}{\mathcal{N}_{total}} \\ & s.t. \quad \begin{cases} 0 \leq \mathcal{N}_{Coop} \leq \mathcal{N}_{total} - 1 \\ \bar{P}_{BER}^{intra} \leq \bar{P}_{BER}^{THR} \\ \bar{P}_{BER}^{inter} \leq \bar{P}_{BER}^{THR} \end{cases} \end{aligned} \quad (4.17)$$

where $\mathcal{N}_{Coop} = 0$ indicates that only the CH participates in the long-haul transmission, while $\mathcal{N}_{Coop} = \mathcal{N}_{total} - 1$ indicates that all devices in the cluster form the CMISO system in the long-haul transmission.

4.3.2 Energy Efficiency CH and Cooperative Devices Selection Algorithm

The capillary gateway executes the CH and Coops selection algorithm using QPSO, after receiving every device's individual information (i.e. residual energy and location).

In this chapter, the quantum position of a particle is composed of the non-CH devices in the cluster, as shown in Figure 4.3. The number of non-CH devices is $\mathcal{N}_{total} - 1$, and thus the dimension of particles is the number of CH candidates $\mathcal{N}_{total} - 1$. The value of quantum position indicates whether the device n in particle m is a Coop in the cluster: $x_{mn}^t = 1$ represents that the candidate n in particle m is a Coop at generation t ; otherwise, the candidate n in particle m is a CM at generation t . Every particle in this chapter represents a possible set of Coops.

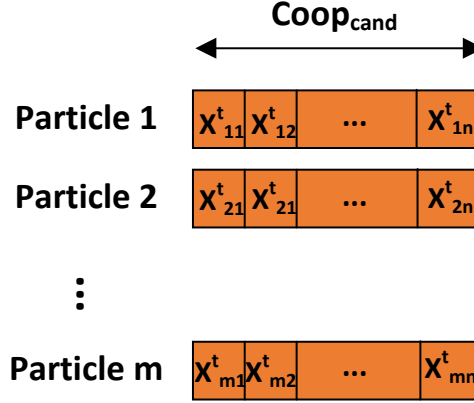


Figure 4.3: Particle position representation for cooperative devices candidates

The CH and Coops selection algorithm aiming at maximising the network lifetime is described in Algorithm 6. Denote the maximum generation to be T_{max} . Firstly, line 2 assumes every device in the cluster to be CH in turn by exhaustive search and iteration ends at line 34. Secondly, the position, velocity, local optimum and global optimum of all particles are initialised, as refer to line 1 to line 12. Thirdly, the swarm updating process is performed from line 13 to line 31. In particular, line 15 to line 19 describes the updating process of a particle, including the regeneration of rotation angle by (2.12), velocity by (2.6) and position by (2.7). Then the fitness value (i.e. network lifetime) of particle is updated by mapping the updated particle position to the selected Coops, as described in line 20. Furthermore, line 21 to line 24 updates the individual optimum in the current generation by comparing the updated fitness value with the previous local optimum fitness value. Then the temporary global optimum at current generation is updated by (2.11) in line 26, which is further compared with global optimum fitness value at previous generation to obtain the final global optimum fitness value at the current generation from line 27 to line 30. Line 32 and line 33 set the maximum fitness value and best set of Coops for the assumed CH. Moreover, Line 35 finds the maximum fitness value from all the fitness values produced in line 32, while line 36 and 37 select the optimum set of CH and Coops, which is returned as the output of this algorithm.

At last, the capillary gateway informs every device about its role (i.e. CH, CM or

Coop) based on the output of Algorithm 6.

4.3.3 Simulation and Conclusions

This subsection describes the simulation scenario, system parameters, simulation platform design, simulation results and conclusions. For the reference, PSO [LTS07] and QGA [GSDL14] are simulated to select the optimum Coops set in this chapter.

4.3.3.1 Scenario Design and System Parameters

Assume 25 devices are randomly distributed located within a square with $100m$ side length. All devices are powered by two AAA Li-FeS2 battery [WIK], which has 1.5-volt nominal voltage and 1200mAh nominal capacity. The capillary gateway is located at position $(150m, 150m)$ if not otherwise specified in the following simulation. The position of devices and capillary gateway are shown in Figure 4.4. All devices are labelled with a number starting from 1 to 25 in the scenario.

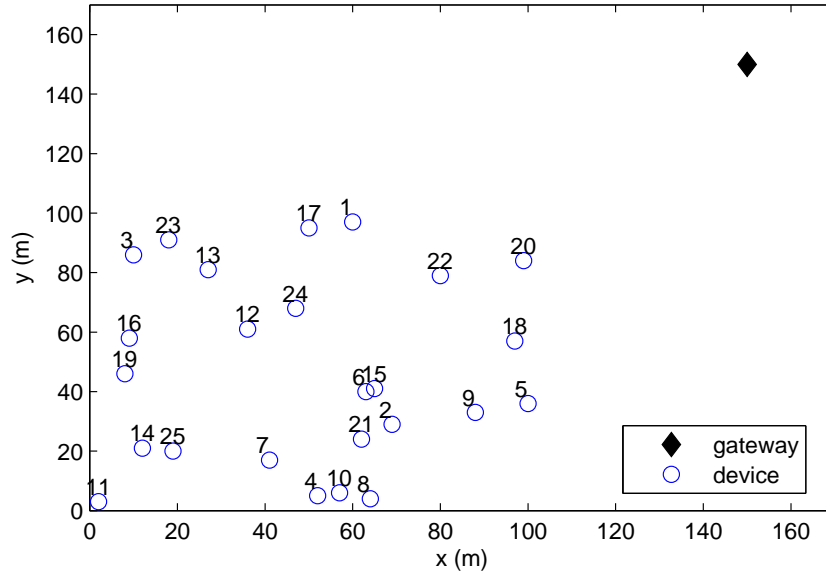


Figure 4.4: Scenario diagram for cluster-based capillary networks using the CMISO system

Algorithm 6: CH and cooperative devices selection algorithm to maximise the network lifetime

```

1 for each  $i \in [1, \mathcal{N}_{total}]$  do
2     /* Exhaustive search to find the optimum CH */
3     Set  $CH = i$ .
4     for each  $m \in [1, 2, \dots, \mathcal{N}_{particle}]$  do
5         for each  $n \in [1, 2, \dots, \mathcal{N}_{total} - 1]$  do
6             Set the quantum position  $x_{mn}^1$  by 0 or 1 randomly
7             Set the quantum velocity  $v_{mn}^1$  to be  $1/\sqrt{2}$ 
8         end
9         Update the network lifetime  $f_m^1$  by (4.17)
10        /* The local optimum is the initialised particles at the first
11        generation */
12        Set the local optimum fitness value  $f_m^{pbest_{max}}$  to be  $f_m^1$ 
13        Set the local optimum position  $\mathbf{x}_m^{pbest_{max}}$  to be  $\mathbf{x}_m^1$ 
14    end
15    /* Update the global optimum */
16    Update the global optimum fitness value  $f^{gbest_{max}}$  and the global optimum
17    position  $\mathbf{x}^{gbest_{max}}$  by (2.11)
18    for each  $t \in [1, 2, \dots, T_{max}]$  do
19        for each  $m \in [1, 2, \dots, \mathcal{N}_{particle}]$  do
20            for each  $n \in [1, 2, \dots, \mathcal{N}_{total} - 1]$  do
21                Update the quantum rotation angle  $\theta_{mn}^{t+1}$  by (2.12)
22                Update the quantum velocity  $v_{mn}^{t+1}$  by (2.6)
23                Update the quantum position  $x_{mn}^{t+1}$  by (2.7)
24            end
25            Update the network lifetime  $f_m^{t+1}$  by (4.17)
26            /* Update local optimum */
27            if  $f_m^{t+1} > f_m^{pbest_{max}}$  then
28                Set the local optimum fitness value  $f_m^{pbest_{max}}$  to be  $f_m^{t+1}$ 
29                Set the local optimum position  $\mathbf{x}_m^{pbest_{max}}$  to be  $\mathbf{x}_m^{t+1}$ 
30            end
31        end
32        Update the temporary global optimum fitness value  $g^{gbest_{max}}$  by (2.11)
33        /* Find the final global optimum */
34        if  $g^{gbest_{max}} > f^{gbest_{max}}$  then
35            Set the final global optimum fitness  $f^{gbest_{max}}$  to be  $g^{gbest_{max}}$ 
36            Update the global optimum position  $\mathbf{x}^{gbest_{max}}$  according to  $g^{gbest_{max}}$ 
37        end
38    end
39    /* Find the optimum set of Coops for CH  $i$  */
40    Set the final optimum network lifetime  $f_{final}(i)$  to be  $f^{gbest_{max}}$ 
41    Set the final optimum set of Coops for CH  $i$   $\mathbf{x}_{final}(i)$  to be  $\mathbf{x}^{gbest_{max}}$ 
42 end
43 /* Find the best CH and its Coops by the results of exhaustive
44 search */
45  $f_{max} = \max\{f_{final}(1), \dots, f_{final}(i), \dots, f_{final}(\mathcal{N}_{total})\}$ 
46 Set the index to obtain  $f_{max}$  to be  $CH_{max}$ 
47 Set the optimum set of Coops to be  $\mathbf{x}_{final}(CH_{max})$ 
48 return  $CH_{max}$  and  $\mathbf{x}_{final}(CH_{max})$  as the optimum set of CH and Coops

```

Most system parameters used in the chapter are as list in Table 3-A and some particular system parameters are list in Table 4-A.

Table 4-A: System Parameters in Scenario Using CMISO system

Parameter	Value	Meaning
t_s	0s [ZCSA10]	the time when battery charge starts
F_{block}	200 [Jay04]	block size of STBC code
ρ_{train}	2 [Jay04]	training symbol parameter
ϕ	0.95 [ZCSA10]	the efficiency of the DC-DC
∇	3volts [ZCSA10]	output voltage of the DC-DC

4.3.3.2 Simulation Platform Design

The simulation process of the proposed CH and Coops selection algorithm aiming at energy efficiency in Subsection 4.3.2 consists of several logic blocks and simulation loops, as shown in Figure 4.5.

A. Scenario Initialisation module

In this module, the individual information of all devices and the capillary gateway are initialised, as shown in Figure 3.6. In specific, the position of capillary gateway is set at (150m, 150m). The battery capacity of all devices is set to be 2400mAh, the position of each device is initialised as shown in Figure 4.4.

B. Exhaustive Search module

This module assumes every device to be CH in turn by exhaustive search technique before and after the QPSO-based Coops selection module. It uses an iteration which starts at the device with label 1 and ends at devices with label \mathcal{N}_{total} (i.e. 25 in the designed scenario).

C. QPSO-based Coops selection module

This module performs QPSO algorithm to select the best Coops for a particular CH.

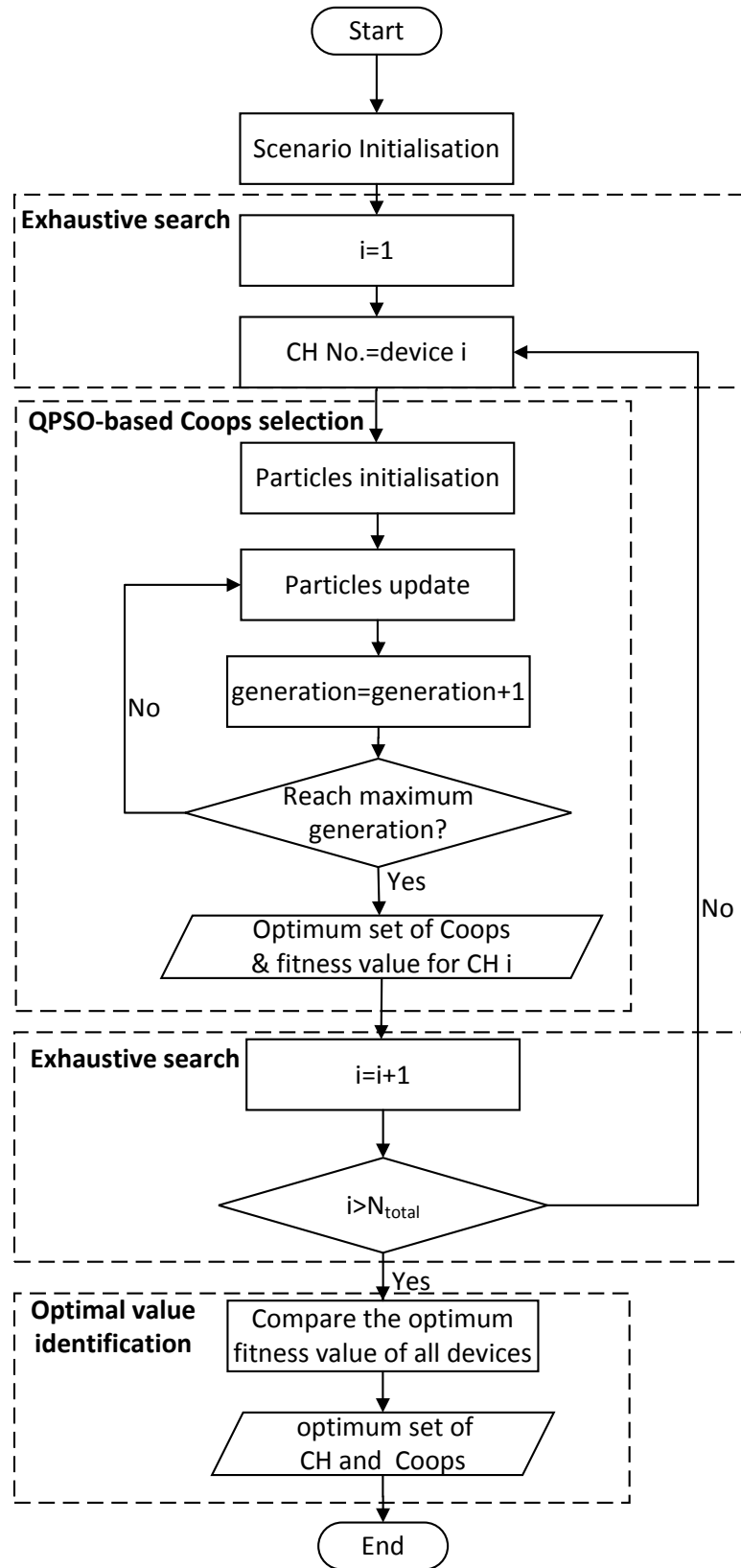


Figure 4.5: Flowchart of the proposed CH and Coops selection algorithm aiming at energy efficiency(Algorithm 6)

It includes particle initialisation and particle updating as described in Subsection 3.5.2, generation iteration process and the output of global optimum fitness value and set of Coops after a predetermined generations.

D. Optimum value identification module

This module finds the maximum fitness value (i.e. network lifetime) from all fitness values produced by exhaustive search module and QPSO-based Coops selection module. It also gets the optimum set of Coops and CH as the output based on the index which leads to the maximum fitness value.

4.3.3.3 Simulation Results

Table 4-B: Particle number and generation number selection in terms of algorithm time complexity

particle number	optimal generation number	function evaluation
4	332	1328
6	205	1230
8	151	1208
10	112	1120
12	101	1212
14	92	1288
16	88	1408
18	81	1458
20	76	1520

As described in Section 3.5.3, the particle number and generation number play important roles in the performance of QPSO. Table 4-B shows the optimum number of generations and function evaluations for different number of particles to converge to the same final optimum global fitness value. The simulation iteration is set to be 50 times. Figure 4.6 shows the trend of optimum generation number of function evaluation in Table 4-B. In Figure 4.6, the optimum generation number decreases dramatically from 4 to 10 particles. This is because more particles means better opportunity to find the optimum fitness value within a limited generations. As the particle number increases

from 10 to 20, the optimum generation number varies within a small range. Focusing on the function evaluations, it can be seen that the minimum FE is achieved at the point where the particle number is 10 and the optimum generation number is 112. In this chapter, the particle number is set to be 10 and the generation number is set to be 120 (around 112) to decrease the algorithm complexity as well as ensure the performance of QPSO.

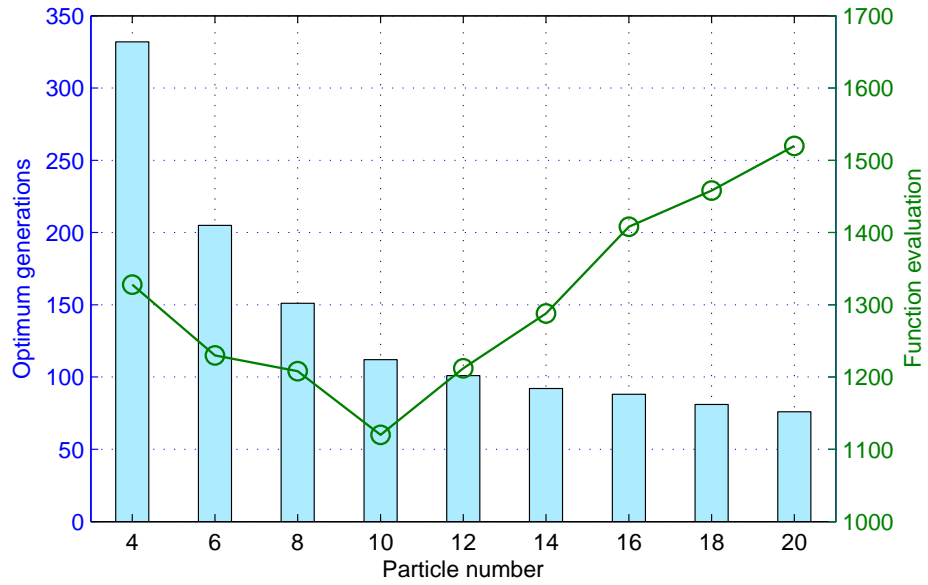


Figure 4.6: Particle number and generation number selection in terms of algorithm time complexity

Next, Figure 4.7 and Figure 4.8 take the location of capillary gateway into consideration. Set \bar{P}_{BER}^{THR} to be 10^{-5} . The location of capillary gateway in Figure 4.7 and Figure 4.8 are set to be the horizontal distance between the updated capillary gateway and the capillary gateway at $(150m, 150m)$ in scenario initialisation. For example, the location of capillary gateway is $50m$ indicates the capillary gateway is located at $(200m, 200m)$. It is observed that the proposed CH and cooperative devices selection algorithm outperforms PSO and QGA in terms of network lifetime by approximately 8% in Figure 4.7. Moreover, the location of capillary gateway is closely related to the long-haul distance, which indicates that the energy consumption in long-haul communication dominates the network lifetime. Figure 4.8 investigates the number of Coops with

respect to the capillary gateway location. With the increment of long-haul distance for all algorithms, more Coops are required to support the long-haul transmission. It is also observed that although the proposed QPSO-based CH and Coops selection algorithm outperforms PSO and QGA algorithms, the number of Coops selected by the proposed algorithm is not the highest, which indicates that higher number of Coops is not necessary. Furthermore, as for the proposed algorithm, the number of Coops remains the same from $150m$ to $250m$, because additional suitable Coops cannot be found.

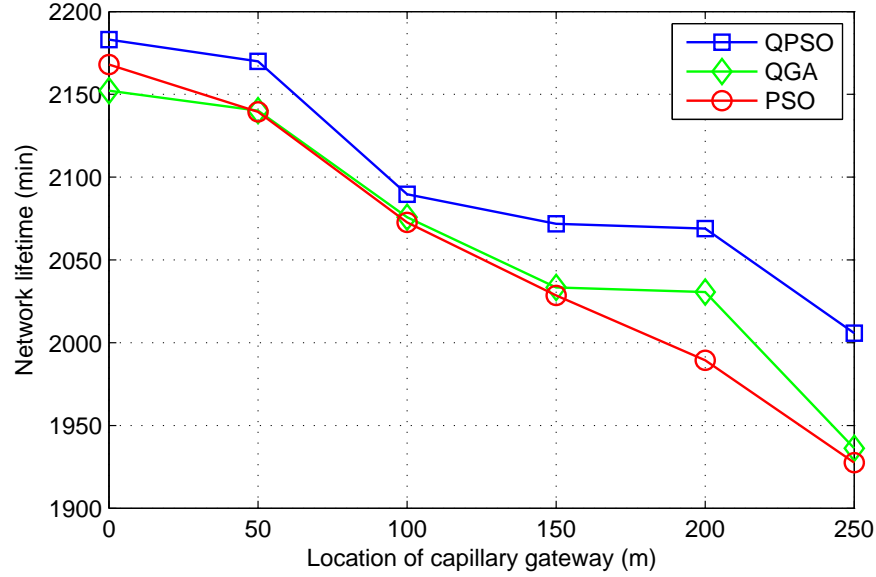


Figure 4.7: Network lifetime with respect to the capillary gateway location

Finally, Figure 4.9 and Figure 4.10 focus on the network lifetime and number of Coops in terms of BER threshold \bar{P}_{BER}^{THR} . In Figure 4.9, the network lifetime increases with the BER threshold. This is because with the increment of BER threshold, more energy can be saved in the long-haul transmission to guarantee the QoS provision. Additionally, due to optimum Coops selected by the proposed QPSO algorithm, it outperforms QGA by approximately 8% and PSO by approximately 12% in terms of network lifetime. However, it can be seen that the number of Coops selected by the proposed QPSO algorithm is also not highest in Figure 4.10, which indicates that the good performance of CMISO system may not require the higher number of Coops. Besides, it is also observed that the

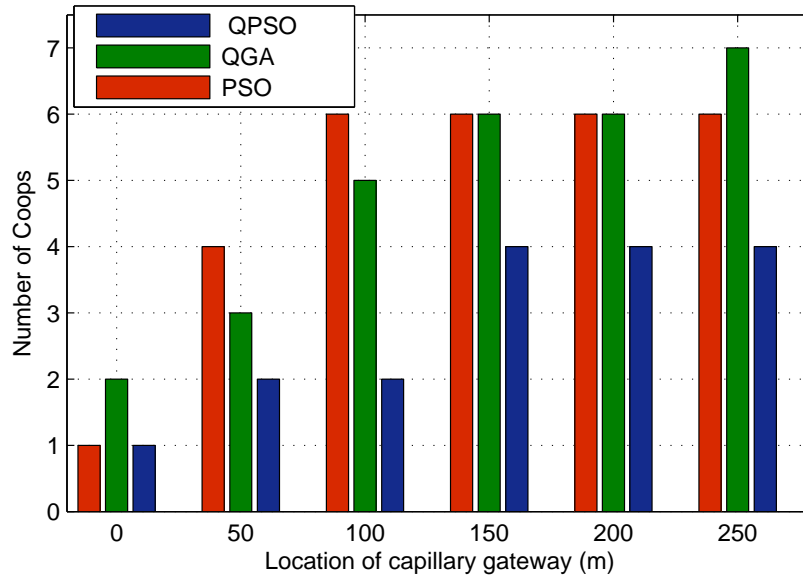


Figure 4.8: Number of Coops with respect to the capillary gateway location

number of selected Coops decreases with the increment of BER threshold. Therefore, it can be concluded that more Coops can be selected in long-haul transmission in order to guarantee better QoS requirement.

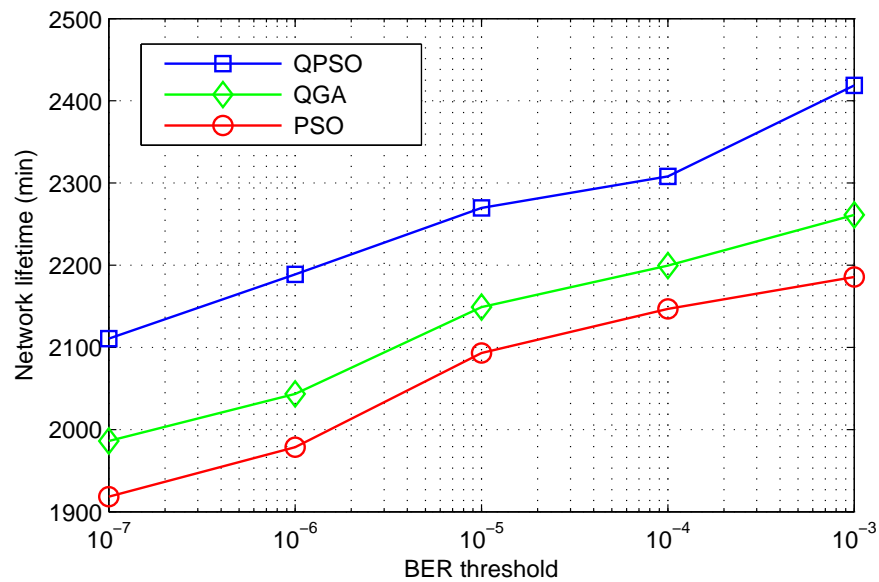


Figure 4.9: Network lifetime with respect to BER threshold

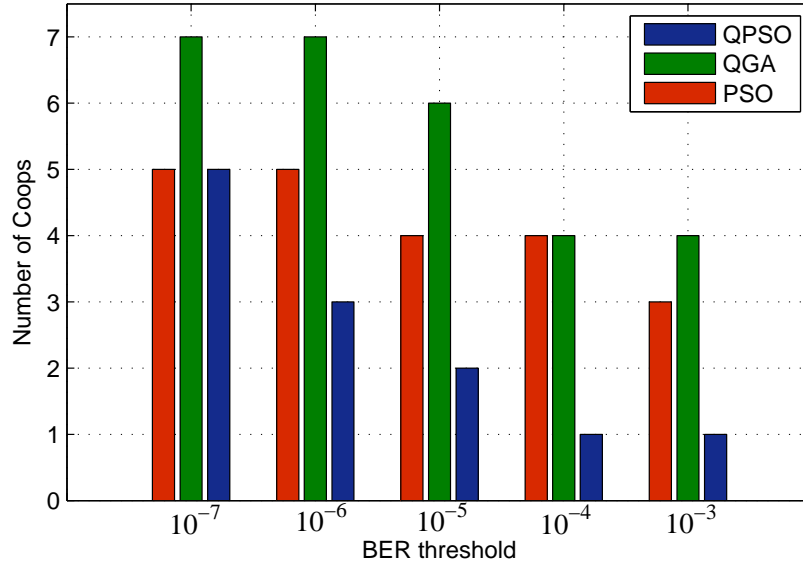


Figure 4.10: Number of Coops with respect to BER threshold

4.3.3.4 Conclusions

In this section, the Coops selection for cluster-based capillary networks is investigated using QPSO algorithm with the aim of maximising the network lifetime. It is shown that the CH and Coops selection plays an important role to prolong the network lifetime. In the proposed algorithm, QPSO algorithm is applied to determined optimum Coops for pre-selected CH. Simulation results show that the proposed QPSO algorithm outperforms PSO and QGA in terms of average network lifetime.

4.4 QoS-based CH and Cooperative Devices Selection

This section investigates the cooperative devices selection using CMISO systems in cluster-based capillary networks with the objective of QoS provision optimisation. The PER minimisation problem formulation is presented first, followed by the proposed CH and cooperative devices selection algorithm and simulation.

4.4.1 QoS-based Problem Formulation

In this subsection, the overall energy consumption of intra-cluster transmission, data aggregation and inter-cluster transmission are formulated. The overall PER is derived and the research problem to minimise the overall PER is presented.

4.4.1.1 Energy Consumption for Intra-cluster Transmission

In the data collection phase, the CH acts as the receiver dissipating the reception power consumption, while both CMs and Coops transmit data to the CH, dissipating the transmission power consumption. As the assumption of squared power path loss, the energy consumption per bit for the data collection phase is expressed as

$$E_b^{DC} = \sum_{i=1}^{\mathcal{N}_{total}-1} (1 + \varphi_{amp}) \frac{(4\pi)^2 M_t N_r}{G_t G_r \lambda^2} \cdot d_{i,CH}^2 \cdot \frac{\bar{E}_b}{N_0} \Big|_{intra} + \frac{(\mathcal{N}_{total} - 1)P_{ct} + P_{cr}}{R_b} \quad (4.18)$$

where $d_{i,CH}$ is the distance between device i and CH. The first term is the energy consumption for power amplifier of all non-CH devices, and the second term is the energy consumption for circuit blocks of all devices.

In the local broadcasting phase, CH acts as the transmitter to broadcast the aggregated data to Coops, dissipating the transmission power consumption, and all Coops receive data information from the CH, dissipating the reception power consumption. Due to the broadcast nature of the wireless channel, if the Coop with the maximum distance, denoted by d_{max} , can receive the aggregated data from the CH, the other Coops can simultaneously receive these data. Then the energy consumption per bit for the local broadcasting phase is given by

$$E_b^{LB} = (1 + \varphi_{amp}) \frac{(4\pi)^2 M_t N_r}{G_t G_r \lambda^2} \cdot d_{max}^2 \cdot \frac{\bar{E}_b}{N_0} \Big|_{intra} + \frac{P_{ct} + \mathcal{N}_{Coop} P_{cr}}{R_b} \quad (4.19)$$

where the first term refers to the energy consumption for the power amplifier of CH,

and the second term is the energy consumption for the circuit blocks for the CH and all Coops.

4.4.1.2 Energy Consumption and Packet Size for Data Aggregation

In this section, the overall energy consumption for data aggregation is as follows

$$E_{agg} = \mathcal{N}_{total} L_{data} E_{bf} \quad (4.20)$$

where E_{bf} is the energy consumption per bit for uniform data aggregation.

The amount of data after aggregation is as follows

$$L_{agg} = \frac{\mathcal{N}_{total}}{\mathcal{N}_{total}\gamma_{agg} - \gamma_{agg} + 1} L_{data} \quad (4.21)$$

where γ_{agg} is the data aggregation factor.

4.4.1.3 Energy Consumption and Packet Size for Long-haul Transmission

In the long-haul cooperative transmission phase, CH and Coops jointly transmit the STBC-coded data to the capillary gateway, dissipating the transmission power consumption. Thus, the energy consumption per bit for the long-haul cooperative transmission phase is expressed as

$$E_b^{LH} = \sum_{i=1}^{\mathcal{N}_{Coop}+1} (1 + \varphi_{amp}) \frac{(4\pi)^2 M_l N_r}{G_t G_r \lambda^2} \cdot d_{i,g}^{\kappa_{i,g}} \cdot \frac{\bar{E}_b}{N_0} \bigg|_{inter} + \frac{(\mathcal{N}_{Coop} + 1) P_{ct}}{R_b} \quad (4.22)$$

where $d_{i,g}$ is the long-haul distance between the Coops/CH i and the capillary gateway, $\kappa_{i,g}$ is the path loss exponent of the long-haul transmission and is in the range between 2 and 3. The first term is the energy consumption for power amplifier of CH and Coops, and the second term is the energy consumption for transmission circuit power blocks of CH and Coops.

Training overhead is introduced into CMISO scheme for channel estimation and the number of required training symbols is proportional to the number of transmit antennas. Therefore, the packet size of Coops and CH in the long-haul transmission is,

$$L_c = \frac{F_{block}}{F_{block} - \rho_{train}(N_{Coop} + 1)} L_{agg} \quad (4.23)$$

where F_{block} is the block size of STBC code, $\rho_{train}(N_{Coop} + 1)$ is the number of training symbols in each block.

4.4.1.4 Overall PER Formulation

The average BER of the intra-cluster communication with a square constellation (i.e. $b = M/2$ is even and b is called the constellation size of MQAM) in AWGN channel [DZ04] is given by

$$\bar{P}_{BER}^{intra} \doteq \frac{4(1 - 1/\sqrt{M})}{\log_2 M} \cdot Q \left(\sqrt{\frac{3 \log_2 M}{M - 1} \cdot \frac{\bar{E}_b}{N_0}} \Big|_{intra} \right) \quad (4.24)$$

where $Q(x) = \int_x^\infty \frac{1}{\sqrt{2\pi}} e^{-\frac{u^2}{2}} du$.

The average BER of the inter-cluster communication with a square constellation MQAM in Rayleigh fading channel [ZD07] is given by

$$\bar{P}_{BER}^{inter} \doteq \frac{4}{\log_2 M} \cdot \left(1 - \frac{1}{\sqrt{M}}\right) \cdot \left(\frac{1 - \mu}{2}\right)^{\mathcal{N}_{Coop} + 1} \cdot \sum_{l=0}^{\mathcal{N}_{Coop}} \binom{\mathcal{N}_{Coop} + l}{l} \cdot \left(\frac{1 + \mu}{2}\right)^l \quad (4.25)$$

where

$$\mu = \sqrt{\frac{\iota}{1 + \iota}} \quad (4.26a)$$

$$\iota = \frac{1}{\mathcal{N}_{Coop} + 1} \cdot \frac{3 \log_2 M}{2(M - 1)} \cdot \frac{\bar{E}_b}{N_0} \Big|_{inter} \quad (4.26b)$$

In terms of BER in the transmission, the PER is derived as $P_{PER} = 1 - (1 -$

$P_{BER})^{L_{packet}}$ [KS05], where L_{packet} is the number of bits in the packet. Moreover, the overall packet size in the data collection phase is $L_{data}(\mathcal{N}_{total} - 1)$, because $(\mathcal{N}_{total} - 1)$ non-CH devices transmit packets of L_{data} bits to the CH. In the local broadcasting phase, \mathcal{N}_{Coop} Coops receive the aggregated data of size L_{agg} from the CH, therefore the overall packet size of this phase is $L_{agg}\mathcal{N}_{Coop}$. In the long-haul transmission phase, the CH and \mathcal{N}_{Coop} Coops transmit the STBC-coded packet of size L_c to the capillary gateway, so the overall packet size of this phase is $L_c(\mathcal{N}_{Coop} + 1)$. Therefore, the PER of the data collection phase, the local broadcasting phase and the long-haul transmission phase are given by

$$\bar{P}_{PER}^{DC} = 1 - (1 - \bar{P}_{BER}^{intra})^{L_{data}(\mathcal{N}_{total}-1)} \quad (4.27a)$$

$$\bar{P}_{PER}^{LB} = 1 - (1 - \bar{P}_{BER}^{intra})^{L_{agg}\mathcal{N}_{Coop}} \quad (4.27b)$$

$$\bar{P}_{PER}^{LH} = 1 - (1 - \bar{P}_{BER}^{inter})^{L_c(\mathcal{N}_{Coop}+1)} \quad (4.27c)$$

As the result, the overall PER during the whole transmission is given by,

$$\bar{P}_{PER}^{overall} = \bar{P}_{PER}^{DC} + (1 - \bar{P}_{PER}^{DC})\bar{P}_{PER}^{LB} + (1 - \bar{P}_{PER}^{DC})(1 - \bar{P}_{PER}^{LB})\bar{P}_{PER}^{LH} \quad (4.28)$$

where the first term indicates that data error occurs in the transmission of the data collection phase, which results in the error transmission of the following local broadcasting phase and long-haul transmission phase; the second term means that the data transmission is successful in the data collection phase while error occurs in the local broadcasting phase, which results in the error transmission in the long-haul transmission phase; the third term indicates that data transmission of both data collection and local transmission phase are successful, however, error occurs in the long-haul transmission phase.

The research problem is to find the optimum set of CH and cooperative devices

$\mathcal{C} = \{CH, Coop_1, \dots, Coop_{\mathcal{N}_{Coop}}\}$ in cluster-based capillary networks, with the objective to minimise the overall packet error rate $\bar{P}_{PER}^{overall}$. Assume the overall sum of energy consumption for all devices in three phases is limited to E_t , the research problem in this section is expressed as

$$\begin{aligned}
 & \underset{\mathcal{C}}{\text{minimise}} \bar{P}_{PER}^{overall} \\
 & \text{s.t.} \quad \begin{cases} 1 + \mathcal{N}_{CM} + \mathcal{N}_{Coop} = \mathcal{N}_{total} \\ 0 \leq \mathcal{N}_{Coop} \leq \mathcal{N}_{total} - 1 \\ LE_b^{DC} + E_{AG} + L_{agg}E_b^{LB} + L_cE_b^{LH} \leq E_t \\ \left. \frac{\bar{E}_b}{N_0} \right|_{intra} = \left. \frac{\bar{E}_b}{N_0} \right|_{inter} \end{cases} \quad (4.29)
 \end{aligned}$$

4.4.2 QoS-based CH and Cooperative Devices Selection Algorithm

The capillary gateway executes the CH and Coops selection process based on QPSO and exhaustive search, after receiving every device's individual information (i.e. residual energy and location).

The QPSO-based CH and Coops selection algorithm aiming at minimising the overall PER is described in Algorithm 7. Denote the maximum generation to be T_{max} . Firstly, line 2 assumes every device in the cluster to be CH in turn by exhaustive search and iteration ends at line 34. Secondly, the position, velocity, local optimum and global optimum of all particles are initialised, as refer to line 1 to line 12. Thirdly, the swarm updating process is performed from line 13 to line 31. In particular, line 15 to line 19 describes the updating process of a particle, including the regeneration of rotation angle by (2.12), velocity by (2.6) and position by (2.7). Then the fitness value (i.e. overall PER) of particle is updated by mapping the updated particle position to the Coop candidates, as described in line 20. Furthermore, line 21 to line 24 updates the individual optimum in the current generation by comparing the updated fitness value

Algorithm 7: CH and cooperative devices selection algorithm to minimise the overall PER

```

1 for each  $i \in [1, \mathcal{N}_{total}]$  do
    /* Exhaustive search to find the optimum CH */
2   Set  $CH = i$ 
3   for each  $m \in [1, 2, \dots, \mathcal{N}_{particle}]$  do
4     for each  $n \in [1, 2, \dots, \mathcal{N}_{total} - 1]$  do
5       Set the quantum position  $x_{mn}^1$  by 0 or 1 randomly
6       Set the quantum velocity  $v_{mn}^1$  to be  $1/\sqrt{2}$ 
7     end
8     Update the overall PER  $f_m^1$  by (4.29)
9     /* The local optimum is the initialised particles at the first generation */
10    Set the local optimum fitness value  $f_m^{pbest_{min}}$  to be  $f_m^1$ 
11    Set the local optimum position  $\mathbf{x}_m^{pbest_{min}}$  to be  $\mathbf{x}_m^1$ 
12  end
13  /* Update the global optimum */
14  Update the global optimum fitness value  $f^{gbest_{min}}$  and the global optimum position  $\mathbf{x}^{gbest_{min}}$  by (2.9)
15  for each  $t \in [1, 2, \dots, T_{max}]$  do
16    for each  $m \in [1, 2, \dots, \mathcal{N}_{particle}]$  do
17      for each  $n \in [1, 2, \dots, \mathcal{N}_{total} - 1]$  do
18        Update the quantum rotation angle  $\theta_{mn}^{t+1}$  by (2.12)
19        Update the quantum velocity  $v_{mn}^{t+1}$  by (2.6)
20        Update the quantum position  $x_{mn}^{t+1}$  by (2.7)
21      end
22      Update the overall PER  $f_m^{t+1}$  by (4.29)
23      /* Update local optimum */
24      if  $f_m^{t+1} < f_m^{pbest_{min}}$  then
25        Set the local optimum fitness value  $f_m^{pbest_{min}}$  to be  $f_m^{t+1}$ 
26        Set the local optimum position  $\mathbf{x}_m^{pbest_{min}}$  to be  $\mathbf{x}_m^{t+1}$ 
27      end
28    end
29    Update the temporary global optimum fitness value  $g^{gbest_{min}}$  by (2.9)
30    /* Find the final global optimum */
31    if  $g^{gbest_{min}} < f^{gbest_{min}}$  then
32      Set the final global optimum fitness value  $f^{gbest_{min}}$  to be  $g^{gbest_{min}}$ 
33      Update the global optimum position  $\mathbf{x}^{gbest_{min}}$  according to  $g^{gbest_{min}}$ 
34    end
35  end
36  Set the final optimum overall PER  $f_{final}(i)$  to be  $f^{gbest_{min}}$ 
37  Set the final optimum set of Coops for CH  $i$   $\mathbf{x}_{final}(i)$  to be  $\mathbf{x}^{gbest_{min}}$ 
38 end
39  $f_{min} = \min\{f_{final}(1), \dots, f_{final}(i), \dots, f_{final}(\mathcal{N}_{total})\}$ 
40 Set the index to obtain  $f_{min}$  to be  $CH_{min}$ 
41 Set the optimum set of Coops to be  $\mathbf{x}_{final}(CH_{min})$ 
42 return  $CH_{min}$  and  $\mathbf{x}_{final}(CH_{min})$  as the optimum set of CH and Coops

```

with the previous local optimum fitness value. Then the temporary global optimum at current generation is updated by (2.9) in line 26, which is further compared with global optimum fitness value at previous generation to obtain the final global optimum fitness value at the current generation from line 27 to line 30. Line 32 and line 33 set the minimum fitness value and best set of Coops for the assumed CH. Moreover, Line 35 finds the minimum fitness value from all the fitness values produced in line 32, while line 36 and 37 select the optimum set of CH and Coops which are returned as the output of this algorithm.

At last, the capillary gateway informs every device about its role (i.e. CH, CM or Coop) based on the result of Algorithm 7.

4.4.3 Simulation and Conclusions

This subsection presents the simulation scenario, system parameters, simulation platform, simulation results and conclusions.

4.4.3.1 Scenario Design and System Parameters

In this subsection, the scenario is the same as the one as described in Subsection 4.3.3.1. The system parameters used in this section are also the same as shown in Table 3-A and Table 4-A.

4.4.3.2 Simulation Platform Design

In this subsection, the simulation platform design is similar to Subsection 4.3.3.2. However, the particles in QPSO-based Coops selection module are updated to find the minimum fitness value (i.e. overall PER) instead of the maximum fitness value (i.e. network lifetime) in Algorithm 6.

4.4.3.3 Simulation Results

Due to the same scenario setting, the particle number and generation number in this simulation is also set to be 10 and 120, respectively.

First, Figure 4.11 illustrates the convergence of QPSO. The overall PER decreases with the number of generations. It can be seen that the final overall PER can be achieved after a certain number of generations for different number of particles, which indicates the convergence of QPSO algorithm.

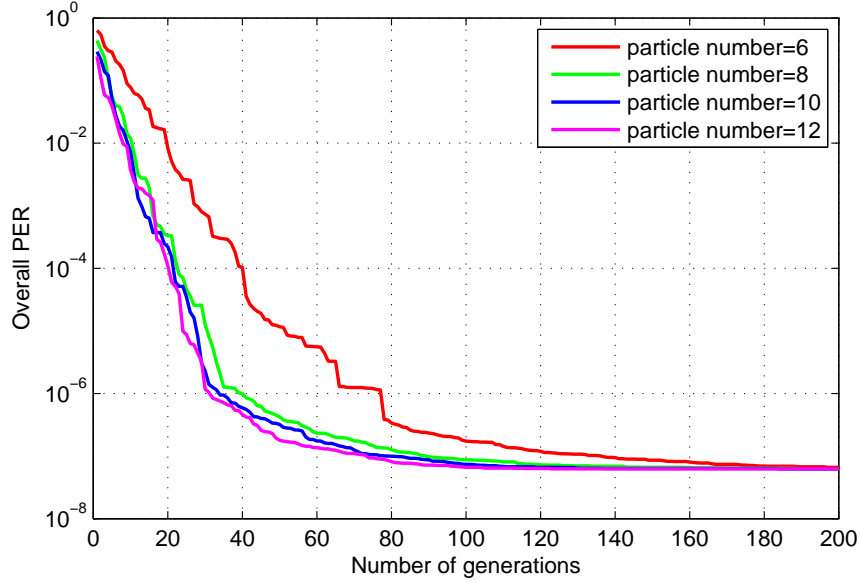


Figure 4.11: Convergence of QPSO

A comparison of overall PER is made in Figure 4.12. It is shown that the overall PER decreases with the increment of energy constraint. This is due to the fact that more Coops can be selected to guarantee the successful packet delivery rate in the case with more energy constraint. In addition, it is obvious that the proposed QPSO-based CH and Coops selection algorithm outperforms PSO and QGA under the same energy constraint. Moreover, as for QPSO, the overall PER is lower than 10^{-5} after the energy constraint is more than $1.2J$, therefore if successful transmission in all phases has to be ensured, the whole network ought to supply at least $1.2J$ and select optimum cooperative

coalition by the proposed CH and Coops selection algorithm.

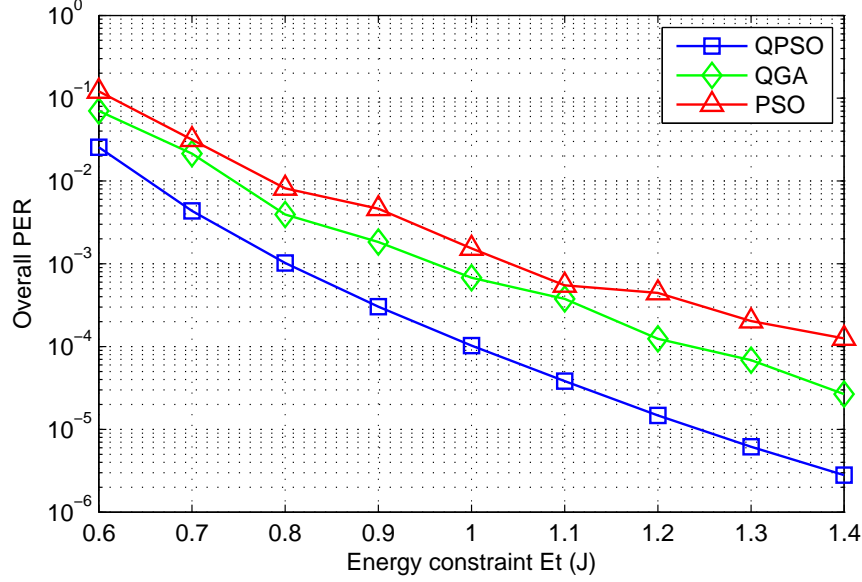
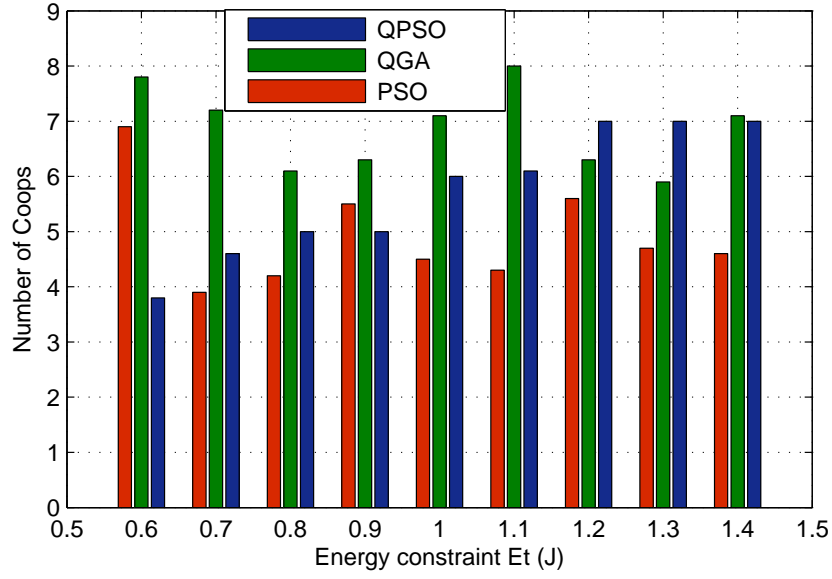


Figure 4.12: Overall PER in terms of energy constraint E_t

Additionally, the number of selected Coops of all algorithms are compared in terms of energy constraint in Figure 4.13. It can be seen that the number of Coops selected by the QPSO is not always the highest. Considering the fact that the overall PER of QPSO outperforms other algorithms in terms of energy constraint as indicated in Figure 4.12, it can be concluded that the proposed QPSO algorithm can select different number of optimum Coops dynamically according to different scenario setting. Moreover, as for the proposed QPSO algorithm, the selected number of coops increases slowly with respect to the energy constraint, because more energy constraint is able to support more Coops in the long-haul transmission. Particularly, the number of Coops remains to be 7 at $1.2J$, $1.3J$ and $1.4J$, because the additional suitable Coops cannot be found.

Figure 4.14 takes the location of capillary gateway into consideration. Set E_b to be $0.8J$. The capillary gateway location has the same definition as described in Section 4.3.3.3. It is observed that the proposed QPSO algorithm outperforms PSO and QGA significantly. Moreover, the location of capillary gateway is closely related to the long-haul distance, which indicates that the PER of long-haul transmission dominates

Figure 4.13: Number of selected Coops in terms of energy constraint E_t

the overall PER. Thus, more energy supply is expected to guarantee successful transmission in scenario of farther capillary gateway.

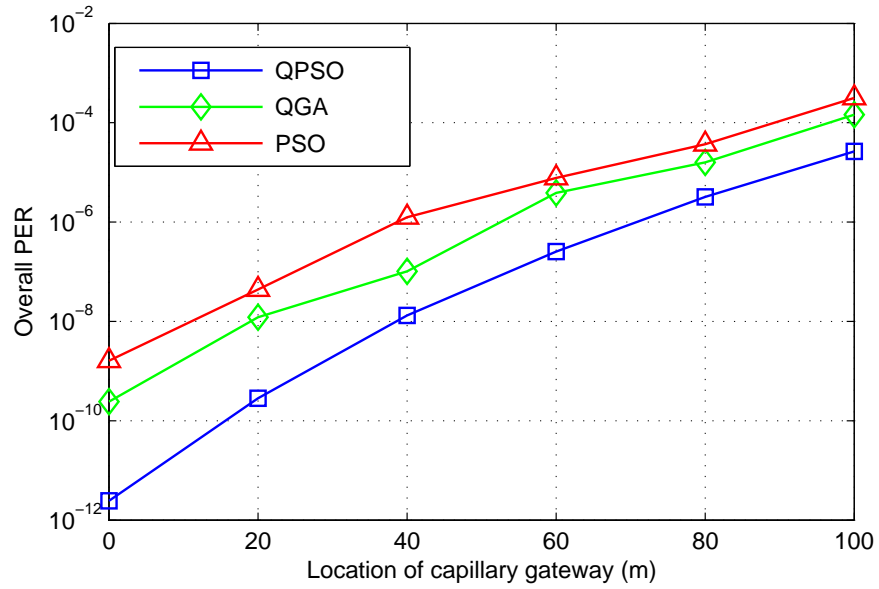


Figure 4.14: Overall PER in terms of capillary gateway location

Finally, Figure 4.15 investigates the number of Coops with respect to the location of capillary gateway. Set E_b to be $0.8J$. In general, more Coops can be selected in order to

decrease the overall PER under the same energy constraint. As for the proposed CH and Coops selection algorithm, the number of optimum Coops decreases with the increment of the capillary gateway location. This can be explained by the fact that the farther the capillary gateway, the higher energy consumption of the long-haul transmission phase, and thus less Coops can be supported under the same energy constraint.

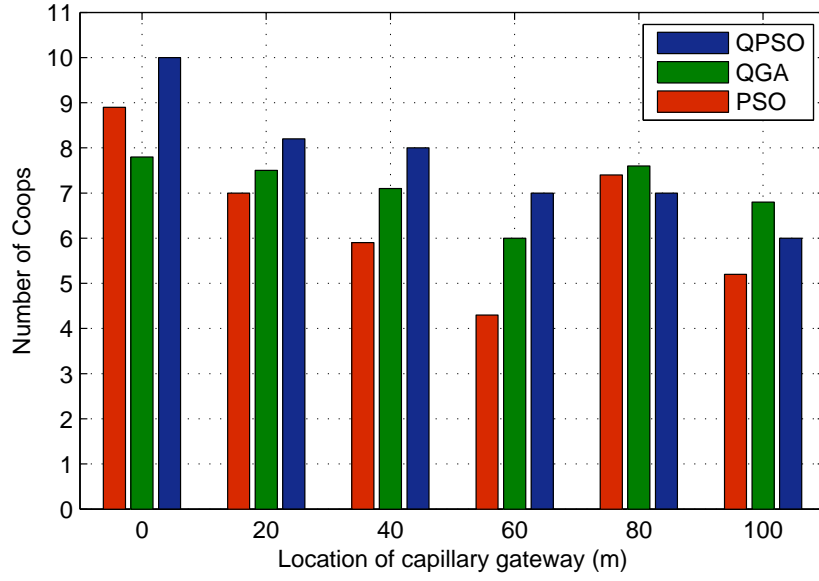


Figure 4.15: Number of Coops in terms of capillary gateway location

4.4.3.4 Conclusions

In this section, the optimum set of CH and Coops selection with the aim of minimising the overall PER is investigated in cluster-based capillary networks. Particularly, QPSO algorithm is applied in order to select best set of Coops for the potential CH, and exhaustive search is used to determine the optimum CH. It is proved that QPSO is competitive to PSO and QGA algorithms with an advantage of employing better evolutionary equations and simpler updating equations with high performance.

4.5 CH and Cooperative Devices Selection for Joint Optimisation

This section focuses on the tradeoff between energy efficiency and QoS provision optimisation using CMISO system by selecting optimum set of CH and Coops.

4.5.1 Joint Optimisation Problem Formulation

Research objectives of energy efficiency and QoS provision optimisation are formulated in this subsection. More specifically, the network lifetime time by (4.17) in Section 4.3 is utilized to optimise energy efficiency, and the overall PER by (4.29) in Section 4.4 is utilized to optimise the QoS provision.

4.5.1.1 Objective 1: Network Lifetime Maximisation

In this section, (4.2) to (4.16) are used to calculate the average battery time \bar{T}_{avg}^{op} , which represents the network lifetime and is expressed as follows

$$\bar{T}_{avg}^{op} = \frac{\sum_{k=1}^{\mathcal{N}_{total}} T^{op}(k)}{\mathcal{N}_{total}} \quad (4.30)$$

4.5.1.2 Objective 2: Overall PER Minimisation

The overall PER is obtained from (4.24) to (4.27) and expressed as follows

$$\bar{P}_{PER}^{overall} = \bar{P}_{PER}^{DC} + (1 - \bar{P}_{PER}^{DC})\bar{P}_{PER}^{LB} + (1 - \bar{P}_{PER}^{DC})(1 - \bar{P}_{PER}^{LB})\bar{P}_{PER}^{LH} \quad (4.31)$$

4.5.1.3 Tradeoff Formulation of Network Lifetime and Overall PER

The research objective is to find the optimum cooperative coalition $\mathcal{C} = \{CH, Coop_1, \dots, Coop_{\mathcal{N}_{Coop}}\}$ in order to achieve the optimal tradeoff between network lifetime and QoS provision, that is,

$$\begin{cases} \underset{\mathcal{C}}{\text{maximise}} \bar{T}_{op}^{avg} \\ \underset{\mathcal{C}}{\text{minimise}} \bar{P}_{PER}^{overall} \end{cases} \quad s.t. \quad 0 \leq \mathcal{N}_{Coop} \leq \mathcal{N}_{total} - 1 \quad (4.32)$$

4.5.2 CH and Coops Selection Algorithm for Joint Optimisation

The capillary gateway executes the CH and Coops selection algorithm based on NSGA-II and QPSO that are called NSQPSO in this thesis, after receiving every device's individual information (i.e. residual energy and location).

The proposed CH and Coops selection algorithm aiming at the optimum tradeoff between network lifetime and overall PER is described in Algorithm 8. The following notations are made in this algorithm:

- Denote the swarm of all particles in the t -th generation to be \mathcal{S}_t , which contains the information for the quantum position, velocity, local optimum and global optimum of all particles.
- Denote the set of non-dominated particles at generation t to be $\hat{\mathcal{S}}_t$.
- Denote $f_m^t(1)$ to be particle m 's fitness value of network lifetime in generation t .
- Denote $f_m^t(2)$ to be particle m 's fitness value of overall PER in generation t .
- Denote the maximum generation to be T_{max} .

Firstly, line 2 assumes every device in the cluster to be CH in turn by exhaustive search and iteration ends at line 31. Secondly, the position, velocity, local optimum and

Algorithm 8: CH and Coops selection algorithm to achieve the optimum tradeoff between energy efficiency and QoS provision

```

1 for each  $i \in [1, \mathcal{N}_{total}]$  do
2   Set  $CH = i$ .
3   for each  $m \in [1, 2, \dots, \mathcal{N}_{particle}]$  do
4     for each  $n \in [1, 2, \dots, \mathcal{N}_{total} - 1]$  do
5       Set the quantum position  $x_{mn}^1$  by 0 or 1 randomly
6       Set the quantum velocity  $v_{mn}^1$  to be  $1/\sqrt{2}$ 
7     end
8     Update the network lifetime  $f_m^1(1)$  by (4.30) and overall PER  $f_m^1(2)$ 
       by (4.31)
9     Set the local optimum fitness value for energy efficiency  $f_m^{pbest_{max}}(1)$  to be
        $f_m^1(1)$ 
10    Set the local optimum fitness value for QoS provision  $f_m^{pbest_{min}}(2)$  to be
        $f_m^1(2)$ 
11    Set the local optimum position  $\mathbf{x}_m^{pbest}$  to be  $\mathbf{x}_m^1$ 
12  end
13  Generate  $\hat{S}_1$  by Algorithm 3 based on  $\mathcal{S}_1$ 
14   $\mathbf{x}^{gbest}$  is chosen from a specified top part (e.g. top 5%) of  $\hat{S}$  randomly
15  for each  $t \in [1, 2, \dots, T_{max}]$  do
16    for each  $m \in [1, 2, \dots, \mathcal{N}_{particle}]$  do
17      for each  $n \in [1, 2, \dots, \mathcal{N}_{total} - 1]$  do
18        Update the quantum rotation angle  $\theta_{mn}^{t+1}$  by (2.12)
19        Update the quantum velocity  $v_{mn}^{t+1}$  by (2.6)
20        Update the quantum position  $x_{mn}^{t+1}$  by (2.7)
21      end
22      Update the network lifetime  $f_m^{t+1}(1)$  by (4.30) and overall PER  $f_m^{t+1}(2)$ 
        by (4.31)
23    end
24     $\mathcal{Z} = \mathcal{S}_t \cup \mathcal{S}_{t+1}$ 
25    Generate  $\hat{S}^{t+1}$  by Algorithm 3 based on  $\mathcal{Z}$ 
26     $\mathbf{x}^{gbest}(i)$  is chosen from a specified top part (e.g. top 5%) of  $\hat{S}^{t+1}$  randomly
27    for each  $m \in [1, 2, \dots, \mathcal{N}_{particle}]$  do
28       $\mathbf{x}_m^{pbest}$  is chosen from  $\hat{S}^{t+1}$  randomly
29    end
30  end
31 end
32 Generate  $\hat{S}^{final}$  by Algorithm 3 based on  $\mathbf{x}^{gbest}$ 
33  $\mathbf{x}_{final}^{gbest}$  is chosen from a specified top part (e.g. top 5%) of  $\hat{S}^{final}$  randomly
34 return  $\mathbf{x}_{final}^{gbest}$ 

```

global optimum of all particles are initialised, as refer to line 3 to 14. In particular, the network lifetime and overall PER are calculated in line 8 after mapping the position of particles to the selected Coops for the assumed CH. And the NSGA-II algorithm is performed in line 13 to sort the initialised particles to the non-dominated particles. Then the global optimum is chosen from a specific top part of the non-dominated particles. Thirdly, the particle updating process is described from line 15 to line 30. Specifically, the quantum rotation angle by (2.12), quantum velocity by (2.6), quantum position by (2.7) and fitness values are updated from line 16 to 23. Then the updated particles merge with previous particles in line 24, and the set of merged particles is sorted according to NSGA-II algorithm in line 25. The global optimum and local optimum are updated from line 26 to 29. At last, line 32 and 33 find the optimum set of CH and Coops by sorting the solutions obtained from line 26 according to NSGA-II. And the optimum set of CH and Coops is returned as the output of this algorithm.

At last, the capillary gateway informs every device about its role (i.e. CH, CM or Coop) based on the result of Algorithm 8.

4.5.3 Simulation and Conclusions

This subsection presents the simulation scenario design, system parameters setting, simulation platform design and the simulation results. In this subsection, the proposed QPSO algorithm focuses on energy efficiency by maximising the network time, denoted as QPSO-EE, and the QPSO algorithm focuses on QoS provision optimisation by minimising the overall PER, denoted as QPSO-QoS, are employed as two reference algorithms.

4.5.3.1 Scenario Design and System Parameters

In this subsection, the scenario is the same as the one as described in Subsection 4.3.3.1. The system parameters used in this section are also the same as shown in Table 3-A and

Table 4-A.

4.5.3.2 Simulation Platform Design

The simulation process of the proposed CH and Coops selection algorithm aiming at the tradeoff optimisation in Subsection 4.5.2 consists of a number of logic blocks and simulation iterations, as shown in Figure 4.16.

The scenario initialisation module and the exhaustive search module are the same as Subsection 4.3.3.2.

A. NSQPSO-based Coops selection Module

This module performs QPSO algorithm to generate and update particles, and also performs the NSGA-II algorithm to generate the non-dominated Pareto solutions which guides the direction of particle updating. It includes particle initialisation block as described in Section 3.5, particle updating block in Section 2.7, particle combination block which merges the updated particles at current generation with previous particles at previous generation, NSGA-II block to obtain the non-dominated swarm, generation iteration process and the output of optimum Coops set for the assumed CH after a pre-determined generations.

The NSGA-II block consists of fast non-dominated sorting sub-block to sort a population into different non-domination levels, the crowded distance calculation sub-block to get an estimate of the density of solutions, and the crowded-comparison sorting sub-block to guide the selection process, as shown in Figure 4.17.

B. Optimal value identification Module

This module finds the final Pareto optimal set of Coops and CH by NSGA-II according to the output of NSQPSO-based selection module. It also gets the Pareto optimal solutions of the optimum network lifetime and the optimum overall PER.

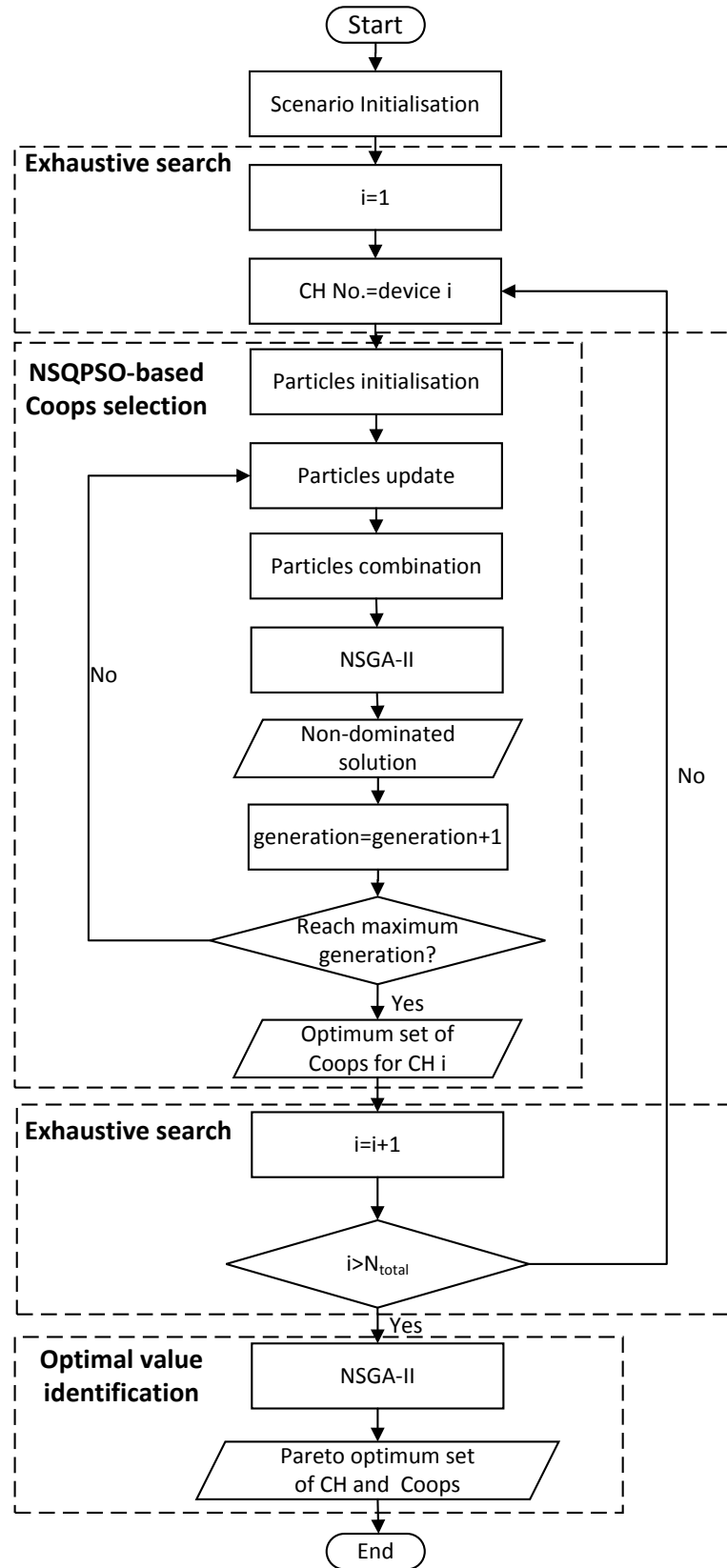


Figure 4.16: Flowchart of the proposed CH and Coops selection algorithm aiming at the tradeoff optimisation (Algorithm 8)

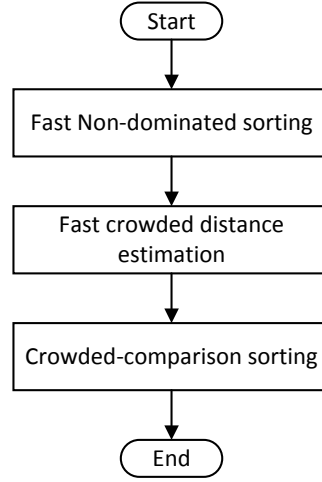


Figure 4.17: Flowchart of NSGA-II module

4.5.3.3 Simulation Results

Due to the same scenario setting, the particle number and generation number in this simulation is also set to be 10 and 120, respectively.

First, Figure 4.18 shows the Pareto optimal solution of the proposed NSQPSO algorithm in terms of 120 generations when setting \bar{E}_b/N_0 to be $18dB$. It can be seen that a longer network lifetime can be achieved but the overall PER is higher at the same time; similarly, the overall PER can be minimised by reducing the network lifetime. In addition, most of the Pareto optimal solutions are in the range of 400-800 min network time and corresponding 0.015-0.025 overall PER. This is because these non-dominated solutions are produced in the particle updating process after certain generations and one of these solutions cannot be said to be better than the others in the absence of any further information.

In addition, Figure 4.19 and Figure 4.20 show the network time and overall PER in terms of SNR per bit \bar{E}_b/N_0 . In Figure 4.19, it is observed that the performance of the proposed NSQPSO algorithm is better than QPSO-QoS algorithm which minimises the overall PER but compromises the energy efficiency. On the other hand, QPSO-EE algorithm outperforms the proposed NSQPSO algorithm in terms of average network

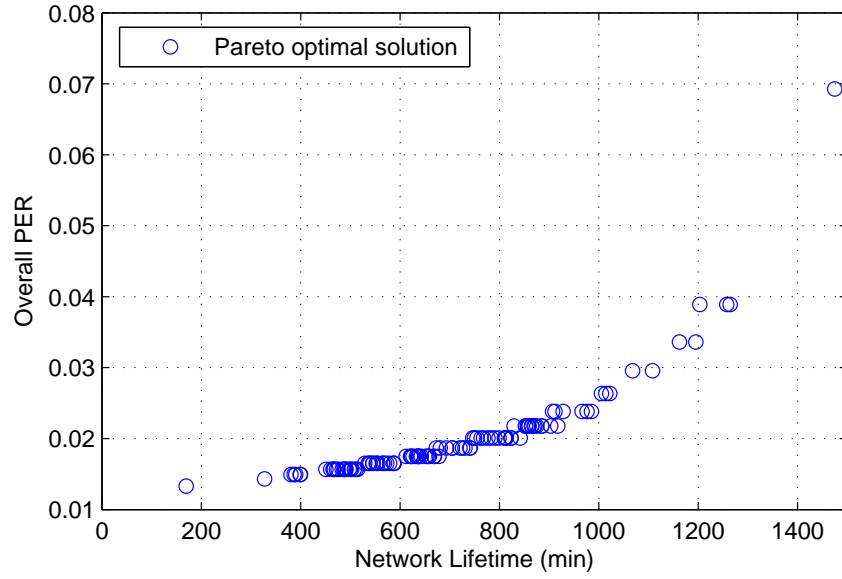


Figure 4.18: Pareto optimal solution of NSQPSO

lifetime, while it compromises the PER as is shown in Figure 4.20. Therefore, it can be concluded that the proposed NSQPSO algorithm is able to achieve the optimal tradeoff between energy efficiency and QoS provision optimisation.

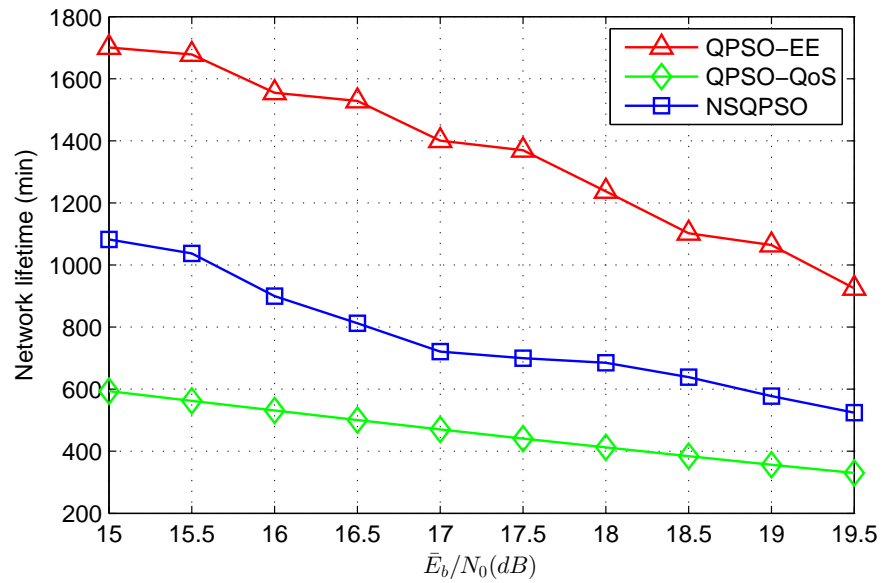
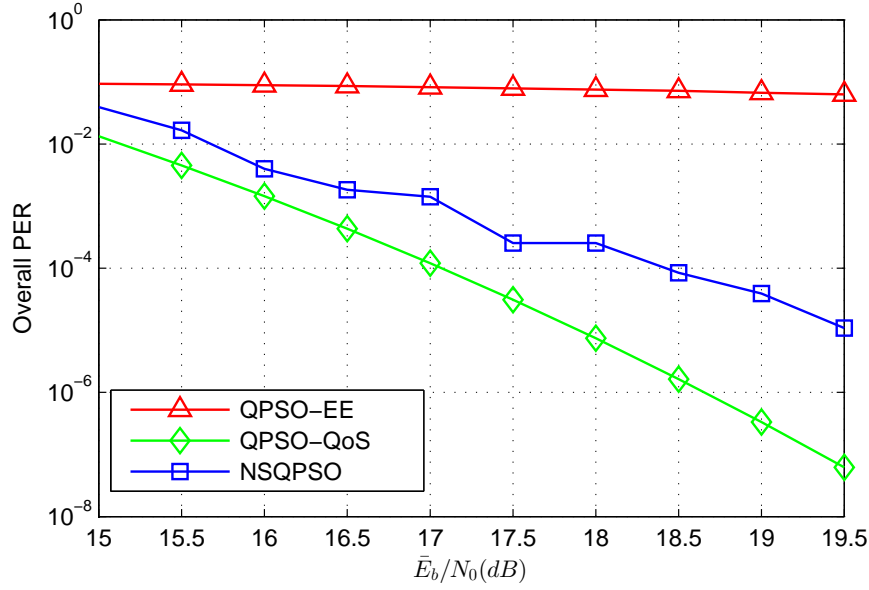
Figure 4.19: Network lifetime with respect to SNR per bit \bar{E}_b/N_0

Figure 4.21 investigates the number of Coops with respect to SNR per bit \bar{E}_b/N_0 .

Figure 4.20: Overall PER with respect to SNR per bit \bar{E}_b/N_0

Note that the number of Coops selected by QPSO-EE algorithm is not illustrated, due to the fact that no Coops participate in the long-haul transmission. This is because the energy consumption per bit increases with respect to \bar{E}_b/N_0 , and thus more Coops is not beneficial to network lifetime. Furthermore, the number of Coops selected by QPSO-QoS algorithm is the highest, because more Coops can decrease BER, thereby decreasing the overall PER. Additionally, it can be seen that the number of Coops selected by NSQPSO algorithm varies with \bar{E}_b/N_0 , because of the diversity of Pareto optimal solutions.

4.5.3.4 Conclusions

In this section, the CH and Coops selection with the aim of optimal tradeoff between energy efficiency and QoS provision is investigated in cluster-based capillary networks. Particularly, exhaustive search is utilised to select the optimum CH, QPSO algorithm is applied to select the best set of Coops for the potential CH, and NSGA-II algorithm is employed for the Pareto solutions to prolong network lifetime and decrease overall PER. It is proved that the proposed NSQPSO algorithm can achieve the optimum tradeoff

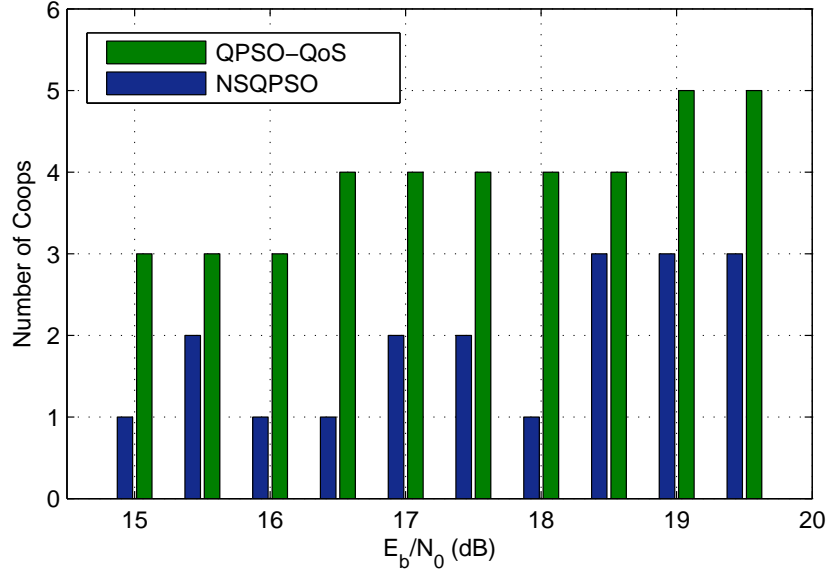


Figure 4.21: Number of selected Coops with respect to SNR per bit \bar{E}_b/N_0

between network lifetime and overall PER.

4.6 Summary

In this chapter, Section 4.1 specified the system model for CMISO systems in cluster-based capillary networks. A novel CH and cooperative devices selection algorithms was developed with different objectives.

First, taking energy efficiency into consideration, Section 4.3 investigated the CH and cooperative devices selection for a CMISO system aiming at network lifetime maximisation. In particular, Subsection 4.3.1 formulated the network lifetime by applying the battery model, evaluating individual power consumption and estimating the transmission time of every device during all transmission phases. Following this, Subsection 4.3.2 applied exhaustive search and QPSO algorithm to select the CH and cooperative devices with the objective to maximise network lifetime. Simulation results in Subsection 4.3.3 demonstrated that the proposed algorithm is able to select better set of cooperative

devices compared with reference algorithms.

Second, Section 4.4 investigated the cooperative devices selection for a CMISO system to optimise the QoS provision. Specifically, the overall PER was adopted to represent the QoS provision. Subsection 4.4.1 formulated the overall PER of all links during the transmission under a given energy constraint and Subsection 4.4.2 proposed an optimum CH and cooperative devices selection algorithm using QPSO to minimise the overall PER. In Subsection 4.4.3, simulation results indicated that the proposed algorithm outperforms QGA and PSO algorithms by selecting better set of cooperative devices.

Finally, since more energy consumption allowed in the network leads to the decrease of overall PER, the tradeoff between energy efficiency and overall PER should be given special attention, which was investigated in Section 4.5. Particularly, Subsection 4.5.1 provided the tradeoff problem formulation by setting two objectives of network lifetime and overall PER optimisation. In Subsection 4.5.2, an optimum cooperative devices selection algorithm was designed to achieve the optimum tradeoff between network lifetime and overall PER. The proposed algorithm applied QPSO to select the optimum set of cooperative devices to assist CH for long-haul transmission, and also employs NSGA-II for the Pareto solutions of the cooperative devices set to prolong network lifetime and decrease overall PER. Simulation results in Subsection 4.5.3 proved that the proposed algorithm is able to achieve the optimal tradeoff between energy efficiency and QoS provision.

Chapter 5

Cooperative Coalitions Selection for Multi-hop Networks

Routing table construction phase is required to decide the routes from the source clusters to the gateway in multi-hop cluster-based networks [RR16]. The cooperative coalitions selection is deployed after the routing table construction phase [DGA04] [NQ10]. A cooperative coalitions in a CMIMO system consists of the source CH and its SCoops as well as the destination CH and its RCoops. This chapter proposes a novel cooperative coalitions selection algorithm in post routing table construction phase. The proposed cooperative coalitions selection algorithm chooses the optimum set of cooperative coalitions with the objectives of energy efficiency, QoS provision, and the tradeoff between energy efficiency and QoS provision.

5.1 System Model

The system model in this chapter considers a multi-hop cluster-based capillary networks with \mathcal{N}_{total} devices, as shown in Figure 5.1. The system model focuses on one routing path from Cluster 1 to the capillary gateway through \mathcal{N}_{hop} hops. All devices in the

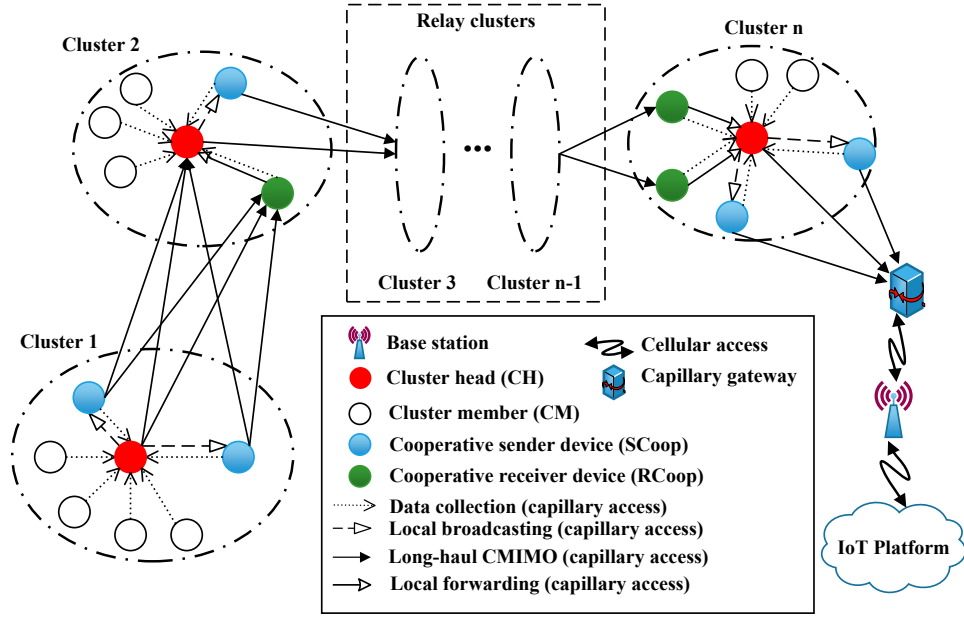


Figure 5.1: System model for CMIMO systems in multi-hop cluster-based capillary networks

routing path have been classified into four categories: CHs, CMs, SCoops and RCoops.

The following notations are made for this chapter:

- Denote the number of CHs in the network to be \mathcal{N}_{CH} , which is also the number of clusters in the routing path.
- Denote the number of CMs in cluster i to be $\mathcal{N}_{CM}(i)$ where $i \in [1, \dots, \mathcal{N}_{CH}]$.
- Denote the number of SCoops in cluster i to be $\mathcal{N}_{SCoop}(i)$ where $i \in [1, \dots, \mathcal{N}_{CH}]$.
- Denote the number of RCoops in cluster i to be $\mathcal{N}_{RCoop}(i)$ where $i \in [1, \dots, \mathcal{N}_{CH}]$.
- Denote the number of all non-CH devices in cluster i to be $\mathcal{N}_{nonCH}(i)$, then $\mathcal{N}_{nonCH}(i) = \mathcal{N}_{CM}(i) + \mathcal{N}_{SCoop}(i) + \mathcal{N}_{RCoop}(i)$.

The number of overall devices in the routing path is express as $\mathcal{N}_{total} = \mathcal{N}_{CH} + \mathcal{N}_{nonCH}$.

The same assumptions in Section 3.1 are also made for this system model. In addition, the battery model in Section 4.3.1.1 are adopted in this chapter.

In Figure 5.1, the data transmission from Cluster 1 to the capillary gateway is through several relay clusters. The long-haul transmission between two neighbouring clusters and the long-haul transmission between the Cluster n and capillary gateway adopt the CMIMO systems to release the burden of CHs. At the transmission side, by forming a virtual multi-antenna diversity systems, CH in Cluster 1 cooperates with its SCoops to send the MIMO-modulated data to Cluster 2. Simultaneously, the CH in Cluster 2 cooperates with its RCoops to receive the MIMO modulated data from Cluster 1 at the reception side. In this way, all the relay clusters in the routing path not only forward their own data but also the MIMO modulated data from their neighbouring clusters to the capillary gateway.

The transmission process in one cluster and between two neighbouring clusters in the routing path consists of following phases:

- Data collection (DC) phase. As shown in Figure 5.2(a), the CH collects and aggregates data from all non-CH devices within the cluster.
- Local broadcasting (LB) phase. As shown in Figure 5.2(b), the CH broadcasts the aggregated data to all SCoops at the transmission side.
- Long-haul cooperative transmission (LH) phase. As shown in Figure 5.3, the CH and its SCoops of the transmission cluster jointly send the MIMO-modulated data to the CH and its RCoops of the reception cluster or the capillary gateway.
- Local forwarding (LF) phase. As shown in Figure 5.2(c), all RCoops transmit the MIMO modulated data obtained from the transmission cluster to their CH at the reception side. Then the reception CH decodes and combines the MIMO modulated data with its cluster data collected in the data collection phase. Finally, the combined data is sent to the next hop.

Figure 5.4 illustrates the time slots of the above four phases for one cluster in TDMA scheduling. Firstly, every non-CH device is allocated with a time slot to transmit the

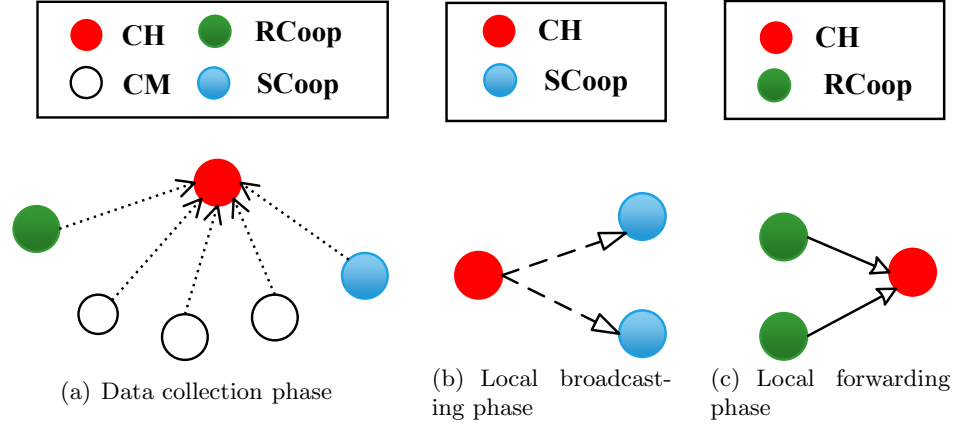


Figure 5.2: Intra-cluster transmission for multi-hop cluster-based capillary networks

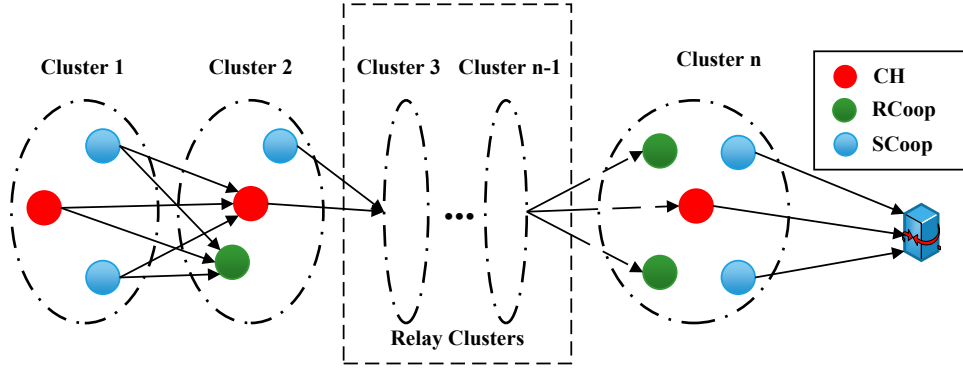


Figure 5.3: Inter-cluster communication for multi-hop cluster-based capillary networks

individual data to the CH in the data collection phase; secondly, every RCoop is allocated with a time slot to send the MIMO-modulated data received from previous hop to the CH in the local forwarding phase; thirdly, the CH uses one time slot to broadcast the combined data to all SCoPs in the local broadcasting phase; finally, the CH together with all RCoops are allocated with different time slots to transmit the MIMO-modulated data to the next hop for the capillary gateway.

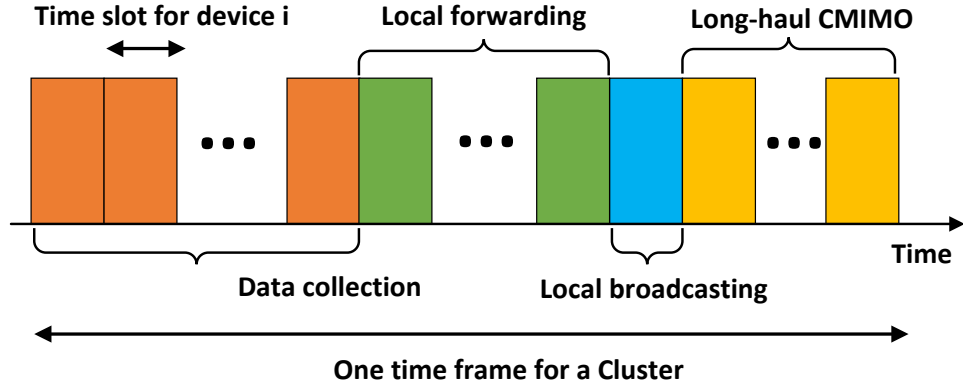


Figure 5.4: Time slots of TDMA scheduling for a cluster using CMIMO systems

5.2 Energy Consumption Model

This chapter uses the energy model of power consumption and intra-cluster communication in Section 3.2. For the inter-cluster communication of long-haul transmission phase, taking CMIMO system into consideration, the average $\left. \frac{\bar{E}_b}{N_0} \right|_{inter}$ with a square constellation MQAM in Rayleigh fading channel [ZD07] is given by

$$\left. \frac{\bar{E}_b}{N_0} \right|_{inter} \doteq N_T \frac{2(M-1)}{3 \log_2 M} \times \left[\frac{1}{4} \left(\frac{4(1 - 1/\sqrt{M})^{(2\mathcal{N}_T\mathcal{N}_R+1)}}{\bar{P}_{BER}^{inter} \log_2 M} \right)^{\frac{1}{\mathcal{N}_T\mathcal{N}_R}} - 1 \right] \quad (5.1)$$

where \bar{P}_{BER}^{inter} is the average BER of inter-cluster communication, \mathcal{N}_T and \mathcal{N}_R are the number of transmitter and reception devices. In this chapter, $\mathcal{N}_T = \mathcal{N}_{SCoop} + 1$ at the transmission side and $\mathcal{N}_R = \mathcal{N}_{RCoop} + 1$ at the reception side.

5.3 Energy Efficient Cooperative Coalitions Selection

This section focuses on selection of the cooperative coalitions in the routing path with the objective of maximising energy efficiency.

5.3.1 Energy Efficient Problem Formulation

This subsection presents the overall power consumption and active time of every device in the routing path, as well as the network lifetime derivation.

5.3.1.1 Power Consumption and Active Time

The part investigates the power consumption and active time of CH, RCoop, SCoop and CM for data collection phase, local broadcasting phase, local forwarding phase and the long-haul cooperative transmission phase.

A. Data collection phase

In the data collection phase, the CH in each cluster acts as the receiver dissipating the reception power consumption, while all CMs, SCoops and RCoops transmit individual data to their corresponding CH, dissipating the transmission path power consumption. As the assumption of squared power path loss, the power consumption per bit of devices in the i -th cluster for the data collection phase are given as follows

$$\begin{aligned}
 P_{CH}^{DC}(i) &= P_{cr} \\
 P_{CM_j}^{DC}(i) &= \frac{(4\pi)^2 M_l N_r}{G_t G_r \lambda^2} R_b d_{j,i}^2 \cdot \frac{\bar{E}_b}{N_0} \Big|_{intra} + P_{ct} \\
 P_{SCoop_m}^{DC}(i) &= \frac{(4\pi)^2 M_l N_r}{G_t G_r \lambda^2} R_b d_{m,i}^2 \cdot \frac{\bar{E}_b}{N_0} \Big|_{intra} + P_{ct} \\
 P_{RCoop_k}^{DC}(i) &= \frac{(4\pi)^2 M_l N_r}{G_t G_r \lambda^2} R_b d_{k,i}^2 \cdot \frac{\bar{E}_b}{N_0} \Big|_{intra} + P_{ct}
 \end{aligned} \tag{5.2}$$

where $j \in [1, \dots, \mathcal{N}_{CM}(i)]$, $m \in [1, \dots, \mathcal{N}_{SCoop}(i)]$ and $k \in [1, \dots, \mathcal{N}_{RCoop}(i)]$. Correspondingly, the active time of devices in the i -th cluster for the data collection phase are

given as follows

$$\begin{aligned}
T_{CH}^{DC}(i) &= (\mathcal{N}_{CM}(i) + \mathcal{N}_{SCoop}(i) + \mathcal{N}_{RCoop}(i)) \frac{L_{data}}{R_b} \\
T_{CM_j}^{DC}(i) &= \frac{L_{data}}{R_b} \\
T_{SCoop_m}^{DC}(i) &= \frac{L_{data}}{R_b} \\
T_{RCoop_k}^{DC}(i) &= \frac{L_{data}}{R_b}
\end{aligned} \tag{5.3}$$

After collecting data from all non-CH devices, the CH performs data aggregation technique. As for the CH, the time duration to aggregate the collected data is rather short compared to other transmission phases [SL13], and thus the active time and power consumption for data aggregation is omitted in this section. In addition, CH i not only transmits its own aggregated data but also all aggregated data in its previous $i - 1$ hop. Therefore, the overall amount of data for CH i is given by

$$L_{agg}(i) = \frac{(1 + \mathcal{N}_{CM}(i) + \mathcal{N}_{SCoop}(i) + \mathcal{N}_{RCoop}(i))}{(\mathcal{N}_{CM}(i) + \mathcal{N}_{SCoop}(i) + \mathcal{N}_{RCoop}(i))\gamma_{agg} + 1} L_{data} + \sum_{n=1}^{i-1} L_{agg}(n) \tag{5.4}$$

where γ_{agg} is the aggregation factor, the first term is the amount of aggregated data for CH i and the second term is the amount of data in previous hops.

B. Local broadcasting phase

In the local broadcasting phase, the CH acts as transmitter to broadcast the aggregated data to all SCoops, dissipating the transmission power consumption, and all SCoops receive the aggregated data from the CH, dissipating the reception power consumption. Due to the broadcast nature of the wireless channel, if the SCoop with the maximum distance from CH i , denoted by $d_{max}(i)$, can receive the data from CH i , the other SCoops can simultaneously receive the data. Then the power consumption per bit of

devices in the i -th cluster for the local broadcasting phase are expressed as follows

$$\begin{aligned}
P_{CH}^{LB}(i) &= \frac{(4\pi)^2 M_l N_r}{G_t G_r \lambda^2} R_b d_{max}^2(i) \cdot \frac{\bar{E}_b}{N_0} \Big|_{intra} + P_{ct} \\
P_{CM_j}^{LB}(i) &= 0 \\
P_{SCoop_m}^{LB}(i) &= P_{cr} \\
P_{RCoop_k}^{LB}(i) &= 0
\end{aligned} \tag{5.5}$$

where $j \in [1, \dots, \mathcal{N}_{CM}(i)]$, $m \in [1, \dots, \mathcal{N}_{SCoop}(i)]$ and $k \in [1, \dots, \mathcal{N}_{RCoop}(i)]$. Correspondingly, the active time of devices in the i -th cluster for the local broadcasting phase are expressed as follows

$$\begin{aligned}
T_{CH}^{LB}(i) &= \frac{L_{agg}(i)}{R_b} \\
T_{CM_j}^{LB}(i) &= 0 \\
T_{SCoop_m}^{LB}(i) &= \frac{L_{agg}(i)}{R_b} \\
T_{RCoop_k}^{LB}(i) &= 0
\end{aligned} \tag{5.6}$$

C. Long-haul transmission phase

In the long-haul transmission phase, CH and SCoops in the i -th cluster jointly transmit the MIMO modulated data to their neighbouring $(i + 1)$ -th cluster or the capillary gateway, dissipating the transmission power consumption, while the CH and RCoops in the $(i + 1)$ -th cluster receives the MIMO modulated data, dissipating the reception power consumption. Considering the broadcasting nature of wireless channels, the long-haul distance for device n is obtained by the maximum distance between the transmitter device in the i -th cluster and the reception device in the $(i + 1)$ -th cluster, denoted by $d_{max}(n)$. Therefore, the power consumption per bit of devices in the i -th cluster at the

transmission side for the long-haul transmission phase are given by

$$\begin{aligned}
P_{CH}^{LH}(i) &= \frac{(4\pi)^2 M_l N_r}{G_t G_r \lambda^2} R_b^{eff} d_{max}^{\kappa_{max}}(i) \cdot \frac{\bar{E}_b}{N_0} \Big|_{inter} + P_{ct} \\
P_{CM_j}^{LH}(i) &= 0 \\
P_{SCoop_m}^{LH}(i) &= \frac{(4\pi)^2 M_l N_r}{G_t G_r \lambda^2} R_b^{eff} d_{max}^{\kappa_{max}}(m) \cdot \frac{\bar{E}_b}{N_0} \Big|_{inter} + P_{ct} \\
P_{RCoop_k}^{LH}(i) &= 0
\end{aligned} \tag{5.7}$$

where $j \in [1, \dots, \mathcal{N}_{CM}(i)]$, $m \in [1, \dots, \mathcal{N}_{SCoop}(i)]$ and $k \in [1, \dots, \mathcal{N}_{RCoop}(i)]$.

Training overhead is introduced into the CMIMO scheme for channel estimation and the number of required training symbols is proportional to the number of transmit antennas. Therefore, the packet size of long-haul transmission is given by

$$L_c(i) = \frac{F_{block}}{F_{block} - \rho_{train}(\mathcal{N}_{SCoop}(i) + 1)} L_{agg}(i) \tag{5.8}$$

where F_{block} is the block size of STBC code, $\rho_{train}(\mathcal{N}_{SCoop} + 1)$ is the number of training symbols in each block. According to [HH03], the effective system bit rate is given by

$$R_b^{eff} = \frac{F_{block} - \rho_{train}(\mathcal{N}_{SCoop}(i) + 1)}{F_{block}} R_b \tag{5.9}$$

Then the active time of devices in the i -th cluster for the long-haul transmission phase are expressed as follows

$$\begin{aligned}
T_{CH}^{LH}(i) &= \frac{L_c(i)}{R_b^{eff}} \\
T_{CM_j}^{LH}(i) &= 0 \\
T_{SCoop_m}^{LH}(i) &= \frac{L_c(i)}{R_b^{eff}} \\
T_{RCoop_k}^{LH}(i) &= 0
\end{aligned} \tag{5.10}$$

At the reception side, the power consumption per bit of devices in the $(i + 1)$ -th cluster for the long-haul transmission phase are expressed as follows,

$$\begin{aligned}
 P_{CH}^{LH}(i + 1) &= P_{cr} \\
 P_{CM_j}^{LH}(i + 1) &= 0 \\
 P_{SCoop_m}^{LH}(i + 1) &= 0 \\
 P_{RCoop_k}^{LH}(i + 1) &= P_{cr}
 \end{aligned} \tag{5.11}$$

where $j \in [1, \dots, \mathcal{N}_{CM}(i + 1)]$, $m \in [1, \dots, \mathcal{N}_{SCoop}(i + 1)]$ and $k \in [1, \dots, \mathcal{N}_{RCoop}(i + 1)]$. Correspondingly, the active time of devices in the $(i + 1)$ -th cluster for the long-haul transmission phase are expressed as follows

$$\begin{aligned}
 T_{CH}^{LH}(i + 1) &= (\mathcal{N}_{RCoop}(i) + 1) \frac{L_c(i)}{R_b^{eff}} \\
 T_{CM_j}^{LH}(i + 1) &= 0 \\
 T_{SCoop_m}^{LH}(i + 1) &= 0 \\
 T_{RCoop_k}^{LH}(i + 1) &= (\mathcal{N}_{RCoop}(i) + 1) \frac{L_c(i)}{R_b^{eff}}
 \end{aligned} \tag{5.12}$$

D. Local forwarding phase

In the local forwarding phase, CH in the $(i + 1)$ -th cluster receives long-haul MIMO data from all RCoops in the same cluster, dissipating the reception power consumption. Meanwhile, RCoops transmit data to their CH, dissipating the transmission power consumption. As a result, the power consumption per bit of devices in the i -th cluster for the local forwarding phase are given by

$$\begin{aligned}
 P_{CH}^{LF}(i + 1) &= P_{cr} \\
 P_{CM_j}^{LF}(i + 1) &= 0 \\
 P_{SCoop_m}^{LF}(i + 1) &= 0 \\
 P_{RCoop_k}^{LF}(i + 1) &= \frac{(4\pi)^2 M_l N_r}{G_t G_r \lambda^2} R_b d_{k,i+1}^2 \cdot \frac{\bar{E}_b}{N_0} \Big|_{intra} + P_{ct}
 \end{aligned} \tag{5.13}$$

where $j \in [1, \dots, \mathcal{N}_{CM}(i+1)]$, $m \in [1, \dots, \mathcal{N}_{SCoop}(i+1)]$ and $k \in [1, \dots, \mathcal{N}_{RCoop}(i+1)]$. Correspondingly, the active time of devices in the $(i+1)$ -th cluster for the long-haul transmission phase can be expressed as follows,

$$\begin{aligned}
 T_{CH}^{LF}(i+1) &= \mathcal{N}_{RCoop}(i+1) \frac{L_c(i)}{R_b} \\
 T_{CM_j}^{LF}(i+1) &= 0 \\
 T_{SCoop}^{LF}(i+1, m) &= 0 \\
 T_{RCoop_k}^{LF}(i+1) &= \frac{L_c(i)}{R_b}
 \end{aligned} \tag{5.14}$$

5.3.1.2 Network Lifetime Formulation

Taking the battery model into consideration, the average current required to power a device during period $[t_s, t_e]$ is obtained by

$$\bar{I}_c = \frac{P_{total}}{\phi \mathbb{V}} \tag{5.15}$$

where P_{total} is the overall power consumption of the device during period $[t_s, t_e]$, ϕ and \mathbb{V} denote the DC-DC converter output efficiency and voltage, respectively [ZCSA09].

The overall power consumption P_{total} of device n is expressed as

$$P_{total}(n) = P^{DC}(n) + P^{LB}(n) + P^{LF}(n) + P^{LH}(n) \tag{5.16}$$

where $P^{DC}(n)$, $P^{LB}(n)$, $P^{LF}(n)$ and $P^{LH}(n)$ can be obtained from (5.2), (5.5), (5.13), (5.7) and (5.11), respectively.

The overall active time during the transmission T_{total} of device n is expressed as

$$T_{total}(n) = T^{DC}(n) + T^{LB}(n) + T^{LF}(n) + T^{LH}(n) \tag{5.17}$$

where $T^{DC}(n)$, $T^{LB}(n)$, $T^{LF}(n)$ and $T^{LH}(n)$ can be obtained from (5.3), (5.6), (5.14), (5.10)

and (5.12), respectively.

Denote the initialising time to be t_0 . The battery operating time of device n can then be expressed as,

$$\begin{aligned} T_{op}(n) &= \frac{C_{avl}(I_c(n), T_{op}(n), t_s(n), t_e(n), \beta^2)}{\bar{I}_c(n)} \\ &= \frac{C_{init}(n)\phi\mathbb{V}}{P_{total}(n)} - (T_{total}(n) - t_0) - 2 \sum_{k=1}^{\infty} \frac{e^{-\beta^2 k^2 (T_{op}(n) - T_{total}(n))} - e^{-\beta^2 k^2 (T_{op}(n) - t_0)}}{\beta^2 k^2} \end{aligned} \quad (5.18)$$

The cooperative coalitions in the i -th cluster can be expressed as follows,

$$\begin{aligned} SCoop(i) &= \{SCoop_1(i), \dots, SCoop_{\mathcal{N}_{SCoop(i)}}(i)\} \\ RCoop(i) &= \{RCoop_1(i), \dots, RCoop_{\mathcal{N}_{RCoop(i)}}(i)\} \\ \mathbb{C}(i) &= RCoop(i) \cup SCoop(i) \end{aligned} \quad (5.19)$$

In this thesis, the network lifetime is represented by the average battery operating time of all devices \bar{T}_{op}^{avg} within the cluster. The research problem is to find the optimum cooperative coalitions of all clusters in the routing path, denoted by $\mathbb{C} = \{\mathbb{C}(1), \dots, \mathbb{C}(i), \dots, \mathbb{C}(\mathcal{N}_{CH})\}$, in order to maximise the network lifetime \bar{T}_{op}^{avg} under given BER threshold \bar{P}_{BER}^{THR} . Therefore, the research problem in this section is expressed as

$$\begin{aligned} \underset{\mathbb{C}}{\text{maximise}} \bar{T}_{op}^{avg} &= \frac{\sum_{n=1}^{\mathcal{N}_{total}} T_{op}(n)}{\mathcal{N}_{total}} \\ \text{s.t.} \quad &\begin{cases} \bar{P}_{BER}^{intra} \leq \bar{P}_{BER}^{THR} \\ \bar{P}_{BER}^{inter} \leq \bar{P}_{BER}^{THR} \end{cases} \end{aligned} \quad (5.20)$$

5.3.2 Energy Efficiency Cooperative Coalitions Selection Algorithm

The capillary gateway executes the cooperative coalitions selection process by QPSO, after receiving every device's individual information (i.e. residual energy and location).

The QPSO-based cooperative coalitions selection algorithm aiming at maximising the network lifetime is described in Algorithm 9.

In this chapter, the quantum position of a particle is composed of all cooperative coalition candidates in the routing path, as shown in Figure 5.5. Denote $SCoop_{cand}(i)$ to be SCoops candidates in cluster i , and $RCoop_{cand}(i)$ to be RCoops in cluster i . Both $SCoop_{cand}(i)$ and $RCoop_{cand}(i)$ are the non-CH devices in cluster i , which suggests that every non-CH device in cluster i has the potential to be a SCoop or RCoop. In the first cluster, there is no RCoops used to receive data from its neighbouring cluster, and thus only the SCoops candidates are taken into consideration for the composition of the particle position. From the second cluster to the last cluster, both RCoops candidates and SCoops candidates make up the particle position. Therefore, the dimension of particles, denoted by \mathcal{N}_{cand} , is $\mathcal{N}_{cand} = \mathcal{N}_{nonCH}(1) + \sum_{i=2}^{\mathcal{N}_{CH}^{(i)}} \mathcal{N}_{nonCH}(i)$. The value of quantum position indicates whether the device n in particle m is a member of the cooperative coalition: $x_{mn}^t = 1$ represents that the candidate n in particle m is a SCoop or RCoop at generation t ; otherwise, the candidate n in particle m is a CM at generation t . Every particle in this chapter represents a possible solution of particular cooperative coalitions.

In Algorithm 9, firstly, the quantum position, quantum velocity, individual optimum and global optimum of all particles are initialised, as described from line 1 to line 10. Secondly, line 11 to line 29 describes the particle updating process to obtain the optimum set of cooperative coalitions. In particular, the quantum rotation angle, quantum velocity and quantum position of particles are updated from line 13 to line 17 by (2.12), (2.6) and (2.7), respectively. Then the updated particle positions are mapped to the selected set of SCoops and RCoops that is further utilized in fitness value (i.e. network lifetime)

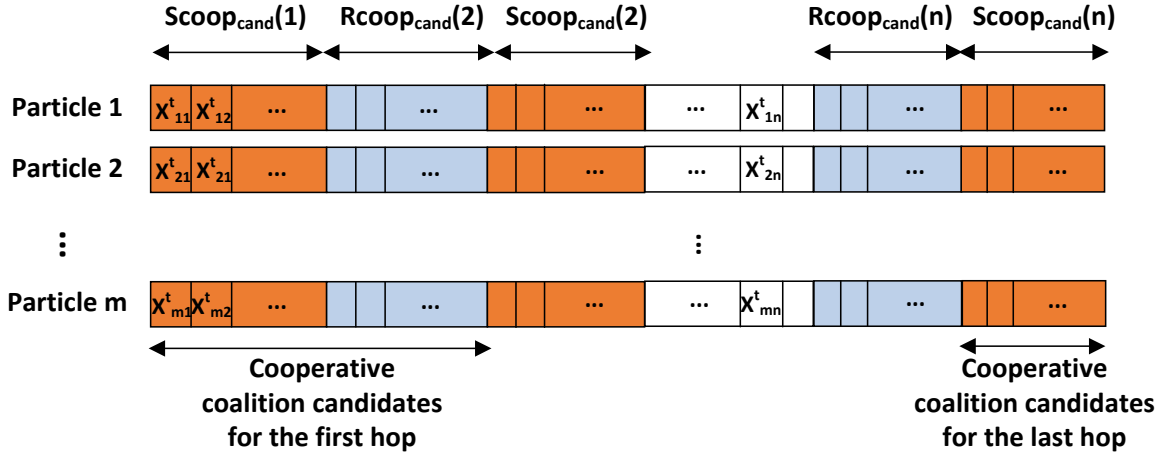


Figure 5.5: Particle position representation for cooperative coalitions candidates

calculation by (5.20) in line 18. Correspondingly, the local optimum and global optimum are updated from line 19 to line 28. Finally, the output of this algorithm is the set of cooperative coalitions in the routing path.

At last, the capillary gateway informs every device about its role (CH, CM, SCoop or RCoop) based on the result of Algorithm 9.

5.3.3 Simulation and Conclusions

This subsection describes the simulation scenario, system parameters, simulation platform design, simulation results and conclusions. In this chapter, the 2×2 MIMO and 3×3 MIMO systems in [LLW⁺13] are simulated as reference.

5.3.3.1 Scenario Design and System Parameters

Assume a scenario with three clusters in one routing path for simplicity, i.e. 3 hops routing, as shown in Figure 5.6. In addition, all devices are powered by two AAA Li-FeS2 battery [WIK], which has 1.5-volt nominal voltage and 1200mAh nominal capacity.

Algorithm 9: Cooperative coalitions selection to maximise the network lifetime

```

1 for each  $m \in [1, 2, \dots, \mathcal{N}_{particle}]$  do
2   for each  $n \in [1, 2, \dots, \mathcal{N}_{cand}]$  do
3     Set the quantum position  $x_{mn}^1$  by 0 or 1 randomly
4     Set the quantum velocity  $v_{mn}^1$  to be  $1/\sqrt{2}$ 
5   end
6   Update the network lifetime  $f_m^1$  by (5.20)
   /* The local optimum is the initialised particles at the first
      generation */
7   Set the local optimum fitness value  $f_m^{pbest_{max}}$  to be  $f_m^1$ 
8   Set the local optimum position  $\mathbf{x}_m^{pbest_{max}}$  to be  $\mathbf{x}_m^1$ 
9 end
   /* Update the global optimum */
10 Update the global optimum fitness value  $f^{gbest_{max}}$  and the global optimum
    position  $\mathbf{x}^{gbest_{max}}$  by (2.11)
11 for each  $t \in [1, 2, \dots, T_{max}]$  do
12   for each  $m \in [1, 2, \dots, \mathcal{N}_{particle}]$  do
13     for each  $n \in [1, 2, \dots, \mathcal{N}_{cand}]$  do
14       Update the quantum rotation angle  $\theta_{mn}^{t+1}$  by (2.12)
15       Update the quantum velocity  $v_{mn}^{t+1}$  by (2.6)
16       Update the quantum position  $x_{mn}^{t+1}$  by (2.7)
17     end
18     Update the network lifetime  $f_m^{t+1}$  by (5.20)
     /* Update local optimum */
19     if  $f_m^{t+1} > f_m^{pbest}$  then
20       Set the local optimum fitness value  $f_m^{pbest}$  to be  $f_m^{t+1}$ 
21       Set the local optimum position  $\mathbf{p}_m$  to be  $\mathbf{x}_m^{t+1}$ 
22     end
23   end
24   Update the temporary global optimum fitness value  $g^{gbest_{max}}$  by (2.11)
   /* Find the final global optimum */
25   if  $g^{gbest_{max}} > f^{gbest_{max}}$  then
26     Set the final global optimum fitness value  $f^{gbest_{max}}$  to be  $g^{gbest_{max}}$ 
27     Update the global optimum position  $\mathbf{x}^{gbest_{max}}$  according to  $g^{gbest_{max}}$ 
28   end
29 end
30 return  $\mathbf{x}^{gbest_{max}}$  as the optimum set of cooperative coalitions in the routing path

```

The simulation scenario in this chapter is illustrated in Figure 5.7. Each cluster consists of 10 devices which are randomly distributed within a circle of $25m$ radius. The CHs are located at $(0m, 0m)$, $(100m, 0m)$, $(200m, 0m)$ in Cluster 1, Cluster 2 and Cluster 3, respectively. The gateway is located at $(300m, 0m)$ if not specified in the

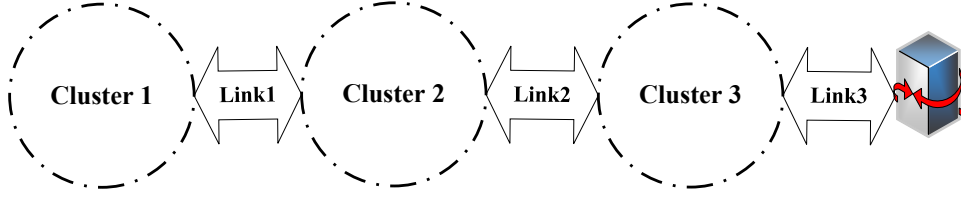


Figure 5.6: Scenario design with three clusters for multi-hop cluster-based capillary networks using CMIMO systems

following subsections. The distance between each cluster and its neighbouring cluster or the capillary gateway is denoted as the long-haul cluster distance the following sections. That is, the long-haul cluster distance in Figure 5.7 is $100m$.

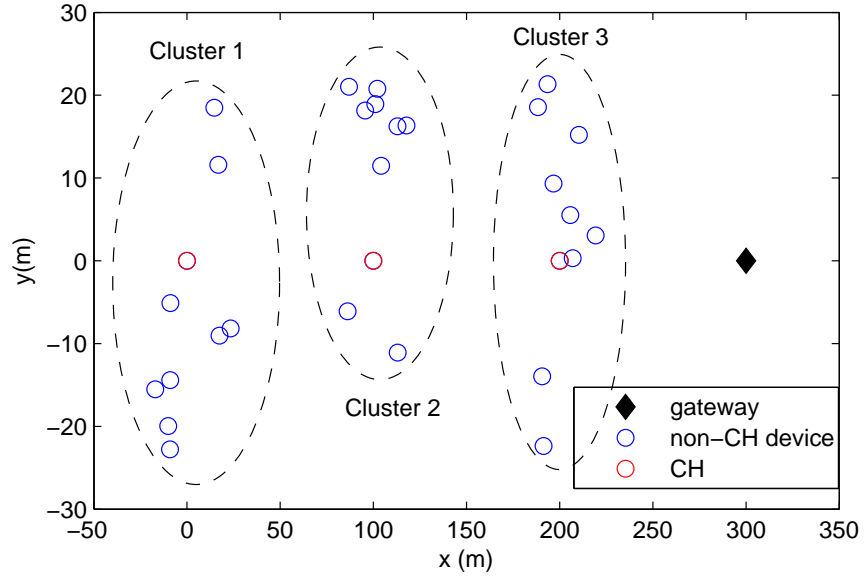


Figure 5.7: Simulation scenario for multi-hop cluster-based capillary networks using CMIMO systems

The system parameters in the chapter are as list in Table 3-A and Table 4-A.

5.3.3.2 Simulation Platform Design

The simulation process of the proposed cooperative coalitions selection algorithm aiming at energy efficiency in Subsection 5.3.2 consists of several logic blocks and simulation loops, as shown in Figure 5.8.

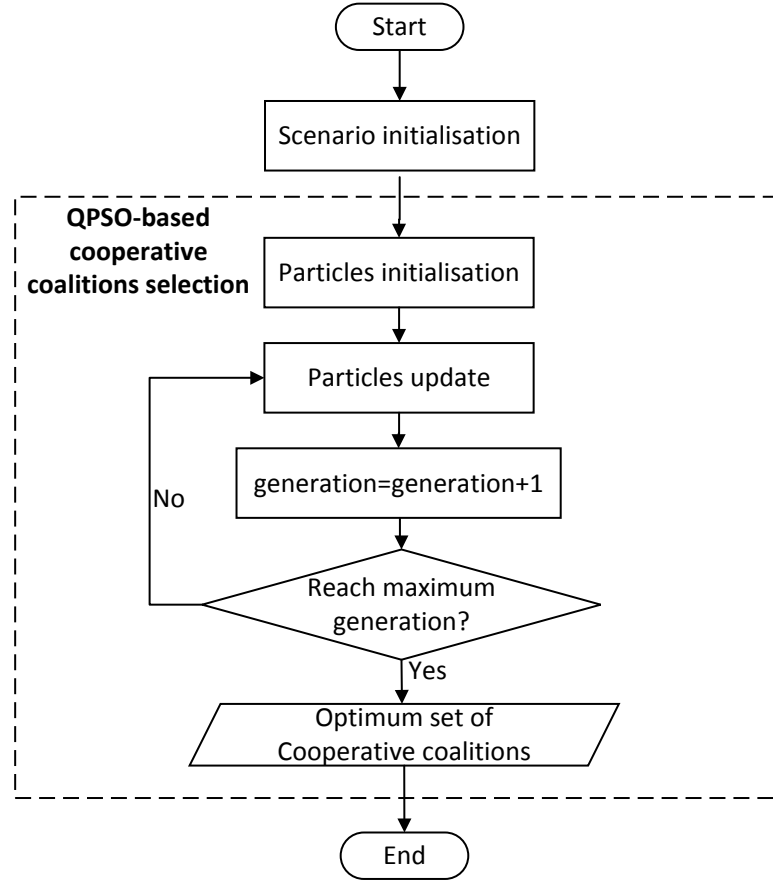


Figure 5.8: Flowchart of the proposed cooperative coalitions selection algorithm aiming at energy efficiency (Algorithm 9)

A. Scenario Initialisation module

In this module, the individual information of all devices and the capillary gateway are initialised. In particular, the position of capillary gateway is set at $(300m, 0m)$. The battery capacity of all devices is set to be $2400mAh$.

B. QPSO-based cooperative coalitions selection module

This module performs QPSO algorithm to select the best set of cooperative coalitions of all clusters in the routing path. It includes particle initialisation and particle updating as described in Subsection 3.5.2, generation iteration process and the output of optimum set of cooperative coalitions after a predetermined generations.

5.3.3.3 Simulation Results

Table 5-A: Particle number and generation number selection in terms of algorithm time complexity

Number of particles($\mathcal{N}_{particle}$)	Optimum number of generations(T_{opt})	Function Evaluations(FE)
4	732	2928
6	445	2670
8	313	2504
10	234	2340
12	189	2268
14	174	2436
16	159	2544
18	147	2646
20	136	2720

As described in Section 3.5.3, the particle number and generation number play important roles in the performance of QPSO. Table 5-A shows the optimum number of generations and function evaluations in terms of different number of particles to converge to the same optimum global fitness value. The simulation iteration is set to be 50 times. In order to emphasize the trend of in Table 5-A, Figure 5.9 shows the convergence time with respect to both optimum number of generations and function evaluations. In Figure 5.9, the optimum number of generations decreases dramatically from 4 to 12 particles. This is explained by the fact that more particles mean better opportunity to find the optimum fitness value. However, as the number of particles increases from 12 to 20, the optimum number of generations decreases slowly, which indicates that the performance of QPSO is not sensitive to the particle number after reaching a certain threshold. In terms of the function evaluation, it can be seen that the minimum function evaluation is achieved at the point where the number of particle is 12 and the optimum number of generation is 189. Therefore, the number of particles is set to be 12 and number of generations to be 200 in the following simulation in order to reduce the algorithm complexity as well as ensure the performance of QPSO.

Figure 5.10 shows the convergence of the QPSO algorithm. It can be seen that the same final fitness value (i.e. network lifetime) can be achieved after several generations

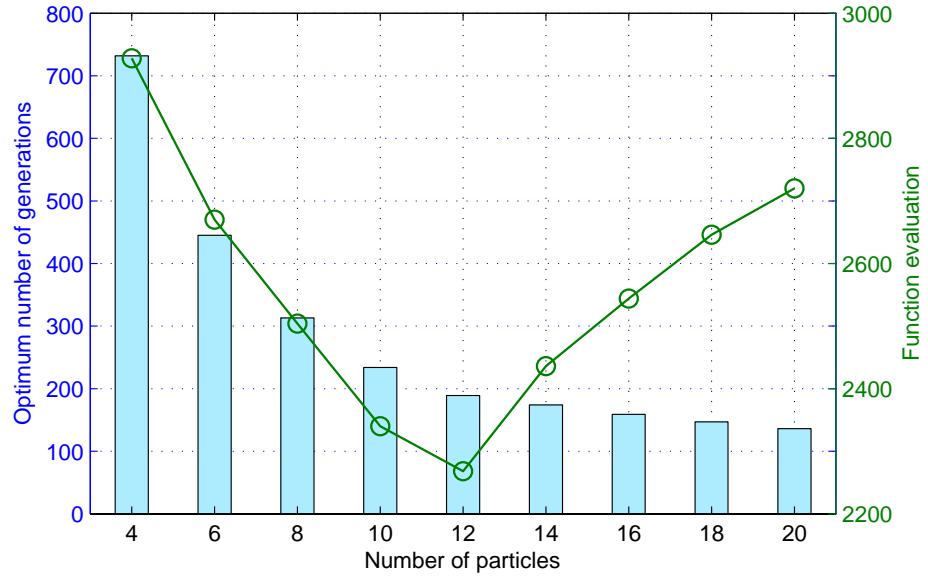


Figure 5.9: Particle number and generation number selection in terms of algorithm time complexity

in terms of different number of particles. In addition, it takes less generations for 12 particles to find the final fitness value, because more particles mean better opportunities to find the optimal solution.

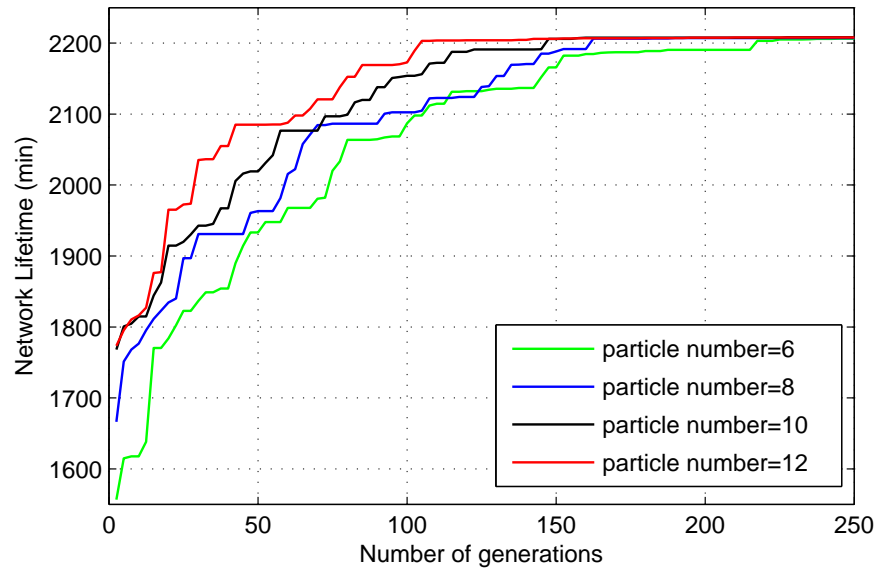


Figure 5.10: Convergence of QPSO algorithm

Next, Figure 5.11 demonstrates network lifetime with respect to the long-haul cluster distance. \bar{P}_{BER}^{THR} is set to be 10^{-4} . It is observed that the proposed QPSO-based cooperative coalitions selection algorithm outperforms the 2×2 MIMO and 3×3 MIMO in terms of network lifetime by approximately 20%. This is because the proposed algorithm is able to select the optimum cooperative coalitions in every link dynamically. In addition, the 2×2 MIMO system outperforms 3×3 MIMO system when the long-haul distance is short, e.g. 100m, due to more circuit energy consumption of 3×3 MIMO system. It is also shown that with the increment of the long-haul distance, the network lifetime decreases, because more RCoops and SCoops are selected to support the long-haul transmission, thereby increasing the energy consumption.

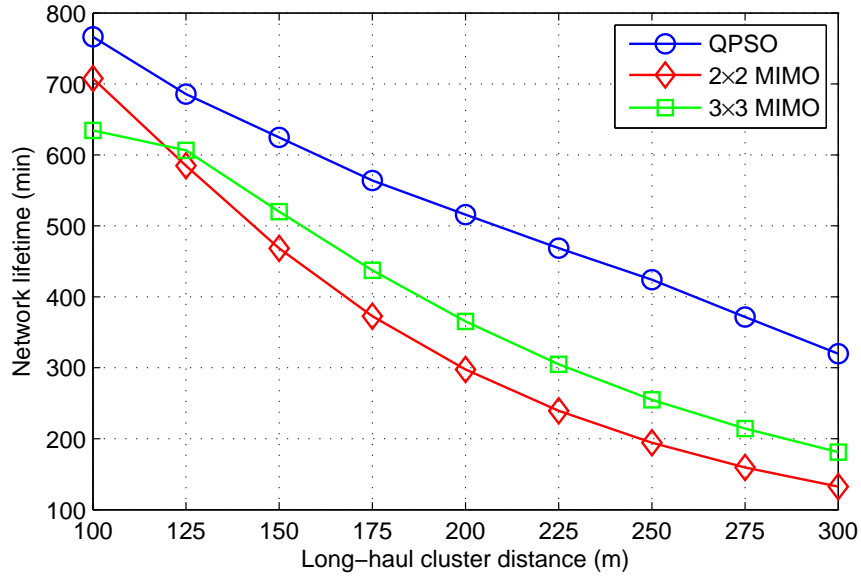


Figure 5.11: Network lifetime in terms of long-haul cluster distance

Table 5-B illustrates the size of cooperative coalitions in each link in terms of the long-haul cluster distance. It can be seen that the size of cooperative coalitions increases from link 1 to link 3 on account of the same long-haul distance, due to the increment of the packet size from line 1 to link 3 in the long-haul transmission. Additionally, it is shown that the size of cooperative coalitions for a particular link also increases with respect to the long-haul distance. However, the size of cooperative coalitions remains

the same when the long-haul distance becomes larger, because no additional suitable SCoops and RCoops can be selected.

Table 5-B: Size of cooperative coalitions in terms of long-haul cluster distance

Long-haul distance (m)	Link 1	Link 2	Link 3
100	$1 \times 2\text{MIMO}$	$2 \times 2\text{MIMO}$	$3 \times 1\text{MIMO}$
125	$1 \times 2\text{MIMO}$	$2 \times 3\text{MIMO}$	$3 \times 1\text{MIMO}$
150	$1 \times 2\text{MIMO}$	$2 \times 3\text{MIMO}$	$4 \times 1\text{MIMO}$
175	$1 \times 2\text{MIMO}$	$3 \times 3\text{MIMO}$	$4 \times 1\text{MIMO}$
200	$1 \times 2\text{MIMO}$	$3 \times 3\text{MIMO}$	$4 \times 1\text{MIMO}$
225	$1 \times 2\text{MIMO}$	$3 \times 3\text{MIMO}$	$5 \times 1\text{MIMO}$
250	$2 \times 2\text{MIMO}$	$3 \times 4\text{MIMO}$	$5 \times 1\text{MIMO}$
275	$2 \times 3\text{MIMO}$	$3 \times 4\text{MIMO}$	$5 \times 1\text{MIMO}$
300	$2 \times 3\text{MIMO}$	$3 \times 4\text{MIMO}$	$5 \times 1\text{MIMO}$

Figure 5.12 depicts the network lifetime in terms of BER threshold \bar{P}_{BER}^{THR} . The long-haul cluster distance is set to be $100m$. As discussed before, the proposed QPSO-based cooperative coalitions selection algorithm is able to choose the optimum cooperative coalitions in each link dynamically, therefore, the proposed algorithm outperforms 2×2 MIMO and 3×3 MIMO systems by about 15%. Furthermore, the 3×3 MIMO outperforms 2×2 MIMO in terms of network lifetime when the BER threshold increases from 10^{-6} to 5×10^{-5} . This is due to the fact that the transmission energy consumption of long-haul transmission dominates the network lifetime. However, the 2×2 MIMO outperforms the 3×3 MIMO system with the increment of BER threshold from 5×10^{-5} to 5×10^{-4} , because the circuit energy consumption dominates the network lifetime in this case.

Finally, the size of cooperative coalitions in each link in terms of BER threshold is investigated in Table 5-C. It is observed that the proposed QPSO algorithm can select the cooperative coalitions dynamically to meet different BER requirement. Besides, it can be seen that more SCoops and RCoops are required to ensure the QoS provision in link 3. This is because cluster 3 is responsible for relaying the data packets of all clusters in the routing path.

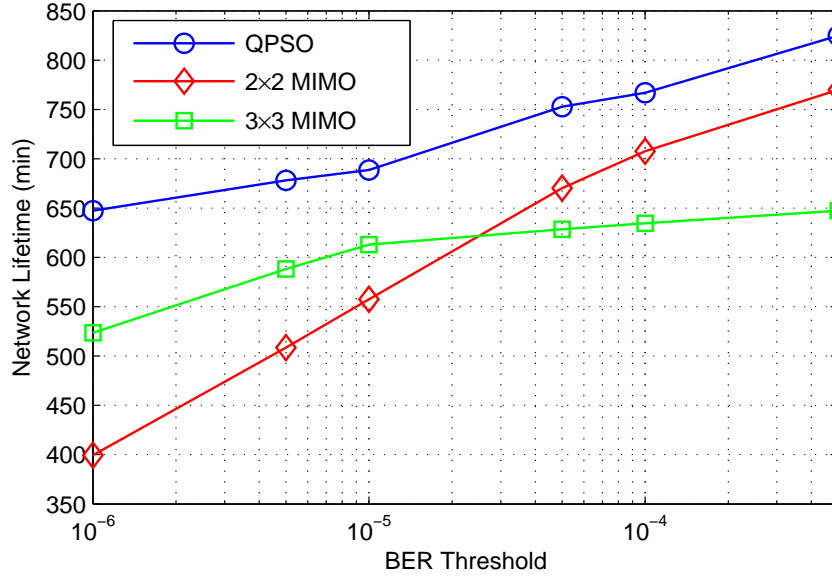


Figure 5.12: Network lifetime in terms of BER threshold

Table 5-C: Size of Cooperative Coalitions in terms of BER threshold

BER Threshold	Link 1	Link 2	Link 3
10^{-6}	$1 \times 3\text{MIMO}$	$3 \times 3\text{MIMO}$	$5 \times 2\text{MIMO}$
5×10^{-6}	$1 \times 3\text{MIMO}$	$3 \times 3\text{MIMO}$	$5 \times 2\text{MIMO}$
10^{-5}	$1 \times 3\text{MIMO}$	$3 \times 2\text{MIMO}$	$5 \times 2\text{MIMO}$
5×10^{-5}	$1 \times 2\text{MIMO}$	$3 \times 2\text{MIMO}$	$4 \times 2\text{MIMO}$
10^{-4}	$1 \times 2\text{MIMO}$	$3 \times 2\text{MIMO}$	$4 \times 2\text{MIMO}$
5×10^{-4}	$1 \times 2\text{MIMO}$	$3 \times 2\text{MIMO}$	$3 \times 2\text{MIMO}$

5.3.3.4 Conclusions

In this section, the cooperative coalitions selection using QPSO algorithm is investigated with the aim of maximising the average network lifetime in multi-hop cluster-based capillary networks. It is shown that the proposed QPSO-based cooperative coalitions selection algorithm can select the optimum cooperative devices dynamically to participate the long-haul transmission. Simulation results show that the proposed QPSO-based MIMO scheme outperforms 2×2 MIMO and 3×3 MIMO in terms of network lifetime.

5.4 QoS-based Cooperative Coalitions Selection

This section focuses on selection of the cooperative coalitions set in one routing path with the objective of minimising overall PER.

5.4.1 QoS-based Problem Formulation

In this subsection, the overall energy consumption of intra-cluster transmission, data aggregation and inter-cluster transmission for all clusters are formulated. The overall PER is derived and the research problem to minimise the overall PER is presented.

5.4.1.1 Energy Consumption for Intra-cluster Transmission

In the data collection phase, all CHs act as the receivers dissipating the reception power consumption, while all CMs, SCoops and RCoops transmit data to their corresponding CH, dissipating the transmission power consumption. As the assumption of squared power path loss, the energy consumption per bit of cluster i for the data collection phase is expressed as

$$\begin{aligned}
 E_b^{DC}(i) = & \sum_{j=1}^{\mathcal{N}_{CM}(i)} \left[(1 + \varphi_{amp}) \frac{(4\pi)^2 M_l N_r}{G_t G_r \lambda^2} \cdot d_{j,i}^2 \cdot \frac{\bar{E}_b}{N_0} \Big|_{intra} + \frac{P_{ct} + P_{cr}}{R_b} \right] \\
 & + \sum_{m=1}^{\mathcal{N}_{SCoop}(i)} \left[(1 + \varphi_{amp}) \frac{(4\pi)^2 M_l N_r}{G_t G_r \lambda^2} \cdot d_{m,i}^2 \cdot \frac{\bar{E}_b}{N_0} \Big|_{intra} + \frac{P_{ct} + P_{cr}}{R_b} \right] \\
 & + \sum_{k=1}^{\mathcal{N}_{RCoop}(i)} \left[(1 + \varphi_{amp}) \frac{(4\pi)^2 M_l N_r}{G_t G_r \lambda^2} \cdot d_{k,i}^2 \cdot \frac{\bar{E}_b}{N_0} \Big|_{intra} + \frac{P_{ct} + P_{cr}}{R_b} \right]
 \end{aligned} \quad (5.21)$$

where $d_{n,i}$ is the distance between device n and CH i , the first term is the data collection energy consumption for CMs in cluster i , the second term is the data collection energy consumption for SCoops in cluster i and the third term is the data collection energy consumption for RCoops in cluster i .

In the local broadcasting phase, CH in the i -th cluster acts as transmitter to broadcast the aggregated data to all SCoops in the i -th cluster, dissipating the transmission power consumption, and all SCoops receive data information from the CH, dissipating the receiving path power consumption. Due to the broadcast nature of the wireless channel, if the SCoop with the maximum distance from CH in the i -th cluster, denoted by $d_{max}(i)$, can receive the data from CH i , the other SCoops can simultaneously receive these data. Then the energy consumption per bit of cluster i for this phase is given by

$$E_b^{LB}(i) = (1 + \varphi_{amp}) \frac{(4\pi)^2 M_l N_r}{G_t G_r \lambda^2} \cdot d_{max}^2(i) \cdot \frac{\bar{E}_b}{N_0} \Big|_{intra} + \frac{P_{ct} + \mathcal{N}_{SCoop}(i) P_{cr}}{R_b} \quad (5.22)$$

In the local forwarding phase, CH $i+1$ receives long-haul MIMO-modulated data from all RCoops in the $(i+1)$ -th cluster, dissipating the receiving path power consumption. Meanwhile, RCoops transmit the MIMO-modulated data to their CH, dissipating the transmission path power consumption. As a result, the energy consumption per bit of cluster $(i+1)$ for the local forwarding phase is as follows

$$E_b^{LF}(i+1) = \sum_{k=1}^{\mathcal{N}_{Rcoop}(i+1)} \left[(1 + \varphi_{amp}) \frac{(4\pi)^2 M_l N_r}{G_t G_r \lambda^2} \cdot d_{k,i+1}^2 \cdot \frac{\bar{E}_b}{N_0} \Big|_{intra} + \frac{P_{ct} + P_{cr}}{R_b} \right] \quad (5.23)$$

5.4.1.2 Energy Consumption and Packet Size for Data Aggregation

The overall energy consumption of data aggregation for CH i is

$$E_{agg}(i) = [\mathcal{N}_{SCoop}(i) + \mathcal{N}_{Rcoop}(i) + \mathcal{N}_{CM}(i)] L_{data} E_{bf} \quad (5.24)$$

where E_{bf} is the energy consumption per bit for uniform data aggregation.

The size of packet after data aggregation is,

$$L_{agg}(i) = \frac{(1 + \mathcal{N}_{CM}(i) + \mathcal{N}_{SCoop}(i) + \mathcal{N}_{Rcoop}(i))}{(\mathcal{N}_{CM}(i) + \mathcal{N}_{SCoop}(i) + \mathcal{N}_{Rcoop}(i))\gamma_{agg} + 1} L_{data} \quad (5.25)$$

where γ_{agg} is the aggregation factor.

5.4.1.3 Energy Consumption and Packet Size for Long-haul Transmission

In the long-haul transmission phase, CH and SCoops in the i -th cluster jointly transmit the MIMO modulated data to their neighbouring $(i + 1)$ -th cluster or the capillary gateway, dissipating the transmission path power consumption, while the CH and RCoops in the $(i + 1)$ -th cluster receives the MIMO modulated data, dissipating the receiving path power consumption. Considering the broadcasting nature of wireless channels, the long-haul distance in the CMIMO communication is obtained by the maximum distance between the transmitter device in the i -th cluster and the reception devices in the $(i + 1)$ -th cluster. Thus, the energy consumption per bit of cluster i and cluster $i + 1$ for this phase $E_b^{LH}(i)$ is

$$\begin{aligned}
 E_b^{LH}(i) = & \sum_{m=1}^{\mathcal{N}_{SCoop}(i)} \left[(1 + \varphi_{amp}) \frac{(4\pi)^2 M_t N_r}{G_t G_r \lambda^2} \cdot d_{max}^{\kappa_{max}}(m) \cdot \frac{\bar{E}_b}{N_0} \Big|_{inter} + \frac{P_{ct}}{R_b^{eff}} \right] \\
 & + \left[(1 + \varphi_{amp}) \frac{(4\pi)^2 M_t N_r}{G_t G_r \lambda^2} \cdot d_{max}^{\kappa_{max}}(i) \cdot \frac{\bar{E}_b}{N_0} \Big|_{inter} + \frac{P_{ct}}{R_b^{eff}} \right] \\
 & + (\mathcal{N}_{RCoop}(i + 1) + 1) \cdot (\mathcal{N}_{SCoop}(i) + 1) \cdot \frac{P_{cr}}{R_b^{eff}}
 \end{aligned} \tag{5.26}$$

where $d_{max}(m)$ is the long-haul distance from SCoop m in cluster i to cluster $(i + 1)$, $d_{max}(i)$ is the long-haul distance from CH i to cluster $(i + 1)$, κ_{max} is the corresponding path loss exponent of the long-haul transmission and is in the range between 2 and 3. In (5.26), the first term is the long-haul energy consumption of all SCoops in cluster i , the second term is the long-haul energy consumption of CH i and the third term is the long-haul energy consumption for the reception circuit blocks of all RCoops and CH in cluster $(i + 1)$.

Training overhead is introduced into the CMIMO scheme for channel estimation and the number of required training symbols is proportional to the number of transmit

antennas. Therefore, the packet size of long-haul transmission is given by,

$$L_c(i) = \frac{F_{block}}{F_{block} - \rho_{train}(\mathcal{N}_{SCoop}(i) + 1)} \sum_{q=1}^i L_{agg}(q) \quad (5.27)$$

where F_{block} is the block size of STBC code, $\rho_{train}(\mathcal{N}_{SCoop} + 1)$ is the number of training symbols in each block. According to [HH03], the effective system bit rate is given by,

$$R_b^{eff} = \frac{F_{block} - \rho_{train}(\mathcal{N}_{SCoop} + 1)}{F_{block}} R_b \quad (5.28)$$

5.4.1.4 Overall PER Formulation

The average BER of the intra-cluster communication with a square constellation (i.e. $b = M/2$ is even and b is called the constellation size of MQAM) and in AWGN channel is given by

$$\bar{P}_{BER}^{intra} \doteq \frac{4(1 - 1/\sqrt{M})}{\log_2 M} Q \left(\sqrt{\frac{3 \log_2 M}{M - 1} \cdot \frac{\bar{E}_b}{N_0}} \right) \quad (5.29)$$

where $Q(x) = \int_x^\infty \frac{1}{\sqrt{2\pi}} e^{-\frac{u^2}{2}} du$.

Denote the number of transmitters to be \mathcal{N}_T and the number of receivers to be \mathcal{N}_R . In this chapter, transmitters in the long-haul transmission include the CH and SCoops at the transmission side, that is, $\mathcal{N}_T = \mathcal{N}_{SCoop}(i) + 1$ in cluster i . The receivers in the long-haul transmission include the CH and RCoops at the reception side, that is, $\mathcal{N}_R = \mathcal{N}_{RCoop}(i) + 1$ in cluster $(i + 1)$. Then the average BER of the inter-cluster communication with a square constellation MQAM in Rayleigh fading channel is given by

$$\bar{P}_{BER}^{inter} \doteq \frac{4}{\log_2 M} \left(1 - \frac{1}{\sqrt{M}} \right) \left(\frac{1 - \mu}{2} \right)^{\mathcal{N}_T \mathcal{N}_R} \times \sum_{l=0}^{\mathcal{N}_T \mathcal{N}_R - 1} \binom{\mathcal{N}_T \mathcal{N}_R - 1 + l}{l} \left(\frac{1 + \mu}{2} \right)^l \quad (5.30)$$

where

$$\mu = \sqrt{\frac{\iota}{1+\iota}} \quad (5.31a)$$

$$\iota = \frac{1}{\mathcal{N}_T} \cdot \frac{3 \log_2 M}{2(M-1)} \cdot \frac{\bar{E}_b}{N_0} \quad (5.31b)$$

In addition, the PER is derived as $P_{PER} = 1 - (1 - P_{BER})^{L_{packet}}$ [KS05], where L_{packet} is the number of bits in the packet. In this section, the overall packet size of cluster i for the data collection phase is $L_{data}(\mathcal{N}_{CM}(i) + \mathcal{N}_{SCoop}(i) + \mathcal{N}_{RCoop}(i))$, because $\mathcal{N}_{CM}(i)$ CMs, $\mathcal{N}_{SCoop}(i)$ SCoops and $\mathcal{N}_{RCoop}(i)$ RCoops transmit packets of L_{data} bits to the CH i . In the local broadcasting phase, $\mathcal{N}_{SCoop}(i)$ SCoops of cluster i receive the aggregated data of size $L_{agg}(i)$ from CH i , therefore the overall packet size is $L_{agg}(i)\mathcal{N}_{SCoop}(i)$. In the long-haul transmission phase, CH i and $\mathcal{N}_{SCoop}(i)$ SCoops at the transmission side send the MIMO-modulated packet of size $L_c(i)$ to $\mathcal{N}_{RCoop}(i+1)$ RCoops and CH $(i+1)$, so the overall packet size is $L_c(i)(\mathcal{N}_{SCoop}(i) + 1)(\mathcal{N}_{RCoop}(i+1) + 1)$. In the local forwarding phase, $\mathcal{N}_{RCoop}(i+1)$ RCoops at cluster $i+1$ transmit a packet of size $L_c(i)$ to their CH $(i+1)$, so the overall packet size is $L_c(i)(\mathcal{N}_{RCoop}(i+1))$. Therefore, the PER of the data collection phase, the local broadcasting phase, the long-haul transmission phase and local forwarding phase are given by

$$\bar{P}_{PER}^{DC}(i) = 1 - (1 - \bar{P}_{BER}^{intra})^{L_{data}(\mathcal{N}_{CM}(i) + \mathcal{N}_{SCoop}(i) + \mathcal{N}_{RCoop}(i))} \quad (5.32a)$$

$$\bar{P}_{PER}^{LB}(i) = 1 - (1 - \bar{P}_{BER}^{intra})^{L_{agg}(i)\mathcal{N}_{SCoop}(i)} \quad (5.32b)$$

$$\bar{P}_{PER}^{LH}(i) = 1 - (1 - \bar{P}_{BER}^{inter})^{L_c(i)(\mathcal{N}_{SCoop}(i)+1)(\mathcal{N}_{RCoop}(i)+1)} \quad (5.32c)$$

$$\bar{P}_{PER}^{LF}(i+1) = 1 - (1 - \bar{P}_{BER}^{inter})^{L_c(i)(\mathcal{N}_{RCoop}(i+1))} \quad (5.32d)$$

Correspondingly, the overall PER of all phases during the transmission from cluster

i to cluster $(i + 1)$ is as follows

$$\begin{aligned} \bar{P}_{PER}(i, i + 1) = & \bar{P}_{PER}^{DC}(i) + (1 - \bar{P}_{PER}^{DC}(i))\bar{P}_{PER}^{LB}(i) + (1 - \bar{P}_{PER}^{DC}(i))(1 - \bar{P}_{PER}^{LB}(i))\bar{P}_{PER}^{LH}(i) \\ & + (1 - \bar{P}_{PER}^{DC}(i))(1 - \bar{P}_{PER}^{LB}(i))(1 - \bar{P}_{PER}^{LH}(i))\bar{P}_{PER}^{LF}(i + 1) \end{aligned} \quad (5.33)$$

where the first term indicates that transmission error occurs in the data collection phase, which results in the error transmission of the following three phases; the second term means that the data transmission is successful in the data collection phase while error occurs in the local broadcasting phase, which results in the error transmission in the long-haul transmission phase and the local forwarding phase; the third term indicates that data transmission of both data collection and local transmission phase are successful, however, error occurs in the long-haul transmission phase, which contributes to the error transmission in the local forwarding phase; and the fourth term means that data transmission of the first three phases are successful, but error occurs in the local forwarding phase.

Therefore, the overall PER of all hops transmission in the routing path is expressed as

$$\bar{P}_{PER}^{overall} = 1 - \prod_{i=1}^{\mathcal{N}_{CH}} [1 - \bar{P}_{PER}(i, i + 1)] \quad (5.34)$$

The research problem is to find the optimum cooperative coalitions of all clusters in the routing path, denoted by $\mathbb{C} = \{\mathbb{C}(1), \dots, \mathbb{C}(i), \dots, \mathbb{C}(\mathcal{N}_{CH})\}$, in order to minimise the overall packet error rate $\bar{P}_{PER}^{overall}$. Assume the overall sum of energy consumption in three phases of all devices is limited to E_t , the research problem in this work is expressed

as

$$\begin{aligned}
 & \text{minimise } \bar{P}_{PER}^{overall} \\
 & \text{s.t. } \begin{cases} 0 \leq \mathcal{N}_{SCoop}(i) \leq \mathcal{N}_{nonCH}(i) \\ 0 \leq \mathcal{N}_{RCoop}(i) \leq \mathcal{N}_{nonCH}(i) \\ \sum_{i=1}^{\mathcal{N}_{CH}} [L_{data} E_b^{DC}(i) + E_{AG}(i) + L_{agg}(i) E_b^{LB}(i) + L_c(i) E_b^{LH}(i) + L_c(i) E_b^{LF}(i+1)] \leq E_t \end{cases}
 \end{aligned} \tag{5.35}$$

5.4.2 QoS-based Cooperative Coalitions Selection Algorithm

The capillary gateway executes the Coops selection process based on QPSO, after receiving every device's individual information (i.e. residual energy and location).

The QPSO-based cooperative coalitions selection algorithm aiming at maximising the network lifetime is described in Algorithm 10. Firstly, the quantum position, quantum velocity, individual optimum and global optimum of all particles are initialised, as described from line 1 to line 10. Secondly, line 11 to line 29 describes the particle updating process to obtain the optimum set of cooperative coalitions. In particular, the quantum rotation angle, quantum velocity and quantum position of particles are updated from line 13 to line 17 by (2.12), (2.6) and (2.7), respectively. Then the updated particle positions are mapped to the selected set of SCoops and RCoops that is further utilized in fitness value (i.e. overall PER) calculation by (5.35) in line 18. Correspondingly, the local optimum and global optimum are updated from line 19 to line 28. Finally, the output of this algorithm is the set of cooperative coalitions in the routing path.

At last, the capillary gateway informs every device about its role (CH, CM, SCoop or RCoop) based on the result of Algorithm 10.

Algorithm 10: Cooperative coalitions selection to minimise overall PER

```

1 for each  $m \in [1, 2, \dots, \mathcal{N}_{particle}]$  do
2   for each  $n \in [1, 2, \dots, \mathcal{N}_{cand}]$  do
3     Set the quantum position  $x_{mn}^1$  by 0 or 1 randomly
4     Set the quantum velocity  $v_{mn}^1$  to be  $1/\sqrt{2}$ 
5   end
6   Update the overall PER  $f_m^1$  by (5.35)
   /* The local optimum is the initialised particles at the first
      generation */
7   Set the local optimum fitness value  $f_m^{pbest_{min}}$  to be  $f_m^1$ 
8   Set the local optimum position  $\mathbf{x}_m^{pbest_{min}}$  to be  $\mathbf{x}_m^1$ 
9 end
   /* Update the global optimum */
10 Update the global optimum fitness value  $f^{gbest_{min}}$  and the global optimum
    position  $\mathbf{x}^{gbest_{min}}$  by (2.9)
11 for each  $t \in [1, 2, \dots, T_{max}]$  do
12   for each  $m \in [1, 2, \dots, \mathcal{N}_{particle}]$  do
13     for each  $n \in [1, 2, \dots, \mathcal{N}_{cand}]$  do
14       Update the quantum rotation angle  $\theta_{mn}^{t+1}$  by (2.12)
15       Update the quantum velocity  $v_{mn}^{t+1}$  by (2.6)
16       Update the quantum position  $x_{mn}^{t+1}$  by (2.7)
17     end
18     Update the overall PER  $f_m^{t+1}$  by (5.35)
19     if  $f_m^{t+1} < f_m^{pbest_{min}}$  then
20       Set the local optimum fitness value  $f_m^{pbest_{min}}$  to be  $f_m^{t+1}$ 
21       Set the local optimum position  $\mathbf{x}_m^{pbest_{min}}$  to be  $\mathbf{x}_m^{t+1}$ 
22     end
23   end
24   Update the temporary global optimum fitness value  $g^{gbest_{min}}$  by (2.9)
   /* Find the final global optimum */
25   if  $g^{gbest_{min}} < f^{gbest_{min}}$  then
26     Set the final global optimum fitness value  $f^{gbest_{min}}$  to be  $g^{gbest_{min}}$ 
27     Update the global optimum position  $\mathbf{x}^{gbest_{min}}$  according to  $g^{gbest_{min}}$ 
28   end
29 end
30 return  $\mathbf{x}^{gbest_{min}}$  as the optimum set of cooperative coalitions in the routing path

```

5.4.3 Simulation and Conclusions

This subsection describes the simulation scenario design, system parameters setting, simulation platform design and the simulation results.

5.4.3.1 Scenario Design and System Parameters

In this subsection, the scenario is the same as the one as described in Subsection 5.3.3.1. The system parameters used in this section are also the same as shown in Table 3-A and Table 4-A.

5.4.3.2 Simulation Platform Design

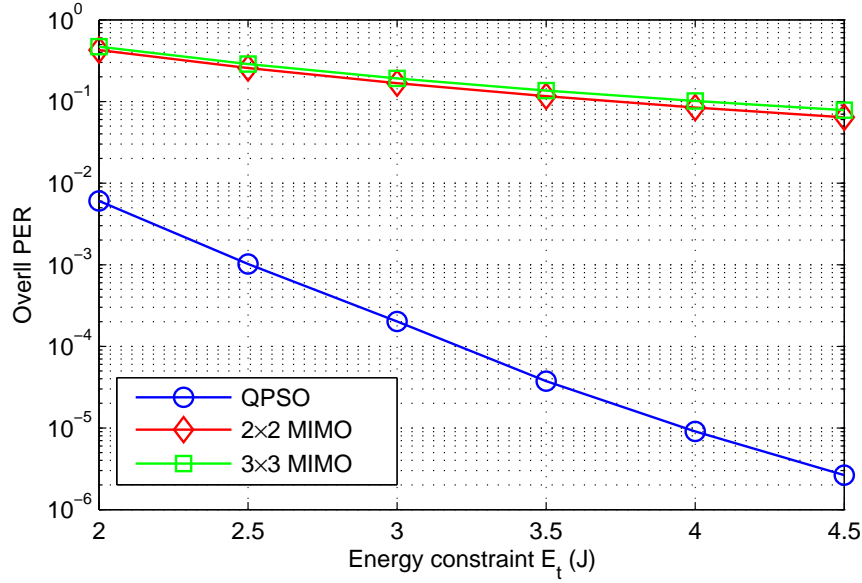
In this subsection, the simulation platform design is similar to Subsection 5.3.3.2. However, the particles in QPSO-based Coops selection module are updated to find the minimum fitness value (i.e. overall PER) in Algorithm 10 instead of the maximum fitness value (i.e. network lifetime) in Algorithm 9.

5.4.3.3 Simulation Results

Due to the same scenario setting, the particle number and generation number in this simulation is also set to be 12 and 200, respectively.

First, Figure 5.13 shows the overall PER in terms of energy constraint E_t . It is observed that the proposed QPSO-based cooperative coalitions selection algorithm outperforms the 2×2 MIMO and 3×3 MIMO by 50% in terms of overall PER dramatically. This is because the proposed algorithm can dynamically select the optimum cooperative coalitions in every link. It is also shown that with the increment of the energy constraint, the overall PER decreases, since more RCoops and SCoops are selected to support the long-haul transmission.

Table 5-D illustrates the size of energy constraint E_t in each link in terms of long-haul distance. It can be seen that the size of cooperative coalitions increases from link 1 to link 3 on account of the same energy constraint, due to the increment of the packet size from link 1 to link 3 in the long-haul transmission. In addition, it is also shown that the size of

Figure 5.13: Overall PER in terms of energy constraint E_t

cooperative coalitions for a particular link increases with more energy constraint. This can be explained by the fact that more energy constraint can support more SCoops and RCoops in the long-haul transmission, and thus decreasing the overall PER. However, the size of cooperative coalitions remains the same when energy constraint increases after a certain threshold, because no optimum SCoops and RCoops can be selected.

Table 5-D: Size of Cooperative Coalitions in terms of Energy Constraint E_t

Energy constraint E_t	Link 1	Link 2	Link 3
$2J$	$1 \times 1\text{MIMO}$	$1 \times 2\text{MIMO}$	$2 \times 1\text{MIMO}$
$2.5J$	$1 \times 1\text{MIMO}$	$2 \times 2\text{MIMO}$	$3 \times 1\text{MIMO}$
$3J$	$2 \times 2\text{MIMO}$	$1 \times 3\text{MIMO}$	$3 \times 1\text{MIMO}$
$3.5J$	$2 \times 2\text{MIMO}$	$1 \times 3\text{MIMO}$	$4 \times 1\text{MIMO}$
$4J$	$2 \times 2\text{MIMO}$	$1 \times 3\text{MIMO}$	$4 \times 1\text{MIMO}$
$4.5J$	$2 \times 2\text{MIMO}$	$1 \times 3\text{MIMO}$	$4 \times 1\text{MIMO}$

Figure 5.14 demonstrates the overall PER in terms of long-haul cluster distance. The energy constraint is set to be $3J$. As discussed before, the proposed QPSO-based algorithm is able to select cooperative coalitions in each link dynamically, therefore, it outperforms 2×2 MIMO and 3×3 MIMO systems significantly. Moreover, the overall PER increases with respect to the long-haul cluster distance. This can be explained by

the fact that limited by the energy constraint, less SCoops and RCoops can be selected in larger long-haul cluster distance.

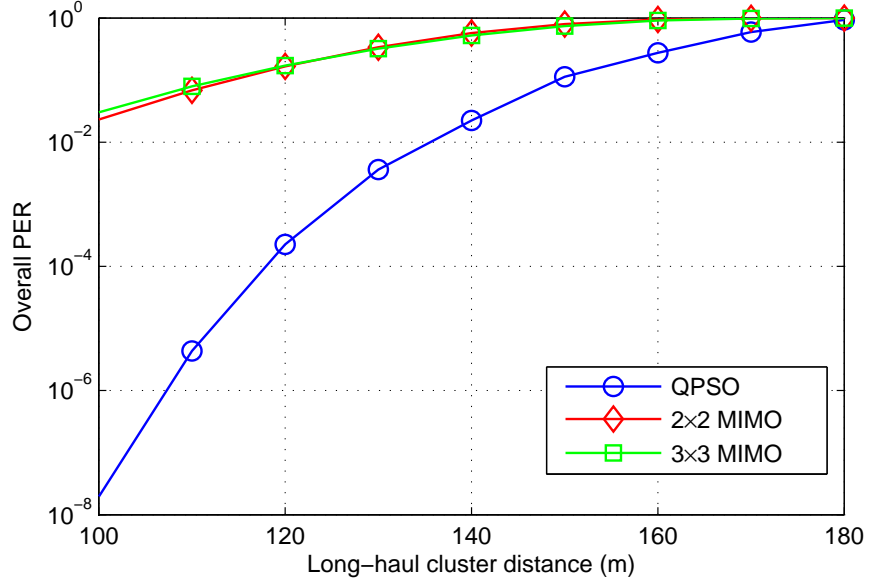


Figure 5.14: Long-haul distance versus overall PER

Finally, the size of cooperative coalitions in each link in terms of energy constraint is investigated in Table 5-E. It can be seen that the proposed QPSO algorithm can select the cooperative coalitions dynamically in scenarios with different energy constraint requirement. In addition, the size of cooperative coalitions becomes smaller with the increment of long-haul cluster distance.

Table 5-E: Size of Cooperative Coalitions versus Long-haul Cluster Distance

Long-haul cluster distance (m)	Link 1	Link 2	Link 3
100	$3 \times 2\text{MIMO}$	$2 \times 4\text{MIMO}$	$5 \times 1\text{MIMO}$
125	$3 \times 2\text{MIMO}$	$2 \times 3\text{MIMO}$	$4 \times 1\text{MIMO}$
150	$3 \times 2\text{MIMO}$	$2 \times 3\text{MIMO}$	$3 \times 1\text{MIMO}$
175	$2 \times 1\text{MIMO}$	$3 \times 2\text{MIMO}$	$2 \times 1\text{MIMO}$
200	$2 \times 1\text{MIMO}$	$3 \times 2\text{MIMO}$	$2 \times 1\text{MIMO}$
225	$2 \times 1\text{MIMO}$	$3 \times 2\text{MIMO}$	$1 \times 1\text{MIMO}$
250	$2 \times 1\text{MIMO}$	$3 \times 2\text{MIMO}$	$1 \times 1\text{MIMO}$
275	$2 \times 1\text{MIMO}$	$3 \times 1\text{MIMO}$	$1 \times 1\text{MIMO}$
300	$2 \times 1\text{MIMO}$	$3 \times 1\text{MIMO}$	$1 \times 1\text{MIMO}$

5.4.3.4 Conclusions

In this section, the cooperative coalitions selection using QPSO algorithm is investigated with the aim of minimising the overall PER in multi-hop cluster-based capillary networks. It is shown that the proposed QPSO-based cooperative coalitions selection algorithm can select the optimum cooperative devices participating the long-haul transmission dynamically. Simulation results show that the proposed QPSO-based MIMO scheme outperforms 2×2 MIMO and 3×3 MIMO in terms of overall PER.

5.5 Cooperative Coalitions Selection for Joint Optimisation

This section focuses on the tradeoff between energy efficiency and QoS provision using CMIMO system by selecting optimum set of cooperative coalitions.

5.5.1 Joint Optimisation Problem Formulation

Research objectives of energy efficiency and QoS provision optimisation are formulated in this subsection. More specifically, the network time by (5.20) in Section 5.3 is utilized to optimise energy efficiency, and the overall PER by (5.35) in Section 5.4 is utilized to optimise the QoS provision.

5.5.1.1 Objective 1: Network Lifetime Maximisation

In this section, (5.2) to (5.20) are used to calculate the average battery time \bar{T}_{avg}^{op} , which represents the network lifetime and is expressed as follows,

$$\bar{T}_{avg}^{op} = \frac{\sum_{k=1}^{\mathcal{N}_{total}} T^{op}(k)}{\mathcal{N}_{total}} \quad (5.36)$$

5.5.1.2 Objective 2: Overall PER Minimisation

The overall PER is obtained from (5.21) to (5.33) and expressed as follows

$$\bar{P}_{PER}^{overall} = 1 - \prod_{i=1}^{\mathcal{N}_{CH}} [1 - \bar{P}_{PER}(i, i+1)] \quad (5.37)$$

5.5.1.3 Tradeoff Formulation of Network Lifetime and Overall PER

The research problem is to find the optimum cooperative coalitions of all clusters in the routing path, denoted by $\mathbb{C} = \{\mathbb{C}(1), \dots, \mathbb{C}(i), \dots, \mathbb{C}(\mathcal{N}_{CH})\}$, in order to achieve the optimal tradeoff between network lifetime and overall PER, that is,

$$\begin{cases} \underset{\mathbb{C}}{\text{maximise}} \bar{T}_{op}^{avg} \\ \underset{\mathbb{C}}{\text{minimise}} \bar{P}_{PER}^{overall} \end{cases} \quad (5.38)$$

s.t. $0 \leq \mathcal{N}_{SCoop}(i) \leq \mathcal{N}_{nonCH}(i)$
 $0 \leq \mathcal{N}_{RCoop}(i) \leq \mathcal{N}_{nonCH}(i)$

5.5.2 Cooperative Coalitions Selection Algorithm for Joint Optimisation

The capillary gateway executes the Coops selection process based on NSGA-II and QPSO (NSQPSO) algorithm, after receiving every device's individual information (i.e. residual energy and location).

The proposed NSQPSO-based Coops selection algorithm aiming at the optimal tradeoff between network lifetime and overall PER is described in Algorithm 11. The notation in Subsection 4.5.2 is used in this section. Firstly, the quantum position, quantum velocity, local optimum and global optimum of all particles are initialised, as refer to line 1 to 12. In particular, the network lifetime and overall PER are calculated in line 6 after

Algorithm 11: Cooperative coalitions selection to achieve the optimum tradeoff between energy efficiency and QoS provision

```

1 for each  $m \in [1, 2, \dots, \mathcal{N}_{particle}]$  do
2   for each  $n \in [1, 2, \dots, \mathcal{N}_{cand}]$  do
3     Set the quantum position  $x_{mn}^1$  by 0 or 1 randomly
4     Set the quantum velocity  $v_{mn}^1$  to be  $1/\sqrt{2}$ 
5   end
6   Update the network lifetime  $f_m^1(1)$  by (5.36) and the overall PER  $f_m^1(2)$ 
   by (5.37)
7   Set the local optimum fitness value for energy efficiency  $f_m^{pbest_{max}}(1)$  to be
    $f_m^1(1)$ 
8   Set the local optimum fitness value for QoS provision  $f_m^{pbest_{min}}(2)$  to be  $f_m^1(2)$ 
9   Set the local optimum position  $\mathbf{x}_m^{pbest}$  to be  $\mathbf{x}_m^1$ 
10 end
11 Generate  $\hat{S}_1$  by Algorithm 3 based on  $\mathcal{S}_1$ 
12  $\mathbf{x}^{gbest}$  is chosen from a specified top part (e.g. top 5%) of  $\hat{S}$  randomly
13 for each  $t \in [1, 2, \dots, T_{max}]$  do
14   for each  $m \in [1, 2, \dots, \mathcal{N}_{particle}]$  do
15     for each  $n \in [1, 2, \dots, \mathcal{N}_{cand}]$  do
16       Update the quantum rotation angle  $\theta_{mn}^{t+1}$  by (2.12)
17       Update the quantum velocity  $v_{mn}^{t+1}$  by (2.6)
18       Update the quantum position  $x_{mn}^{t+1}$  by (2.7)
19     end
20     Update the network lifetime  $f_m^{t+1}(1)$  by (5.36) and overall PER  $f_m^{t+1}(2)$ 
     by (5.37)
21   end
22    $\mathcal{Z} = \mathcal{S}_t \cup \mathcal{S}_{t+1}$ 
23   Generate  $\hat{S}^{t+1}$  by Algorithm 3 based on  $\mathcal{Z}$ 
24    $\mathbf{x}^{gbest}(i)$  is chosen from a specified top part (e.g. top 5%) of  $\hat{S}^{t+1}$  randomly
25   for each  $m \in [1, 2, \dots, \mathcal{N}_{particle}]$  do
26      $\mathbf{x}_m^{pbest}$  is chosen from  $\hat{S}^{t+1}$  randomly
27   end
28 end
29 return  $\mathbf{x}^{gbest}$  as the optimum set of cooperative coalitions in the routing path

```

mapping the position of particles to the selected cooperative coalitions. And the NSGA-II algorithm is performed in line 11 to sort all particles. Then the global optimum is chosen from a specific top part of the sorted particles. Secondly, the particle updating process are described from line 15 to line 19. Specifically, the rotation angle by (2.12), velocity by (2.6), position by (2.7) and fitness values are updated in line 20. Then the

updated particles merge with previous particles in line 22, and the set of merged particles is sorted according to NSGA-II algorithm in line 23. The global optimum and local optimum are updated from line 24 to 27. Finally, the best set of cooperative coalitions for the routing path is returned as the output of this algorithm.

At last, the capillary gateway informs every device about its role (CH, CM or Coop) based on the result of Algorithm 11.

5.5.3 Simulation and Conclusions

This subsection describes the simulation scenario design, system parameters setting, simulation platform design and the simulation results.

5.5.3.1 Scenario Design and System Parameters

In this subsection, the scenario is the same as the one as described in Subsection 5.3.3.1. The system parameters used in this section are also the same as shown in Table 3-A and Table 4-A.

5.5.3.2 Simulation Platform Design

The simulation process of the proposed cooperative coalitions selection algorithm aiming at the tradeoff optimisation in Subsection 5.5.2 consists of a number of logic blocks and simulation loops, as shown in Figure 5.15.

A. Scenario initialisation module

The scenario initialisation module is the same as Subsection 5.3.3.2.

B. NSQPSO-based cooperative coalitions selection Module

This module performs QPSO algorithm to generate and update particles, and also per-

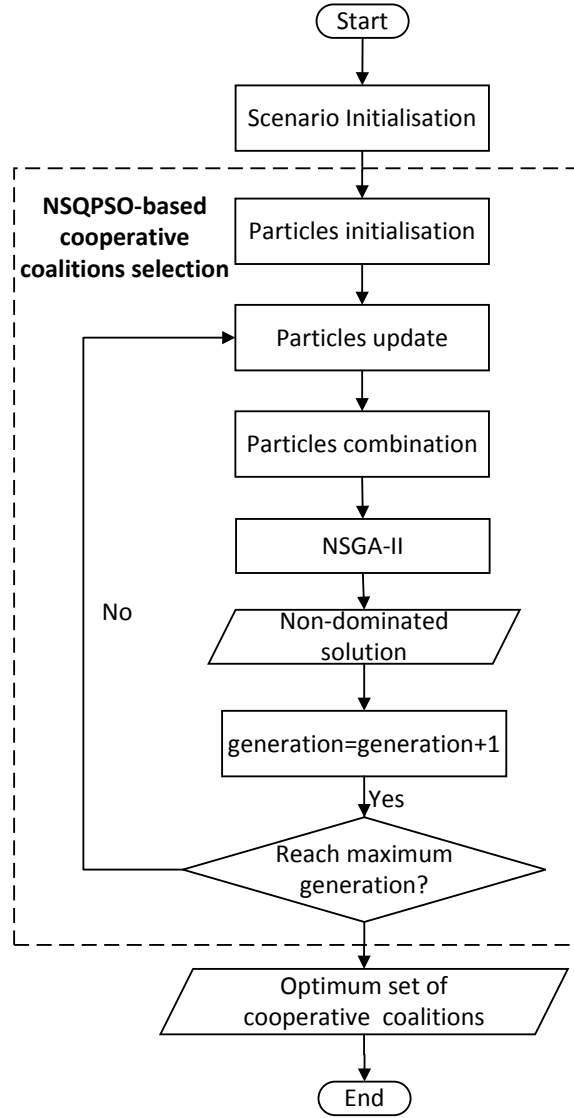


Figure 5.15: Flowchart of the proposed cooperative coalitions selection algorithm aiming at the tradeoff optimisation (Algorithm 11)

forms the NSGA-II algorithm to generate the non-dominated Pareto solutions which guides the direction of particle updating. It includes particle initialisation and particle updating as described in Subsection 3.5.2, particle combination block which merges the updated particles at current generation with previous particles at previous generation, NSGA-II block to obtain the non-dominated swarm, generation iteration process and the output of cooperative coalitions in the routing path after a pre-determined generations.

The NSGA-II block consists of non-dominated sorting sub-block to sort all solutions

into non-dominated fronts, as described in Subsection 4.5.3.

5.5.3.3 Simulation Results

Due to the same scenario setting, the particle number and generation number in this simulation is also set to be 12 and 200, respectively. In this subsection, the QPSO algorithm focuses on energy efficiency by maximising the network lifetime, denoted as QPSO-EE, and the QPSO algorithm focuses on QoS provision optimisation by minimising the overall PER, denoted as QPSO-QoS, are employed as two reference algorithms.

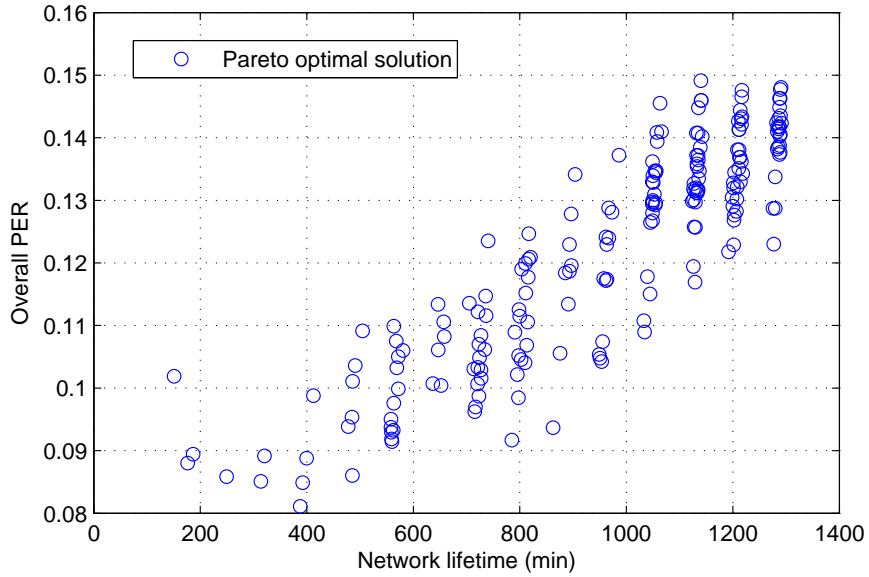


Figure 5.16: Pareto optimal solution of NSQPSO

First, Figure 5.16 shows the Pareto optimal solution of the proposed NSQPSO algorithm when setting \bar{E}_b/N_0 to be $20dB$. It can be seen that a longer network lifetime can be achieved but the overall PER is higher at the same time; similarly, the overall PER can be minimised by reducing the network lifetime. In addition, most of the Pareto optimal solutions are in the range between 1000-1400 min network lifetime. This is because these non-dominated solutions are produced in the particle updating process after certain generations and one of these solutions cannot be said to be better than the

in the absence of any further information.

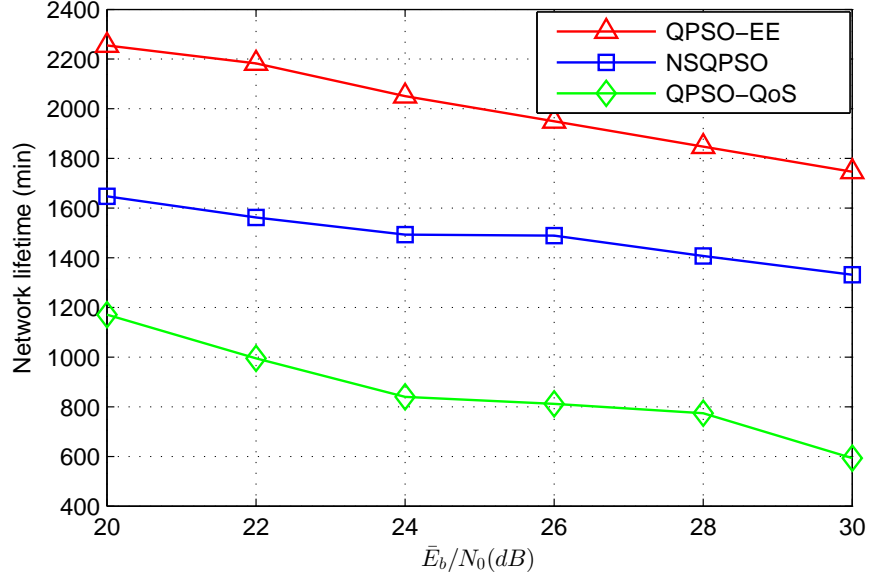
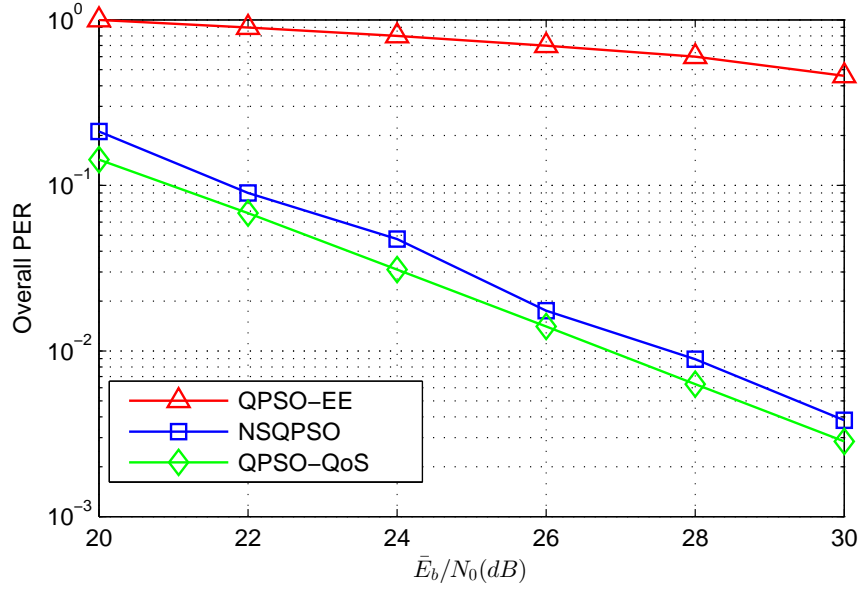


Figure 5.17: \bar{E}_b/N_0 versus network lifetime

In addition, Figure 5.17 and Figure 5.18 show the network lifetime and overall PER in terms of SNR per bit \bar{E}_b/N_0 . In Figure 5.17, it is observed that the performance of the proposed NSQPSO algorithm is better than QPSO-QoS algorithm which minimises the overall PER but compromises the energy efficiency. On the other hand, QPSO-EE algorithm outperforms the proposed NSQPSO algorithm in terms of network lifetime, while it compromises the PER as is shown in Figure 5.18. It can be concluded that the proposed NSQPSO algorithm is able to achieve the optimal tradeoff between energy efficiency and QoS provision by selecting optimum set of cooperative coalitions in the routing path.

Finally, the size of cooperative coalitions for link 1, link 2 and link 3 are list in Table 5-F, Table 5-G and Table 5-H, respectively. It has been proved in [DCSI07] that the BER decreases with the increment of \bar{E}_b/N_0 , and thus the energy consumption per bit increases with respect to \bar{E}_b/N_0 . In this case, the cooperative coalitions selected by QPSO-EE in the routing path is 1×1 MIMO. On the contrary, QPSO-QoS is able to select different cooperative coalitions with the objective of overall PER minimisation.

Figure 5.18: \bar{E}_b/N_0 versus overall PER

Additionally, more SCoops and RCoops for each link are selected by QPSO-QoS with the increment of \bar{E}_b/N_0 . It can also be observed that the size of cooperative coalitions selected by the proposed NSQPSO varies dynamically with respect to \bar{E}_b/N_0 . This is because there are many different Pareto optimal solutions of cooperative coalitions which can achieve the optimum tradeoff between network lifetime and overall PER and the proposed NSQPSO algorithm selects one of them randomly as the optimum cooperative coalitions.

Table 5-F: Size of Cooperative Coalitions for Link 1 in terms of \bar{E}_b/N_0

\bar{E}_b/N_0 (dB)	QPSO-EE	QPSO-QoS	Proposed NSQPSO
20	1 × 1MIMO	2 × 3MIMO	4 × 3MIMO
22	1 × 1MIMO	2 × 3MIMO	4 × 4MIMO
24	1 × 1MIMO	2 × 4MIMO	3 × 5MIMO
26	1 × 1MIMO	2 × 4MIMO	3 × 4MIMO
28	1 × 1MIMO	2 × 4MIMO	3 × 3MIMO
30	1 × 1MIMO	2 × 4MIMO	5 × 4MIMO

Table 5-G: Size of Cooperative Coalitions for Link 2 in terms of \bar{E}_b/N_0

$\bar{E}_b/N_0(dB)$	QPSO-EE	QPSO-QoS	Proposed NSQPSO
20	$1 \times 1\text{MIMO}$	$1 \times 4\text{MIMO}$	$2 \times 4\text{MIMO}$
22	$1 \times 1\text{MIMO}$	$1 \times 5\text{MIMO}$	$2 \times 4\text{MIMO}$
24	$1 \times 1\text{MIMO}$	$1 \times 5\text{MIMO}$	$3 \times 4\text{MIMO}$
26	$1 \times 1\text{MIMO}$	$1 \times 5\text{MIMO}$	$4 \times 4\text{MIMO}$
28	$1 \times 1\text{MIMO}$	$1 \times 5\text{MIMO}$	$5 \times 2\text{MIMO}$
30	$1 \times 1\text{MIMO}$	$1 \times 5\text{MIMO}$	$4 \times 3\text{MIMO}$

Table 5-H: Size of Cooperative Coalitions for Link 3 in terms of \bar{E}_b/N_0

$\bar{E}_b/N_0(dB)$	QPSO-EE	QPSO-QoS	Proposed NSQPSO
20	$1 \times 1\text{MIMO}$	$3 \times 1\text{MIMO}$	$5 \times 1\text{MIMO}$
22	$1 \times 1\text{MIMO}$	$5 \times 1\text{MIMO}$	$3 \times 1\text{MIMO}$
24	$1 \times 1\text{MIMO}$	$5 \times 1\text{MIMO}$	$5 \times 1\text{MIMO}$
26	$1 \times 1\text{MIMO}$	$5 \times 1\text{MIMO}$	$4 \times 1\text{MIMO}$
28	$1 \times 1\text{MIMO}$	$5 \times 1\text{MIMO}$	$6 \times 1\text{MIMO}$
30	$1 \times 1\text{MIMO}$	$6 \times 1\text{MIMO}$	$4 \times 1\text{MIMO}$

5.5.3.4 Conclusions

In this section, the cooperative coalitions selection using QPSO and NSGA-II algorithm is investigated with the aim of the optimum tradeoff between energy efficiency and QoS provision in multi-hop cluster-based capillary networks. It is shown that the proposed QPSO-based cooperative coalitions selection algorithm selects the optimum cooperative devices dynamically to participate the long-haul transmission. Simulation results show that the proposed QPSO-based MIMO can strike the optimum tradeoff between average network lifetime and overall PER.

5.6 Summary

In this chapter, Section 5.1 specified the system model for CMIMO systems in multi-hop cluster-based capillary networks.

In order to improve energy efficiency, an optimum cooperative coalitions selection algorithm was developed to achieve the network lifetime maximisation in Section 5.3.

Similar to Subsection 4.3.1, the network lifetime was formulated by applying the battery model, evaluating individual power consumption and estimating the transmission time of every device during all intra-cluster and inter-cluster transmission in Subsection 5.3.1. The proposed cooperative coalitions selection algorithm in Subsection 5.3.2 applies QPSO to select the cooperative coalitions for every hop in a particular routing path, which aims to maximise the network lifetime. Simulation results in Section 5.3.3 have shown that the proposed cooperative coalitions selection algorithm achieves more than 10% increase of battery network lifetime than 2×2 MIMO and 3×3 MIMO.

In addition, taking the QoS provision optimisation into account, an optimum cooperative coalitions selection in multi-hop cluster-based capillary networks was investigated to minimise the overall PER of all links for the routing path in Section 5.4. Subsection 5.4.1 presented the overall PER calculation and Subsection 5.4.2 designed the cooperative coalitions selection algorithm that uses QPSO to choose the optimum set of cooperative coalitions in a particular routing path with the objective of overall PER minimisation. Simulation results in Section 5.4.3 demonstrated that the proposed algorithm outperforms 2×2 MIMO and 3×3 MIMO in terms of overall PER.

Furthermore, Section 5.5 focused on the tradeoff between network lifetime and overall PER in multi-hop cluster-based capillary networks using CMIMO systems. Subsection 5.5.1 presented the tradeoff problem formulation by setting two objectives of network lifetime and overall PER optimisation. Subsection 5.5.2 proposed NSQPSO algorithm to select the optimum set of cooperative coalitions, which applies QPSO to select the optimum set of cooperative senders and cooperative receivers of each cluster in the routing path, and also NSGA-II for the Pareto solutions of cooperative coalitions to prolong network lifetime and decrease overall PER. The simulation results in Subsection 5.5.3 proved that the proposed NSQPSO algorithm is able to achieve the optimal tradeoff between energy efficiency and QoS provision.

Chapter 6

Conclusions and future work

6.1 Conclusions

This thesis proposed several node selection algorithms based on clustering and cooperative communication for capillary networks. The proposed algorithms aimed to prolong network lifetime, minimise overall PER and achieve the optimum tradeoff between network lifetime and PER.

First, a QoS aware energy efficient CHs selection algorithm is proposed by using QPSO to maximise the network lifetime. Simulation results proved that the proposed algorithm is able to prolong network lifetime by selecting the optimum set of CHs, and outperforms PSO and QGA algorithms by 10% in terms of network lifetime.

Second, CH and cooperative devices selection algorithms for one-hop cluster-based capillary networks based on CMISO are proposed to maximise the network lifetime, minimise the PER, and also achieve the optimum tradeoff between network lifetime and PER. Simulation results proved that the proposed algorithms effectively achieve different objectives by selecting the optimum set of cooperative devices. In addition, it is demonstrated that the proposed algorithms outperforms PSO and QGA by 8% in

terms of network lifetime.

Finally, cooperative coalitions selection algorithms for multi-hop cluster-based capillary networks based on multi-hop CMIMO are proposed to maximise the network lifetime, minimise the PER, and also achieve the optimum tradeoff between network lifetime and PER. Simulation results demonstrated that the proposed cooperative coalition selection algorithms effectively achieve different objectives by selecting the optimum set of cooperative senders and cooperative receivers of each cluster in the routing path. It was also shown that the proposed algorithms outperforms 2×2 MIMO and 3×3 MIMO by 20% in terms of network lifetime.

6.2 Future work

6.2.1 Cooperative Coalitions Selection in Energy Harvesting Networks

Due to the tremendous increase in the number of battery-powered wireless devices over the past decade, the energy harvesting has become an important research area as a mean of prolonging lifetime of such devices [PS05]. Apart from the conventional renewable energy sources such as solar and wind, radio frequency signals radiated by ambient transmitters can be treated as a viable new source for energy harvesting. Thus, the wireless signals can be used to deliver information as well as energy [Shi11].

Taking energy harvesting technique into consideration, the research on cooperative communication enabled capillary networks is limited and still in its infancy. For the capillary networks employing CMISO or CMIMO systems, the new cooperative coalitions selection algorithms is indispensable, and there are at least two aspects that should be taken into account:

- a) The discontinuous energy level of CHs may result in different optimum long-haul cooperative transmission scheme selection. As such, the new cooperative coalitions selec-

tion algorithm should address the flexibility to switch between single-input-single-output (SISO), MISO, single-input-multiple-output (SIMO) and MIMO cooperative transmission schemes.

- b) Due to the random nature of the harvested energy, cooperative coalitions may not be suitable to support the long-haul transmission during a long time period. Therefore, it is vital to develop an effective low time complexity cooperative coalitions selection algorithm which can be executed frequently to adjust the continuous changing energy level of all devices.

Therefore, it comes to the conclusion that cooperative coalitions selection in cooperative communication enabled capillary networks is a promising research avenue.

6.2.2 Cooperative Coalitions Selection in Heterogeneous Wireless Networks

The future wireless network architecture is heterogeneous, with macro-cells, pico-cells and femto-cells, along with a number of heterogeneous devices using different radio access technologies [HLIK13]. Cooperative communication can be used in such emerging networks by employing heterogeneous devices and infrastructures as the cooperating nodes. For the cooperative schemes in heterogeneous networks, different devices or infrastructures are allowed to share resources and channel information to implement collaboration [ZFK06].

However, cooperative coalitions selection in heterogeneous wireless networks is a very challenging research topic, due to the dynamic subjective status (e.g. battery status and CPU processing capability) of heterogeneous devices and infrastructures. In addition, by implementing the cooperative communication, a large variety of coexisting radio access technologies (i.e. Zigbee, Wi-Fi, cellular) among heterogeneous devices and infrastructures can result in the co-channel interference.

Therefore, novel cooperative coalition selection algorithms are open issues worth to be addressed.

Appendix A

Simulation Validation

In order to testify the performance of the proposed algorithms, the theoretical problem formulation is translated to the Matlab code. In the simulation, the typical parameter values specified in related IoT standards and research work are adopted, as shown in Table 3-A and Table 4-A. All codes are checked by the debugger, and the mathematical correctness of the implemented algorithm is checked line by line.

To verify the correctness of Matlab coding, reproduction of the related work is carried out. Figure 2.9 shows that the final convergence value of Rastrigin function using qubit-based QPSO is about 10^{-5} , and the final convergence value of Rastrigin function using PSO and QGA are about 10^{-1} , which agrees with the result of Figure 5 in [CZZ⁺14]. Additionally, Figure 2.10 shows that the qubit-based QPSO outperforms PSO and QGA by about 50% in terms of the convergence value of Griewank function, which matches the simulation result of Figure 4 in [CZZ⁺14]. Therefore, the correctness of Matlab codes in Chapter 2 can be verified. By substituting the particle representation and the fitness function, the Matlab codes of PSO, QGA and qubit-based QPSO used in Chapter 2 are also executed in the simulations of Chapter 3 and Chapter 4.

To evaluate the proposed algorithms in Chapter 5, the performance of proposed algorithms are compared with existing algorithms, thereby ensuring the trend of the

simulation results is reasonable. In Chapter 5, Figure 5.18 indicates that the overall PER decreases with the increment of SNR for both the proposed algorithm in Section 5.5 and existing algorithm in [LLW⁺13], and this trend agrees with the result of Figure 3 in [LLW⁺13]. In addition, Chapter 5 executes the same Matlab codes of qubit-based QPSO which is used and has been verified in Chapter 2.

References

- [ABBR⁺12] I. Augé-Blum, K. Boussetta, H. Rivano, R. Stanica, and F. Valois. Capillary networks: a novel networking paradigm for urban environments. In *Proceedings of the first workshop on Urban networking*, pages 25–30. ACM, 2012.
- [AK10] Asaduzzaman and H. Y. Kong. Energy efficient cooperative leach protocol for wireless sensor networks. *Journal of Communications and Networks*, 12(4):358–365, 2010.
- [APW08] I. Ahmed, M. Peng, and W. Wang. Uniform energy consumption through adaptive optimal selection of cooperative mimo schemes in wireless sensor networks. In *IEEE Vehicular Technology Conference (VTC Spring)*, pages 198–202, May 2008.
- [AY05] K. Akkaya and M. Younis. A survey on routing protocols for wireless sensor networks. *Journal of Ad Hoc Networks*, 3:325–349, 2005.
- [AY07] A. A. Abbasi and M. Younis. A survey on clustering algorithms for wireless sensor networks. *Computer communications Journal*, 30(14):2826–2841, 2007.
- [Bác96] T. Bäck. *Evolutionary algorithms in theory and practice*. Oxford University Press, 1996.
- [Bat11] All About Battery. Find the energy contained in standard battery sizes. <http://www.allaboutbatteries.com/Energy-tables.html>, 2011.
- [BC03] S. Bandyopadhyay and E. J. Coyle. An energy efficient hierarchical clustering algorithm for wireless sensor networks. In *Twenty-Second Annual Joint Conference of the IEEE Computer and Communications (INFOCOM)*, volume 3, pages 1713–1723, March 2003.
- [BS13] S. Bandyopadhyay and S. Saha. Some single- and multi-objective optimization techniques. In *Unsupervised Classification: Similarity Measures, Classical and Metaheuristic Approaches, and Applications*, pages 17–58, Berlin, Heidelberg, 2013. Springer Berlin Heidelberg.

- [BZL08] L. Bai, L. Zhao, and Z. Liao. Energy balance in cooperative wireless sensor network. In *14th European Wireless Conference*, pages 1–5, June 2008.
- [CADM91] N. Cooke, H. Adams, P. Dell, and T. Moore. *Basic mathematics for electronics*. McGraw-Hill, Inc., 1991.
- [CEC05] L. Cagnina, S. C. Esquivel, and C. Coello. A particle swarm optimizer for multi-objective optimization. *Journal of Computer Science and Technology*, 5, 2005.
- [CGB04] S. Cui, A.J. Goldsmith, and A. Bahai. Energy-efficiency of mimo and cooperative mimo techniques in sensor networks. *IEEE Journal on Selected Areas in Communications*, 22(6):1089–1098, 2004.
- [CL15] W. Chang and T. W. Lin. A novel cluster head reselection and edge sub-clustering lifetime prolongation scheme for modern sensor networks. In *2015 IEEE 81st Vehicular Technology Conference (VTC Spring)*, pages 1–5, May 2015.
- [CMBR14] S. Chen, J. Montgomery, and A. Bolufé-Röhler. Measuring the curse of dimensionality and its effects on particle swarm optimization and differential evolution. *Journal of Applied Intelligence*, 42(3):514–526, 2014.
- [CSSI06] A.D. Coso, S. Savazzi, U. Spagnolini, and C. Ibars. Virtual mimo channels in cooperative multi-hop wireless sensor networks. In *2006 40th Annual Conference on Information Sciences and Systems*, pages 75–80, 2006.
- [CVAG12] N. Chu, S. Vural, J. Annoville, and N. Gligoric. Device management. Technical report, EXALTED, October 2012.
- [CZZ⁺14] J. Cao, T. Zhang, Z. Zeng, Y. Chen, and K. K. Chai. Multi-relay selection schemes based on evolutionary algorithm in cooperative relay networks. *International Journal of Communication Systems*, 27(4):571–591, April 2014.
- [CZZL13] J. Cao, T. Zhang, Z. Zeng, and D. Liu. Interference-aware multi-user relay selection scheme in cooperative relay networks. In *Globecom Workshops (GC Wkshps), 2013 IEEE*, pages 368–373, Dec 2013.
- [Das10] A. Das. Digital modulation techniques. In *Digital Communication:*

- Principles and System Modelling*, pages 111–141, Berlin, Heidelberg, 2010. Springer.
- [DCSI07] A. Del Coso, U. Spagnolini, and C. Ibars. Cooperative distributed mimo channels in wireless sensor networks. *IEEE Journal on Selected Areas in Communications*, 25(2):402–414, February 2007.
- [DDCM02] E. Diaz-Dorado, J. Cidras, and E. Miguez. Application of evolutionary algorithms for the planning of urban distribution networks of medium voltage. *IEEE Transactions on Power Systems*, 17(3):879–884, Aug 2002.
- [DGA04] M. Dohler, A. Gkelias, and H. Aghvami. A resource allocation strategy for distributed mimo multi-hop communication systems. *IEEE Communications Letters*, 8(2):99–101, Feb 2004.
- [Dic06] P. A. Dick, G. and Whigham. Spatially-structured evolutionary algorithms and sharing: Do they mix? In *6th International Conference on Simulated Evolution and Learning*, pages 457–464, Berlin, Heidelberg, 2006. Springer Berlin Heidelberg.
- [DK01] K. Deb and D. Kalyanmoy. *Multi-Objective Optimization Using Evolutionary Algorithms*. John Wiley & Sons, Inc., New York, NY, USA, 2001.
- [DPAM02] K. Deb, A. Pratap, S. Agarwal, and T. Meyarivan. A fast and elitist multiobjective genetic algorithm: Nsga-ii. *IEEE Transactions on Evolutionary Computation*, 6(2):182–197, Apr 2002.
- [DZ04] L. Dai and Q. Zhou. Energy efficiency of mimo transmission strategies in wireless sensor networks. In *International Conference on Computing, Communications and Control Technologies (CCCT)*, volume 1, page 2, 2004.
- [Fal98] E. Falkenauer. *Genetic Algorithms and Grouping Problems*. John Wiley & Sons, Inc., New York, NY, USA, 1998.
- [FGZW10] L. Fei, Q. Gao, J. Zhang, and G. Wang. Energy saving in cluster-based wireless sensor networks through cooperative mimo with idle-node participation. *Journal of Communications and Networks*, 12(3):231–239, 2010.
- [Fog97] D. Fogel. The advantages of evolutionary computation. In *Biocomputing and Emergent Computation: Proceedings of BCEC97*, pages 1–11. World

Scientific Press, 1997.

- [GCD11] H. Gao, J. Cao, and M. Diao. A simple quantum-inspired particle swarm optimization and its application. *Information Technology Journal*, 10(12):2315–2321, 2011.
- [GGP⁺15] D. Greiner, B. Galván, J. Periaux, N. Gauger, K. Giannakoglou, and G. Winter. *Advances in Evolutionary and Deterministic Methods for Design, Optimization and Control in Engineering and Sciences*. Springer, 2015.
- [GP10] N. Gautam and J. Y. Pyun. Distance aware intelligent clustering protocol for wireless sensor networks. *Journal of Communications and Networks*, 12:122–129, April 2010.
- [GSDL14] J. Guo, L. Sun, X. Du, and L. Liu. Clustering protocol based on data aggregating scheme for wireless sensor networks. *WIT transaction on information and communication technology*, 51:379–386, 2014.
- [HCB00] W.R. Heinzelman, A. Chandrakasan, and H. Balakrishnan. Energy-efficient communication protocol for wireless microsensor networks. In *System Sciences, 2000. Proceedings of the 33rd Annual Hawaii International Conference on*, pages 10 pp. vol.2–, 2000.
- [HCB02] W. B. Heinzelman, A. P. Chandrakasan, and H. Balakrishnan. An application-specific protocol architecture for wireless microsensor networks. *IEEE Transactions on Wireless Communications*, 1(4):660–670, Oct 2002.
- [HH03] B. Hassibi and B. M. Hochwald. How much training is needed in multiple-antenna wireless links? *IEEE Transactions on Information Theory*, 49(4):951–963, April 2003.
- [HLIK13] M. E. Helou, S. Lahoud, M. Ibrahim, and K. Khawam. A hybrid approach for radio access technology selection in heterogeneous wireless networks. In *19th European Wireless Conference*, pages 1–6, April 2013.
- [HOKK12] Z. Huang, H. Okada, K. Kobayashi, and M. Katayama. A study on cluster lifetime in multi-hop wireless sensor networks with cooperative miso scheme. *Journal of Communications and Networks*, 14(4):443–450, Aug 2012.
- [Jay04] S. K. Jayaweera. Energy analysis of mimo techniques in wireless sensor

- networks. In *38th Conference on Information Sciences and Systems*, 2004.
- [KCY⁺08] J. Kim, S. H. Chauhdary, W. Yang, D. Kim, and M. Park. Produce: a probability-driven unequal clustering mechanism for wireless sensor networks. In *IEEE 22nd International Conference on Advanced Information Networking and Applications-Workshops*, pages 928–933, 2008.
- [KE95] J. Kennedy and R. Eberhart. Particle swarm optimization. In *IEEE International Conference on Neural Networks*, volume 4, pages 1942–1948 vol.4, Nov 1995.
- [KPHC08] J. M. Kim, S. H. Park, Y. J. Han, and T. M. Chung. Chef: Cluster head election mechanism using fuzzy logic in wireless sensor networks. In *10th International Conference on sAdvanced Communication Technology*, volume 1, pages 654–659, Feb 2008.
- [KS05] R. Khalili and K. Salamatian. A new analytic approach to evaluation of packet error rate in wireless networks. In *Proceedings of the 3rd Annual Communication Networks and Services Research Conference*, pages 333–338, May 2005.
- [Lan06] J . Laneman. Cooperative communications in mobile ad hoc networks. *IEEE Signal Processing Magazine*, 1053:18–29, 2006.
- [Lee05] K. Lee. *Modern Heuristic Optimization Techniques With Applications To Power Systems*. John Wiley & Sons, 2005.
- [LES08] K. Y. Lee and M. A. El-Sharkawi. *Modern heuristic optimization techniques: theory and applications to power systems*, volume 39. John Wiley & Sons, 2008.
- [LG97] C. R. Lin and M. Gerla. Adaptive clustering for mobile wireless networks. *IEEE Journal on Selected areas in Communications*, 15(7):1265–1275, 1997.
- [LKH93] F. Lin, C. Kao, and C. Hsu. Applying the genetic approach to simulated annealing in solving some np-hard problems. *Systems, Man and Cybernetics, IEEE Transactions on*, 23(6):1752–1767, Nov 1993.
- [LLM07] F.G. Lobo, C.F. Lima, and Z. Michalewicz. *Parameter Setting in Evolutionary Algorithms*. Springer Publishing Company, Incorporated, 1st edition,

2007.

- [LLW⁺13] B. Li, H. Li, W. Wang, Q. Yin, and H. Liu. Performance analysis and optimization for energy-efficient cooperative transmission in random wireless sensor network. *Wireless Communications, IEEE Transactions on*, 12(9):4647–4657, 2013.
- [LTS07] N.M.A. Latiff, C.C. Tsimenidis, and B.S. Sharif. Energy-aware clustering for wireless sensor networks using particle swarm optimization. In *IEEE 18th International Symposium on Personal, Indoor and Mobile Radio Communications (PIMRC 2007)*, pages 1–5, 2007.
- [LTSL08] N.M.A. Latiff, C.C. Tsimenidis, B.S. Sharif, and C. Ladha. Dynamic clustering using binary multi-objective particle swarm optimization for wireless sensor networks. In *IEEE 19th International Symposium on Personal, Indoor and Mobile Radio Communications (PIMRC)*, pages 1–5, Sept 2008.
- [LW03] J. N. Laneman and G. W. Wornell. Distributed space-time-coded protocols for exploiting cooperative diversity in wireless networks. *IEEE Transactions on Information Theory*, 49(10):2415–2425, Oct 2003.
- [LZM10] L. Liu, X. Zhang, and H. Ma. Optimal node selection for target localization in wireless camera sensor networks. *IEEE Transactions on Vehicular Technology*, 59(7):3562–3576, Sept 2010.
- [MMBF05] S. D. Muruganathan, D. C. F. Ma, R. I. Bhasin, and A. O. Fapojuwo. A centralized energy-efficient routing protocol for wireless sensor networks. *IEEE Communications Magazine*, 43(3):S8–13, March 2005.
- [MQ10] A. S. Malik and S. A. Qureshi. Analyzing the factors affecting network lifetime for cluster-based wireless sensor networks. *Pakistan Journal of Engineering and Applied Science*, 6:9–16, 2010.
- [MR13] P. N. Malleswari and G. V. Rao. An energy efficient virtual mimo communication for cluster-based wireless sensor networks. In *International Journal of Engineering Research and Technology*, volume 2. ESRSA Publications, 2013.
- [NBO⁺15] O. Novo, N. Beijar, M. Ocak, J. Kjällman, M. Komu, and T. Kauppinen.

- Capillary networks-bridging the cellular and iot worlds. In *2015 IEEE 2nd World Forum on Internet of Things (WF-IoT)*, pages 571–578. IEEE, 2015.
- [NQ10] M. Nasim and S. Qaisar. Hierarchical mimo: A clustering approach for ad hoc wireless sensor networks. In *2010 44th Annual Conference on Information Sciences and Systems (CISS)*, pages 1–6, March 2010.
- [PLC12] S. Park, W. Lee, and D. Cho. Fair clustering for energy efficiency in a cooperative wireless sensor network. In *2012 IEEE 75th Vehicular Technology Conference (VTC Spring)*, pages 1–5, May 2012.
- [PS05] J. A. Paradiso and T. Starner. Energy scavenging for mobile and wireless electronics. *IEEE Pervasive computing*, 4(1):18–27, 2005.
- [Rap14] RapidTables. How to convert mah to wh. <http://www.rapidtables.com/convert/electric/mah-to-wh.htm>, 2014.
- [RD16] A. Ray and D. De. Energy efficient clustering protocol based on k-means (eepk-means)-midpoint algorithm for enhanced network lifetime in wireless sensor network. *IET Wireless Sensor Systems*, 6(6):181–191, 2016.
- [RR16] D. S. Rao and P. N. Rao. A cluster based scalable and energy efficient multi path routing protocol for manet. *International Journal of Engineering Science*, 2016.
- [RV01] D.N. Rakhmatov and S.B.K. Vrudhula. An analytical high-level battery model for use in energy management of portable electronic systems. In *IEEE/ACM International Conference on Computer Aided Design*, pages 488–493, Nov 2001.
- [SB12] C. C. L. Sibanda and A. B. Bagula. Network selection for mobile nodes in heterogeneous wireless networks using knapsack problem dynamic algorithms. In *2012 20th Telecommunications Forum (TELFOR)*, pages 174–177, Nov 2012.
- [SBE⁺14] J. Sachs, N. Beijar, P. Elmdahl, J. Melen, F. Militano, and P. Salmela. Capillary networks a smart way to get things connected. *Ericsson Review*, pages 2 –7, September 2014.
- [SBY⁺12] Z.W. Siew, A. Bono, H.P. Yoong, K.B. Yeo, and K.T.K. Teo. Cluster for-

- mation of wireless sensor nodes using adaptive particle swarm optimisation. *International Journal of Simulation Systems*, 13:38–44, June 2012.
- [SFX04] J. Sun, B. Feng, and W. Xu. Particle swarm optimization with particles having quantum behavior. In *Congress on Evolutionary Computation*, volume 1, pages 325–331 Vol.1, 2004.
- [SH11] S. Singh and K. Huang. A robust m2m gateway for effective integration of capillary and 3gpp networks. In *2011 Fifth IEEE International Conference on Advanced Telecommunication Systems and Networks (ANTS)*, pages 1–3. IEEE, 2011.
- [Shi11] N. Shinohara. Power without wires. *IEEE Microwave Magazine*, 12(7):S64–S73, 2011.
- [SL13] A. Sinha and D. K. Lobiyal. Performance evaluation of data aggregation for cluster-based wireless sensor network. *Human-Centric Computing and Information Sciences*, 3(1):1, 2013.
- [Sud08] D. Sudholt. Computational complexity of evolutionary algorithms, hybridizations, and swarm intelligence, 2008.
- [SYY⁺13] Z. Sheng, S. Yang, Y. Yu, A. V. Vasilakos, J. A. Mccann, and K. K. Leung. A survey on the ietf protocol suite for the internet of things: standards, challenges, and opportunities. *IEEE Wireless Communications*, 20(6):91–98, December 2013.
- [TKS14] M. Tarhani, Y. S. Kavian, and S. Siavoshi. Seech: Scalable energy efficient clustering hierarchy protocol in wireless sensor networks. *IEEE Sensors Journal*, 14(11):3944–3954, Nov 2014.
- [TNNY10] H. Taheri, P. Neamatollahi, M. Naghibzadeh, and M. H. Yaghmaee. Improving on heed protocol of wireless sensor networks using non probabilistic approach and fuzzy logic (heed-npf). In *2010 5th International Symposium on Telecommunications*, pages 193–198, Dec 2010.
- [TT10] M. C. M. Thein and T. Thein. An energy efficient cluster-head selection for wireless sensor networks. In *2010 International Conference on Intelligent Systems, Modelling and Simulation*, pages 287–291, Jan 2010.

- [WCZW12] D. Wu, Y. Cai, L. Zhou, and J. Wang. A cooperative communication scheme based on coalition formation game in clustered wireless sensor networks. *IEEE Transactions on Wireless Communications*, 11(3):1190–1200, 2012.
- [WHC99] A. Wang, W.R. Heinzelman, and A.P. Chandrakasan. Energy-scalable protocols for battery-operated microsensor networks. In *1999 IEEE Workshop on Signal Processing Systems*, pages 483–492, 1999.
- [WIK] WIKIPEDIA. Aaa battery. https://en.wikipedia.org/wiki/AAA_battery/. Accessed February 8, 2016.
- [Woe03] G. J. Woeginger. Exact algorithms for np-hard problems: A survey. In *Combinatorial OptimizationEureka, You Shrink!*, pages 185–207. Springer, 2003.
- [YCK06] Y. Yuan, M. Chen, and T. Kwon. A novel cluster-based cooperative mimo scheme for multi-hop wireless sensor networks. *EURASIP Journal on Wireless Communications and Networking*, 2006(2):38–38, April 2006.
- [YF04] O. Younis and S. Fahmy. Heed: a hybrid, energy-efficient, distributed clustering approach for ad hoc sensor networks. *IEEE Transactions on Mobile Computing*, 3(4):366–379, Oct 2004.
- [YHC06] Y. Yuan, Z. He, and M. Chen. Virtual mimo-based cross-layer design for wireless sensor networks. *IEEE Transactions on Vehicular Technology*, 55(3):856–864, May 2006.
- [ZCSA09] J. Zhang, S. Ci, H. Sharif, and M. Alahmad. A battery-aware deployment scheme for cooperative wireless sensor networks. In *IEEE Global Telecommunications Conference*, pages 1–5, Nov 2009.
- [ZCSA10] J. Zhang, S. Ci, H. Sharif, and M. Alahmad. Modeling discharge behavior of multicell battery. *IEEE Transactions on Energy Conversion*, 25(4):1133–1141, Dec 2010.
- [ZD07] Y. Zhang and H. Dai. Energy-efficiency and transmission strategy selection in cooperative wireless sensor networks. *Journal of Communications and Networks*, 9(4):473–481, Dec 2007.
- [ZFK06] Q. Zhang, F.H.P. Fitex, and M. Katz. Evolution of heterogeneous wireless

networks: towards cooperative networks. In *3rd International Conference of the Center for Information and Communication Technologies (CICT)*, 2006.